



The University of  
**Nottingham**

Advanced Drug Delivery and Tissue Engineering Group

School of Pharmacy, University of Nottingham

**DEVELOPMENT OF A NOVEL POROUS  
SCAFFOLD: ASSESSMENT OF ITS SUITABILITY  
FOR CARDIAC MUSCLE ENGINEERING**

**Lilia Araida Hidalgo-Bastida, BSc.**

Thesis submitted to the University of Nottingham for the degree of  
Doctor of Philosophy,

June 2008

## Abstract

Cellular transplantation, a current therapy for cardiac failure, does not consider the need for a physical support or biochemical factors required by the cardiomyocyte. The aim of this project was to establish the Extra Cellular Matrix (ECM), architectural and mechanical properties of a flexible scaffold to assist the maintenance of a cardiac cell line cultured under mechanical stimuli. Previously, mechanical stimulation has been proved to have an effect in cardiomyocytes similar to that of growth factors on other cells and promotes protein expression, differentiation and survival [1]. Poly-(1,8-octanediol-co-citric acid) [POC] is an elastomer that can be processed into scaffolds for tissue engineering. Mechanical properties of the POC were compared at different porosity, storage method and strain rate. POC, with an ultimate elongation of 60-160%, did support cardiac cell attachment when coated with fibronectin. Seeding strategies were evaluated to find optimal conditions and static seeding resulted more favourable for cell adhesion and survival than other dynamics approaches. In collaboration with the University of Leeds, cardiomyocytes were cultured in a dynamic bioreactor, Tencell, under continuous and discontinuous stretching regimes. Mechano-stimulation of cardiac constructs encouraged cell survival in the discontinuous regime and up-regulated the expression of *actc1* and *nppa* genes regardless of the treatments. It was concluded that although mechanical stimulation had a positive effect on cell survival and gene expression, tissue formation was not promoted.

**Keywords:** Scaffold, Poly-(1,8-octanediol-co-citric acid) [POC], Elastomer, Cardiomyocyte, Tissue Engineering.

## **Acknowledgments**

I would like to thank my supervisor, Kevin M Shakesheff, for his guidance and for giving me the opportunity to work on such a new project within the group.

I am sincerely grateful to Felicity RAJ Rose for her helpful suggestions, stimulating advice and valuable training during my time in this research group.

I would like to express my thanks to Lee D Buttery, Ian P Hall and William C Claycomb for their comments and collaboration.

I also extend my gratitude to Eileen Ingham and Joanne Ingram for providing the Tencell system to test my constructs, without their cooperation this project would never be completed.

My thanks to John JA Barry for his kind support in the elaboration and analysis of copolymers and scaffolds; to Nicola M Everitt, for her advice on mechanical test procedures and analysis. Also to Franco H Falcone, Andrew Hall and Gerard Byrne, for their guidance and training on molecular techniques.

Special thanks to Ruby Majani, for all the help with the SEM processing and imaging while I could not handle hazardous chemicals, and to Lisa J White, for her help with the microCT imaging and analysis.

I also thank the Department of Microbiology at the University of Leeds, the Tissue Engineering Group, the Clean Technology Group and the technical staff at the School of Pharmacy, from the University of Nottingham, for their assistance and advice.

Thanks to all the friends who I met during or because of this PhD, to Yolanda, Neil, Sophie, Gracia, Cuitlahuac, Ale, Ulysses, Paula, Lisa, Mieke, Chayanin, Ruby, Maria and all the guys from the Mexican band. In one way or another, each of you contributed to this work with your moral support and priceless friendship.

Special gratitude to my parents and my brother, who have encouraged and supported me in all possible ways to pursue my dreams. Thanks Mum for teaching me never to give up and for always being there for me.

I am very grateful to my husband Jesús, whose patient and understanding love enabled me to complete this work and who never stopped believing in me. You have showed me that *love is patient and kind...bears all things, believes all things, hopes all things, endures all things...*

Last, but not least, thanks to Sebastian: you have been my ultimate reason to finish this PhD.

Finally thanks to the Mexican Science and Technology Council (CONACYT), the Mexican Ministry of Education (SEP) and the British Council for funding this project.

# Table of Contents

<b>ACKNOWLEDGMENTS</b> .....	<b>3</b>
<b>TABLE OF CONTENTS</b> .....	<b>5</b>
<b>LIST OF FIGURES</b> .....	<b>9</b>
<b>LIST OF TABLES</b> .....	<b>14</b>
<b>ABBREVIATIONS</b> .....	<b>15</b>
<b>ABBREVIATIONS</b> .....	<b>15</b>
<b>1 CARDIAC DISEASES: CURRENT THERAPIES AND RESEARCH</b> .....	<b>19</b>
1.1 CARDIAC DISEASES: CURRENT THERAPIES AND RESEARCH.....	20
1.2 CARDIAC DISEASES, MORTALITY AND MORBIDITY.....	20
1.2.1 <i>Cardiac Anatomy</i> .....	21
1.2.2 <i>Diseases</i> .....	28
1.3 CARDIAC REGENERATION & TREATMENTS.....	29
1.3.1 <i>The Challenge of Cardiac Regeneration</i> .....	29
1.3.2 <i>Available Treatments</i> .....	30
1.4 TISSUE ENGINEERING.....	32
1.4.1 <i>Cells for in vitro development of cardiac muscle</i> .....	34
1.4.2 <i>Biomaterials</i> .....	35
1.4.3 <i>Scaffolds for Tissue Engineering</i> .....	43
1.4.4 <i>Bioreactors</i> .....	57
1.5 AIMS OF THE STUDY.....	63
1.5.1 <i>Objectives</i> .....	63
<b>2 GENERAL MATERIALS AND METHODS</b> .....	<b>65</b>
2.1 POLYMER PREPARATION, PROCESSING AND CHARACTERISATION.....	66
2.1.1 <i>Polymer synthesis</i> .....	66
2.1.2 <i>Scaffold manufacture</i> .....	66
2.1.3 <i>Polymer Characterisation</i> .....	69
2.2 CELL CULTURE METHODS.....	72
2.2.1 <i>Culture of HL-1 cardiomyocytes</i> .....	72
2.2.2 <i>Culture of c2c12 myocytes</i> .....	73
2.3 CULTURE OF CELL SEEDED SCAFFOLDS.....	73
2.3.1 <i>Preparation of POC films and scaffolds</i> .....	73
2.3.2 <i>Modification of POC surface with ECM proteins</i> .....	74
2.3.3 <i>Seeding cells into non-porous POC films</i> .....	74
2.3.4 <i>Seeding cells into porous POC scaffolds</i> .....	75

2.3.5	<i>Static culture</i> .....	76
2.3.6	<i>Tencell culture</i> .....	76
2.4	BIOCHEMICAL AND MOLECULAR ASSAYS .....	78
2.4.1	<i>Alamar Blue</i> .....	78
2.4.2	<i>Quantitative RT-PCR</i> .....	79
2.5	IMAGING OF CELLS .....	81
2.5.1	<i>Evaluation of Cell Morphology and Contraction Rate</i> .....	81
2.5.2	<i>Video recording of HL-1 cells</i> .....	82
2.5.3	<i>Immunofluorescence staining for sarcomeric-actin</i> .....	82
2.5.4	<i>Live/Dead assay for Stereo and Confocal microscopy</i> .....	83
2.5.5	<i>SEM</i> .....	83
2.6	STATISTICAL ANALYSIS.....	84
<b>3</b>	<b>PROCESSING, CHARACTERISATION AND MECHANICAL PROPERTIES OF POLY-(1,8 OCTANEDIOL-CO-CITRIC ACID) [POC] POROUS SCAFFOLDS FOR CARDIAC MUSCLE TISSUE ENGINEERING .....</b>	<b>85</b>
3.1	PROCESSING BIOMATERIALS INTO SCAFFOLDS .....	86
3.1.1	<i>Polymers and elastomers</i> .....	86
3.1.2	<i>Processing polymers into porous scaffolds</i> .....	87
3.1.3	<i>Methods for scaffold characterisation</i> .....	91
3.1.4	<i>Mechanical properties of scaffolds</i> .....	93
3.1.5	<i>Degradation</i> .....	98
3.1.6	<i>Aims of this study</i> .....	99
3.2	MATERIALS AND METHODS .....	99
3.2.1	<i>Synthesis of POC</i> .....	99
3.2.2	<i>Gas foaming of POC</i> .....	99
3.2.3	<i>Salt leaching of POC</i> .....	100
3.2.4	<i>Characterisation of POC scaffolds</i> .....	100
3.3	RESULTS AND DISCUSSION.....	100
3.3.1	<i>POC processing</i> .....	101
3.3.2	<i>POC scaffold characterisation</i> .....	111
3.4	CONCLUSIONS .....	132
<b>4</b>	<b>OPTIMISATION OF SEEDING CONDITIONS FOR MYOCYTES IN POLY (1,8-OCTANEDIOL-CO-CITRIC ACID) FILMS AND SCAFFOLDS.....</b>	<b>134</b>
4.1	INTRODUCTION.....	135
4.1.1	<i>Cardiomyocyte culture</i> .....	135
4.1.2	<i>Cell adhesion</i> .....	136

4.1.3	<i>Seeding strategies for scaffolds</i> .....	141
4.1.4	<i>Aims</i> .....	142
4.2	<b>MATERIALS AND METHODS</b> .....	143
4.2.1	<i>Manufacture of POC films</i> .....	143
4.2.2	<i>Casting of POC scaffolds</i> .....	143
4.2.3	<i>Cell culture</i> .....	144
4.2.4	<i>Seeding cells into scaffolds</i> .....	144
4.2.5	<i>Surface modification</i> .....	145
4.2.6	<i>Analysis of cell viability</i> .....	145
4.2.7	<i>Inverted microscopy and total area</i> .....	146
4.2.8	<i>Imaging of cells on scaffolds</i> .....	146
4.2.9	<i>Statistical analysis</i> .....	146
4.3	<b>RESULTS AND DISCUSSION</b> .....	147
4.3.1	<i>Monolayer culture of c2c12 and HL-1 cells</i> .....	147
4.3.2	<i>3D culture of c2c12 and HL-1 in POC scaffolds</i> .....	149
4.3.3	<i>Surface coating with Extracellular Matrix (ECM) Proteins</i> .....	149
4.3.4	<i>Analysis of the effect of different porosities on the proliferation of HL-1s</i> .....	154
4.3.5	<i>3D culture - Static vs. dynamic seeding</i> .....	158
4.4	<b>CONCLUSIONS</b> .....	165
<b>5</b>	<b>COMPARISON OF CULTURE OF CARDIOMYOCYTE CONSTRUCTS ON A MECHANICAL STIMULATED BIOREACTOR AND STATIC CULTURE</b> .....	<b>166</b>
5.1	<b>INTRODUCTION</b> .....	167
5.1.1	<i>Mechanical stimuli in cardiomyocytes</i> .....	167
5.1.2	<i>Cardiac gene markers</i> .....	168
5.1.3	<i>Dynamic Bioreactors</i> .....	170
5.1.4	<i>Aims</i> .....	177
5.2	<b>MATERIALS AND METHODS</b> .....	177
5.2.1	<i>Preparation of Scaffolds</i> .....	177
5.2.2	<i>Cell culture</i> .....	177
5.2.3	<i>Culture of cell-seeded scaffolds</i> .....	177
5.2.4	<i>Analysis of constructs</i> .....	178
5.3	<b>RESULTS AND DISCUSSION</b> .....	180
5.3.1	<i>Differences in seeding concentration and in situ incubation</i> .....	180
5.3.2	<i>Survival after mechanical load</i> .....	184

5.3.3	<i>Gene expression</i> .....	187
5.3.4	<i>Protein expression</i> .....	191
5.3.5	<i>Imaging of constructs</i> .....	191
5.4	CONCLUSIONS .....	200
<b>6</b>	<b>GENERAL DISCUSSION AND CONCLUSIONS</b> .....	<b>201</b>
	<b>REFERENCES</b> .....	<b>207</b>
	<b>APPENDIX 1 – VIDEO OF HL-1 CARDIOMYOCYTES, CULTURED IN TCP, CONTRACTING AT CONFLUENCE</b> .....	<b>241</b>
	<b>APPENDIX 2 – PUBLICATIONS AND PRESENTATIONS</b> .....	<b>242</b>

## List of Figures

Figure 1-1 Diagram of the heart anatomy adapted from [5] .....	22
Figure 1-2 Phase contrast image of HL-1 cardiomyocytes at lower magnification (10x) shows phenotypical elongated morphology .....	25
Figure 1-3 Oligomerisation of citric acid and 1,8-octanediol .....	42
Figure 1-4 Principle of a bioreactor .....	58
Figure 2-1 Digital image of the supercritical Carbon Dioxide (scCO <sub>2</sub> ) system .....	67
Figure 2-2 Schematic diagram of a cone beam X-ray microtomography system [86] .....	70
Figure 2-3 Diagram of the Tencell bioreactor .....	77
Figure 3-1 Elastic behaviour of polymers and elastomers [119] .....	96
Figure 3-2 Digital images of POC discs crosslinked for (A) 3 days at 120°C, (B) 7 days at 120°C and (C) 7 days at 80°C .....	102
Figure 3-3 Digital images of (A) non processed POC disc compared to porous POC structures processed by scCO <sub>2</sub> for 2 hours, foamed only in the superior part of the disc. (B) POC processed for 4 hours compared to an untreated disc and (C-D) fully foamed POC discs after 16 hours of supercritical processing .....	104
Figure 3-4 SEM images of (A-B) POC discs crosslinked for 10 days and processed with scCO <sub>2</sub> for 6 hours showing solid internal structure with pores only in the surface. (C-D) POC crosslinked for 14 days and then foamed for 6 hours showed the same effect with a resultant solid core. ....	105
Figure 3-5 Digital images of (A-B) salt leached POC discs of 10 mm diameter and 8 mm thick. Magnified images of (C) pores shaped like the porogen and (D) interconnected pores .....	107
Figure 3-6 Digital images of Teflon moulds and the resultant POC discs and rectangular films after solvent casting process .....	109
Figure 3-7 (A-B) SEM and (C-D) microCT images of salt leached POC 70% porous scaffolds confirming full porous structure and interconnectivity .....	110
Figure 3-8 MicroCT images from sections of (A) 60%, (B) 70% and (C) 80% porous POC scaffolds stored at room temperature; (D) 60%, (E) 70% and (F) 80% POC porous	

scaffolds stored at -20°C and of (G) 60%, (H) 70% and (I) 80% POC/cellulose scaffolds stored at room te.....	113
Figure 3-9 SEM images from sections of (A) 60%, (B) 70% and (C) 80% porous POC scaffolds stored at room temperature; (D) 60%, (E) 70% and (F) 80% POC porous scaffolds stored at -20°C and of (G) 60%, (H) 70% and (I) 80% POC/cellulose scaffolds stored at room temperature.....	114
Figure 3-10 pH neutralisation of a POC scaffold washed in (A) 100 ml and (B) 4,000 ml of PBS .....	122
Figure 3-11 pH variation of POC scaffolds washed in scCO <sub>2</sub> compared to untreated POC scaffolds overtime .....	123
Figure 3-12 Degradation overtime of POC films incubated in PBS at 37°C (mean values ± SD, n=3).....	125
Figure 3-13 MicroCT images of 60, 70 and 80% porous scaffolds after incubation in PBS at 37°C to mimic degradation in physiological conditions. Scaffolds after 26 weeks were solid POC films.....	126
Figure 3-14 Young's modulus of POC scaffolds stored (A) at room temperature, (B) at -20°C and (C) POC/cellulose scaffolds strained at 18, 180, 300 and 500 mm/min. (mean value ± SD, n=3).....	128
Figure 3-15 Maximum elongation of POC scaffolds stored (A) at room temperature, (B) at -20°C and (C) POC/cellulose scaffolds strained at 18, 180, 300 and 500 mm/min. (mean value ± SD, n=3).....	130
Figure 4-1 Images of c2c12 myocytes cultured on untreated (A) TCP and (B) POC film and HL-1 cardiomyocyte monolayer cultures on (C) untreated TCP, (D) untreated POC, (E) treated TCP and (F) treated POC. TCP images are on day 3 while in POC are on day 1. ....	148
Figure 4-2 Images at low and high magnification of (A-B) c2c12 cells and (C-D) HL-1 cells cultured on un-conditioned POC scaffolds for 24 hours. Poor attachment is caused by the low affinity of the cell surface receptors to POC ligands, absence of proteins on the surface and acidic conditions. Arrows show dead cells. ....	150

Figure 4-3 Representative images of area coverage of HL-1 cells after 18 hours cultured on poly(1,8-octanediol-co-citric acid) [POC] films coated with proteins at different concentrations: Fibronectin (A) 400  $\mu\text{g}/\text{cm}^2$  (B) 40  $\mu\text{g}/\text{cm}^2$ , (C) 4  $\mu\text{g}/\text{cm}^2$  and (D) control-PBS; Collagen (E) 10  $\mu\text{g}/\text{cm}^2$ , (F) 1  $\mu\text{g}/\text{cm}^2$ , (G) 0.1  $\mu\text{g}/\text{cm}^2$ , and (H) control-PBS; Laminin (I) 2  $\mu\text{g}/\text{cm}^2$ , (J) 0.2  $\mu\text{g}/\text{cm}^2$ , (K) 0.02  $\mu\text{g}/\text{cm}^2$  and (L) control-PBS. .... 151

Figure 4-4 Total area coverage of HL-1 cells after 18 hours of culture on poly (1,8-octanediol-co-citric acid) [POC] films coated with fibronectin, collagen or laminin at concentrations [ $\mu\text{g}/\text{cm}^2$ ] as indicated (n=3, mean + SD, \*\*\* indicates  $p < 0.001$ ). ..... 152

Figure 4-5 (A) Standard curve for number cell and Alamar blue absorbance and (B) Survival of HL-1 cells after 24 hours when seeded on POC scaffolds with different porosities (mean  $\pm$  SD, n=9, # indicates  $p > 0.05$ ). ..... 156

Figure 4-6 Fluorescent images of HL-1 cells stained with Live/Dead after 24 hours of culture in (A) 60%, (B) 70% and (C) 80% POC scaffolds ..... 157

Figure 4-7 Images of HL-1 cells after 24 hours of culture in POC 70% scaffolds coated with fibronectin at 400  $\mu\text{g}/\text{cm}^2$  seeded by (A-C) centrifugation, (D-F) static, (G-I) 100 rpm, (J-L) 200 rpm and (M-O) 300 rpm ..... 159

Figure 4-8 Images of c2c12 cells after 24 hours of culture when seeded on 70% POC film scaffolds coated with fibronectin at 400  $\mu\text{g}/\text{cm}^2$  seeded by (A-C) static method and by (D-F) 100 rpm dynamic seeding. .... 160

Figure 4-9 Graph of cell survival of HL-1 and c2c12 cells after 24 hours of being seeded statically, by centrifugation of at 100, 200 or 300 rpm (n=9, mean  $\pm$ SD, \*\*\* indicates  $p < 0.001$ ). ..... 162

Figure 4-10 Fluorescent images of 70% POC film scaffolds seeded with (A) c2c12 cells by static seeding, (B) c2c12 cells seeded at 100 rpm, (C) HL-1 cardiomyocytes statically and (D) HL-1 cardiomyocytes seeded dynamically at 100 rpm. Samples imaged after 24 hours using UV microscopy after Live/Dead staining. .... 163

Figure 5-1 Commercial dynamic bioreactors (A) BioDynamics by Bose/Enduratec, (B) Flexcell, (C) RCCS, and (D) DynaGens by TGT [232-236]..... 172

Figure 5-2 Digital images of custom-made multi-station dynamic bioreactors: (A) Miniature Load and Strain-Controlling Bioreactor (Northeastern University, USA), (B) Bioreactor

for controlled stretch and flexure of soft biological materials under cell-culture conditions (University of Pittsburgh, USA) and (C) Tencell (Leeds University, UK) [92, 229, 230].	173
Figure 5-3 Digital images of 70% porous POC scaffolds (A) before cell culture preparation and (B) compared to a pH buffered scaffold characterised by the change of colour from white to pale yellow. POC scaffolds dimensions (C) and clamp marked areas (D) are shown. Resultant constructs after cell culture in the Tencell with change of colour caused by the culture medium (E) and clamp marks (F)	181
Figure 5-4 Diagram of a Tencell chamber showing (A) lateral view of a construct held by one static clamp and by one mechanically coupled clamp. (B) Superior view of the chamber containing the construct surrounded by media	182
Figure 5-5 Digital image of HL-1/POC constructs (A) after 20 hours of static culture in the Tencell. (B) Constructs incubated in Alamar blue exhibit a change in colour from purple/blue to bright pink. Constructs in the central box were incubated in a plate whereas constructs in the discontinuous line box were in the Tencell. No metabolic activity can be seen where the clamps were whilst the central constructs show metabolic activity through all the structure	182
Figure 5-6 Survival of HL-1 cells after 20 hours of static culture. Cells were seeded at two different concentrations, $55 \times 10^3$ cells and $110 \times 10^3$ cells per scaffold; and in two conditions: incubated in 8-well non tissue cultured plates or directly into the Tencell chambers. There was no statistical significant difference in the survival of any of the groups (mean $\pm$ SD, # indicates $p > 0.05$ , $n=3$ ). However, when seeded at lower concentration, the overall survival was higher than seeded at higher concentration	183
Figure 5-7 Survival of HL-1 cells after 1 week of culture in the Tencell cultured at different stretching regimen. There is a significant difference between survival in the Tencell static culture and the stretching for four hours per day but not between static and continuous culture (mean $\pm$ SD, *** indicates $p < 0.001$ , # indicates $p > 0.05$ , $n=3$ )	185
Figure 5-8 Melt curves of the primers for (A) hprt1, (B) rpl32, (C) actc1, (D) myh6 and (E) nppa. Several peaks are observed in the myh6 melt curve indicating the amplification of additional sequences	189

Figure 5-9 REST statistical analysis of *actc1* and *nppa* in (A) continuously stretched and (B) discontinuously stretched normalised with *rpl32* as housekeeping gene. *Actc1* was up-regulated in both cases, although a 4-fold up-regulation is observed in discontinuous regimen. No significant difference was found according to the statistical method (mean  $\pm$  SD, # indicates  $p > 0.05$ ,  $n=9$ )..... 190

Figure 5-10 Fluorescent micrographs of actin filaments in HL-1 cells stretched (A) discontinuously and (B) continuously loaded in the Tencell bioreactor. .... 192

Figure 5-11 Composed image of fluorescent stereo-micrographs of a HL-1/POC construct cultured in the Tencell stained for Live/Dead. Non-fluorescent lateral areas correspond to the clamps that hold the construct in position and therefore no cell attachment nor proliferation is visible. .... 194

Figure 5-12 Fluorescent image of HL-1 cells in a POC scaffolds ..... 195

Figure 5-13 Fluorescent stereo-micrographs of HL-1 constructs cultured (A, B) statically, (C, D) under continuous mechanical load and (E,F) in a stretching regime of four hours per day..... 196

Figure 5-14 Confocal micrographs of HL-1s cultured (A,B) statically and (C,D) in the Tencell..... 197

Figure 5-15 SEM microphotographs of POC constructs seeded with HL-1 cells and statically cultured for a week in a 8-well plate and in the Tencell. Continuous arrows indicate dead cells and discontinuous arrows show structures that resemble aligned myofibres..... 198

Figure 5-16 SEM microphotographs of POC constructs seeded with HL-1 cells and cultured for a week in the Tencell with continuous and discontinuous stretching regime. Continuous arrows indicate dead cells and discontinuous arrows show cardiomyocytes of typical phenotype..... 199

## List of Tables

Table 1-1 Location and function of the different types of cells present in the heart [5].....	24
Table 1-2 Function and protein involved in typical cardiac junctions [5] .....	24
Table 1-3 Comparison of characteristics between atrial and ventricular cardiomyocytes [5] ...	27
Table 1-4 Tissue healing models [29].....	33
Table 1-5 Synthetic and natural polymers with medical applications [37-39] .....	38
Table 1-6 Physical properties of citric acid and 1,8-octanediol [39] .....	40
Table 1-7 Description of the key characteristics in scaffolds design [40-41].....	44
Table 1-8 Standard techniques for biomaterial processing into porous scaffolds [33, 41, 50-57] .....	48
Table 1-9 State of the art in stimulated cardiac systems [75-84].....	56
Table 2-1 qRT-PCR primer sequences designed for mouse cells.....	80
Table 3-1 Porosity of POC scaffolds (n=3 for microCT; n=9 for He pycnometry).....	115
Table 3-2 Mean Pore size (StDev) of POC scaffolds (n=3 for microCT; n=9 for He pycnometry).....	115
Table 3-3 Pore size between RT, -20, + cellulose (microCT) (n=3 for microCT; n=9 for He pycnometry).....	120
Table 3-4 Density of POC scaffolds at different porosity values (mean values $\pm$ SD, n=3)....	120
Table 4-1 Principal ECM proteins used in surface modification of biomaterials for cell adhesion [161-163] .....	140
Table 4-2 Relative survival of HL-1 cells after 24 hours of culture in POC scaffolds of different porosities analysed with Alamar Blue .....	157
Table 5-1 Characteristics of different bioreactors for cell culture [243].....	171

## Abbreviations

%	per cent
$\rho$	density
$\Delta L$	change of length
$\mu\text{m}$	micrometer
$\pm$	plus or minus
$^{\circ}\text{C}$	degree Celsius
$\mu\text{CT}$	micro computed tomography scan
$\mu\text{L}$	microlitre
2D	two-dimensional
3D	three-dimensional
$A_0$	original cross-sectional area through the force is applied
ANF	Atrial Natriuretic Factor
ANP	Atrial Natriuretic Peptide
ATP	adenosine tri-phosphate
AV	Atrioventricular
BMP-2	bone morphogenic protein 2
BNP	Brain Natriuretic Peptide
BPR	back pressure regulator
cDNA	complementary Deoxyribonucleic acid
CG	collagen-glycosaminoglycan
CHD	congenital heart diseases
CICR	Calcium-Induced, Calcium-Released
CK-MM	creatine kinase MM
$\text{cm}^2$	square centimetre

CO <sub>2</sub>	Carbon Dioxide
CONACYT	Mexican Science and Technology Council
CT	computed tomography scan,
CVD	cardiovascular disease
Cx43	Conexin 43
DMEM	Dulbecco's modified Eagle's medium
DNA	deoxyribonucleic acid
<i>E</i>	Young's modulus or elastic modulus,
ECCAC	European collection of cell cultures
ECG	electrocardiogram
ECM	extra cellular matrix
ESC	embryonic stem cells
<i>F</i>	force applied to the object,
FD	freeze dried
h	hour
H <sub>2</sub> O	water
HARV	high aspect ratio vessel
Hg	Mercury
HMDS	hexamethyldisilazane
HSC	haematopoietic stem cells
Hz	Hertz
ITEMS	Intelligent tissue engineering via mechanical stimulation
kPa	kiloPascals
kV	kilovolts
<i>L</i> <sub>0</sub>	initial length of the material before a load is applied,

LV	left ventricle
mA	milliamperes
MHC	myosin heavy chain
mL	millilitre
MLC	myosin light chains
mm	millimetre
MPa	Megapascals
mRNA	messenger ribonucleic acid
ms	milliseconds
MSC	mesenchymal or bone-marrow stem cells
NASA	National Aeronautics and Space Administration
PBS	Phosphate Buffered Saline
PCL	poly(caprolactone)
PDLA	poly(DL-lactic acid)
PE	Polyethylene
PEG	Poly(ethylene glycol)
PGA	poly(glycolic acid)
PGS	poly(glycerol-sebacate)
pH	measure of acidity/alkalinity
PHEMA	Poly(hydroxyethyl methacrylate)
PLLA	poly(L-lactic acid)
POC	Poly-(1,8-octanediol-co-citric acid)
PP	Polypropylene
Psi	pounds per square inch
PU	Polyurethanes

qRT-PCR	quantitative Reverse Transcriptase -Polymerase Chain Reaction
RGD	arginine-glycine-aspartine
Rpm	revolutions per minute
RT	room temperature
SA	Sinoatrial
scCO <sub>2</sub>	supercritical carbon dioxide
SCPL	solvent casting and particle leaching
sd	standard deviation
SEM	scanning electron microscopy
SEP	Mexican Ministry of Education
SFF	solid free-form fabrication
SLA	stereo lithography
STLV	slow turning lateral vessel
TCP	tissue culture plastic
TEFLON	poly-(tetrafluoroethylene)
Tg	glass transition temperature
TGFβ	Transforming Growth Factor beta
U	Units
UK	United Kingdom
USA	United States of America
UV	ultraviolet
V	volume
VEGF	vascular endothelial growth factor
w	weight
YIGSR	tyrosine-isoleucine-glycine-serine-arginine

# 1 Cardiac Diseases: Current Therapies and Research

*This first chapter presents the significance impact of heart diseases on healthcare systems and patient quality of life. Conventional therapies and new approaches to treat cardiac patients will be discussed. It particularly focuses on the role of tissue engineering as an emerging clinical alternative and describes its key elements: cells, biomaterials and bioreactors. This literature review establishes the basis for this work; the main aim of which is to evaluate a mechanically stimulated 3D culture of cardiac cells contained with flexible structures.*

## **1.1 Cardiac Diseases: Current Therapies and Research**

This work evolved as a consequence of the increasing number of deaths related to cardiac causes and the few alternatives available to cure these diseases; all these resulting in poor quality of life for patients and a significant cost to healthcare services.

Regenerative medicine has re-emerged in recent years as one of the applied sciences with potential impact in daily life. However before testing any new therapy in patients, all the processes involved need to be optimised and run through several phases of clinical trials to ensure the safety and efficacy of the treatment. This work endeavours to contribute to the development of *in vitro* cardiomyocyte structures engineered under dynamic conditions by considering all the elements involved in such a task.

## **1.2 Cardiac Diseases, Mortality and Morbidity**

The need for heart replacement therapies is evident in the increasing figures of morbidity and mortality due to heart disease in most Western countries, where this disease is the major cause of deaths. In Europe, cardiovascular disease (CVD) causes nearly half of all deaths, 47%, with cardiac diseases (coronary heart diseases and stroke) comprising 40% of CVD [1]. The prevalence of risk factors among the European population is increasing in such levels that projections for consequent years still consider CVD as the main cause of death and the most common chronic disease on this continent.

In the United Kingdom, cardiovascular diseases were the most reported common cause of death with 260,000 deaths per annum (42%) in 2005 [2].

Cardiac disease deaths are included in the latter statistic with an average number of deaths of 206,000 (32%) per year in England, Scotland, Ireland, and Wales and is the main cause of premature death. In addition, the population with some level of cardiac disease is currently 2.6 million people (4.5% of total population) who are in treatment to control or cure their condition [3].

In the United States of America (USA), the figures are similar to Europe with 38% of deaths caused by heart disease and 43% of all cardiovascular causes. A history of a heart attack is held by 2.5% of Americans, whereas 22% of the American population suffers some kind of cardiovascular disease and 6% suffer from heart disease [4].

### **1.2.1 Cardiac Anatomy**

#### **Structure And Function Of The Heart**

The cardiovascular system includes the heart, blood and blood vessels. The heart is a highly vascularised organ that weighs an average of 300-350 grams and contains 120 millilitres of blood in adult humans. It is well protected as it is flanked by the ribcage and protected by the breastbone, lungs, diaphragm and pericardium. The heart is essentially a muscle that pumps oxygenated or deoxygenated blood around the body including the lungs. The heart is formed by four chambers and four valves. Superior chambers are called atria and the inferior, ventricles (Figure 1-1). The muscle of the ventricle walls is thicker than those of the atria because of the high pressures required to be generated. The heart is not only a pump but also an endocrine organ: the myocardium has a stock of active natriuretic peptides (polypeptide hormones) that are released

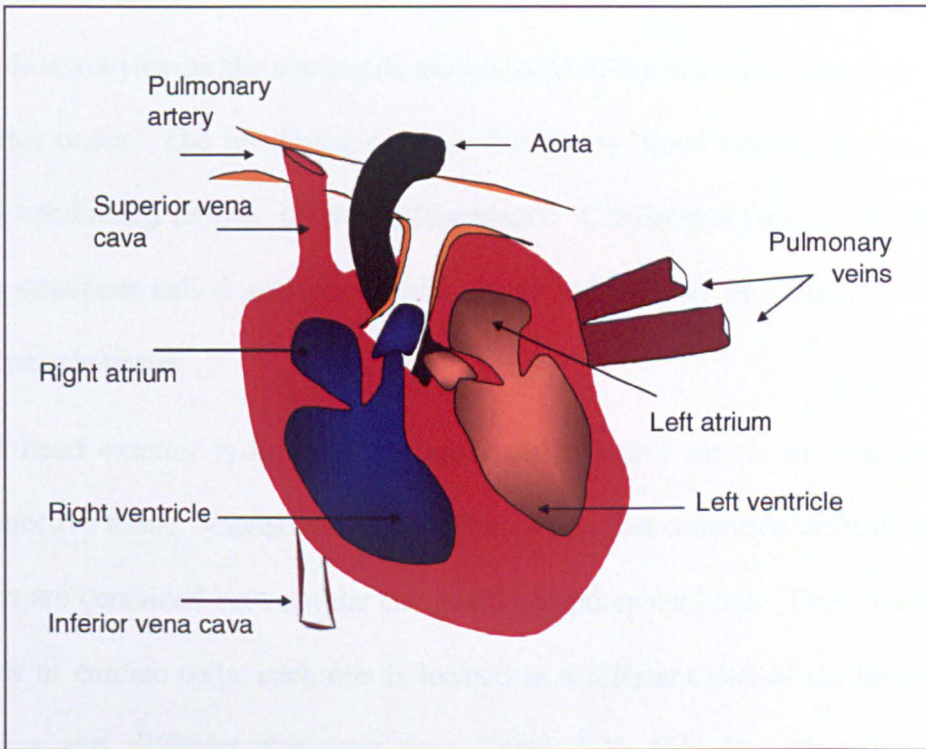


Figure 1-1 Diagram of the heart anatomy adapted from [5]

during stretching of the atria and increased serum levels indicate cardiac hypertrophy [5].

### **Cellular Structure**

Cardiomyocytes are the contractile muscle cells of the heart and constitute 75% of this organ. The remaining organ is formed by blood vessels, pacemakers and conducting tissues, including fibroblasts. Cardiomyocytes are organised into structures called myofibres which are bound together by collagen to form the muscle tissue.

The heart exterior is lined by epicardial cells over a matrix of fibro-elastic connective tissue, whereas the myocardium fibres that constitute the wall of the heart are contained between the endocardium and epicardium. There are three types of cardiac cells; each one is located in a different part of the heart and carries out different functions (see Table 1-1) [5]. The electrical and mechanical connection between cardiac cells is completed by intercalated disks. These cell-to-cell junctions are specialised and depending on each function, express different proteins (see Table 1-2).

#### **1.2.1.a.1 Cardiomyocytes**

Cardiomyocytes (Figure 1-2) have an average diameter of 10-20  $\mu\text{m}$ , length of 50-100  $\mu\text{m}$  and a single central nucleus. Each cell contains 100-150 thin sarcomere myofibrils composed of seven major proteins arranged in thin and thick filaments of actin, myosin heavy and light chains (MHC, MLC), tropomyosin and troponin proteins. The interaction of the myosin and actin that

CELL	LOCATION	FUNCTION
Myocytes	Atria and ventricles	Contraction
Purkinje fibres	Atrioventricular (AV) bundle, branches and ventricular endocardium.	Rapid conduction with intercalated disks
Nodal cells	Sinoatrial (SA) & AV nodes	Pacemaker activity and atrioventricular conduction

**Table 1-1 Location and function of the different types of cells present in the heart [5]**

JUNCTION	FUNCTION	PROTEIN
Gap	Electrical communication	Connexin 43 (Cx43)
Fascia adherence	Mechanical linkage	Actin and $\alpha$ -actin
Desmosome	Electrical communication	Desmin

**Table 1-2 Function and protein involved in typical cardiac junctions [5]**

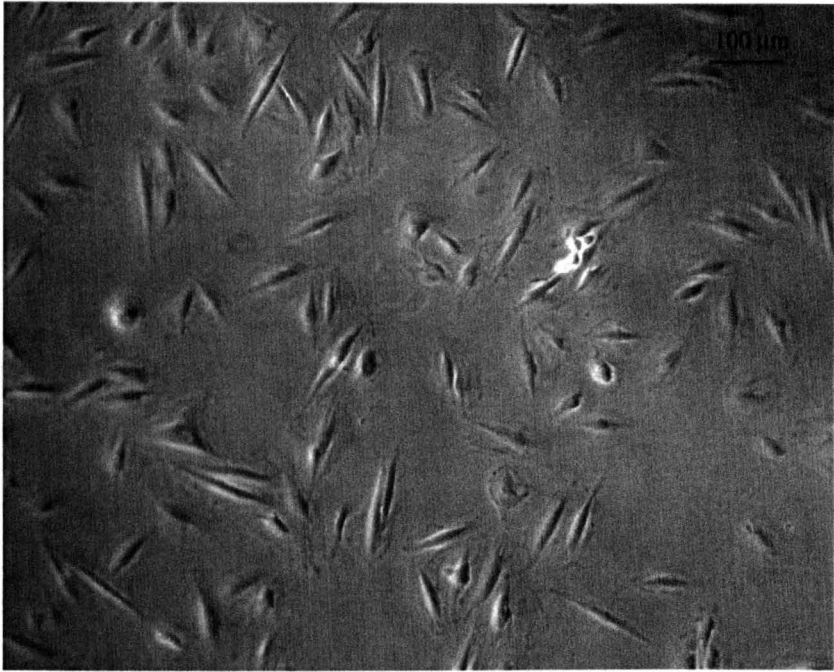


**Figure 1-2 Phase contrast image of HL-1 cardiomyocytes at lower magnification (10x) shows phenotypical elongated morphology**

induces contraction is controlled by the intracellular calcium concentration. The orientation of the myofibrils is important for the conduction of the electrical wave. Around the left ventricle (LV) the myofibrils are arranged in a circumferential direction whilst the myofibrils within the other regions of the heart are arranged in a longitudinal orientation. The shortening of these myofibrils result in the contraction of heart chambers. Cardiomyocytes differ depending on if they are ventricular or atrial. As reported above, substantial differences lie between ventricular and atrial structure and functions; atrial and ventricular myocyte characteristics are reported in Table 1-3 [5].

#### **1.2.1.a.2 Electrical Coupling and Contraction**

Electrical coupling occurs via a calcium biochemical pathway. Calcium-Induced, Calcium-Released (CICR) channels transport the calcium influx. High levels of intra-cellular calcium induce myosin-actin contact, decreasing sarcomere length and producing a contraction. This transport requires energy, which is supplied by adenosine tri-phosphate (ATP) molecules. When calcium returns to the sarcoplasmic reticulum it triggers a sodium-calcium channel that decreases calcium levels resulting in myocardial relaxation. The contractile process is mainly controlled by the proteins myosin, actin, tropomyosin and troponin C, I and T [6]. Diastole and systole are common terms in the medical field, the first is related to cardiac relaxation and the second one to cardiac contraction [7,8].

CHARACTERISTIC	VENTRICULAR MYOCYTES	ATRIAL MYOCYTES
Shape	Long and narrow	Elliptical
Length (μm)	50-100	About 20
Diameter (μm)	10-25	5-6
T tubules	Plentiful	Rare or none
Intercalated disk and gap junction	Prominent end-to-end transmission	Side-to-side and end-to-end transmission
General appearance	Mitochondria and sarcomeres, very abundant; rectangular bundles with little interstitial collagen	Bundles of atrial tissue separated by wide areas of collagen

**Table 1-3 Comparison of characteristics between atrial and ventricular cardiomyocytes**  
[5]

Heart contraction is due to electrical impulses generated and conducted along the muscle. The sequence of these events determines the normal behaviour of the heart. The electrical signal is activated spontaneously; some zones are polarised whilst others depolarised. The waves are propagated first to the right atrium, then to the left atrium, and after that to the ventricles.

### **1.2.2 Diseases**

The most common heart disease is heart failure which denotes a weak contractile function of the heart because of a blocked vessel. This blockage decreases the pump ability and therefore the oxygen supply to the body, including the heart. This leads to a myocardial infarction which is the death of part of the cardiac muscle because of this lack of oxygen [4].

Other less common diseases are endocarditis or inflammation of the inside of the heart cavities or heart valves, and congenital heart diseases (CHD), caused by abnormal heart development during pregnancy, that affects the structure and function of the heart.

In order to gain an accurate diagnosis, multiple tests must be performed on each patient, such as physical examination (irregular heartbeat, heart sounds, breath sounds), coronary angiography, echocardiogram, chest X-ray, chest computed tomography (CT) scan, electrocardiogram (ECG), heart biopsy and lab tests (complete blood count, coronary risk profile, blood chemistries and cardiac enzymes), because of the wide range of symptoms. These diagnostic tests as well as the therapy result in a high cost to the health services, moreover

the low long-term effectiveness of these therapies represents a national health issue [4].

### **1.3 Cardiac Regeneration & Treatments**

#### **1.3.1 The Challenge of Cardiac Regeneration**

Researchers believe that cell regeneration will vary depending on the type of cellular death. Necrosis induces an inflammatory response, collagen deposition for scar tissue and fibroblast activation whilst apoptosis does not [9]. Adult mammalian cardiac tissue cannot regenerate. Cardiomyocyte proliferation starts decreasing from birth and they are not able to re-enter the cell cycle again after an injury [10]. After cardiomyocyte death, non contractile scar tissue (formed of collagen fibrils) replaces the cardiac muscle along with hardening of the damaged myocardium. This initial damage and subsequent remodelling of the heart tissue starts with chained cellular events that lead to heart failure. This failure is caused by the inability of the organ to pump blood with a normal cardiac output and therefore fulfil the body's requirements of nutrients and oxygen [11]. Some researchers have reported spontaneous cardiac regeneration after a myocardial infarction carried out by myofibroblasts. However, these fibroblast-like contractile cells do not achieve total regeneration of the damaged tissue [12, 13]. For a functional recovery after ischemia, there is a need to incorporate functional cardiomyocytes and paracrine factors. This will cue the repair mechanism, limit the scar tissue and improve the vascularisation through angiogenesis, inducing the formation of new capillaries and vessels [14].

### **1.3.2 Available Treatments**

The treatments for heart disease depend on several factors: cause, age, risks and the clinical history of each patient. Available treatments include medication, dietary and lifestyle changes, and surgery. However, current treatments are not effective for more than 2 years and only delay progression and congestive failure in most cases [4]. Cardiac transplantation, the best therapy available, is restricted by the shortage of donors, the risk of tissue rejection, infection and pathogen transfer, and the high cost of the complex long-term intensive care.

Recent research has concentrated on three main strategies: cellular transplantation, tissue replacement and tissue regeneration. Cardiomyoplasty could potentially improve outcomes both in terms of morbidity and mortality. This therapy involves transplanting different kind of cells and tissues into the affected zone [15]. Strategies for this repopulation include direct transplantation of cells, mobilisation of endogenous stem cells to the damaged area and initiation of the cardiomyocyte cell cycle in the surviving cells. In cellular cardiomyoplasty, different sources of cells have been tried in order to improve heart performance following infarction [16]. These include primary cells such as adult cardiomyocytes, smooth muscle cells, skeletal myoblasts and fibroblasts. Stem cells are a novel source that includes specific adult stem cells (SC), mesenchymal or bone-marrow stem cells (MSC), circulating or haematopoietic stem cells (HSC) and embryonic stem cells (ESC). In the case of the latter, some concerns have arisen regarding the risk of ES-derived tumours and arrhythmias following transplantation [17].

The most important characteristic for a suitable cell type for cellular therapies is the ability to differentiate into a specific and functional cardiac cell but also to couple physically, as well as electrically, to the host tissue in order to develop synchronic contractions. Research in cardiac muscle repair has been focused on two alternatives, cellular transplantation and cardiac tissue engineered grafts. In the last ten years several pre-clinical and clinical phase I and II trials of cell transplantation have been conducted in cardiac patients, including direct injection or percutaneous application of myoblasts derived from skeletal muscle satellite cells, stem cell-derived cardiomyocytes, skeletal ventricle muscle and tissular wraps [18]. Most of the reports, generated from European and American studies, indicate that cellular cardiomyoplasty is an easy and effective therapy for cardiac failure [19]. Some researchers have started phase I clinical trials to show the feasibility of intracardiac autologous skeletal myoblast implantation in humans with good results. Clinical data showed an improvement in the contractile function when the transplantation was combined with a bypass procedure [20]. Food and Drugs Administration (FDA) approval has been granted to Bioheart Inc. to practice this therapy. More than 450 patients have taken this option without further complications although long-term results are still missing to determine its complete success[21].

Tissular cardiomyoplasties have not been assessed to the same extent as cellular. The main limitation is the limited range of patients suitable for this procedure, mainly in early stages of CHF [22].

Tissue regeneration aims to prompt biochemical and physical signals to induce the heart to self-regenerate the damaged areas. This approach still requires further understanding of cardiac signalling pathway and gene expression [23].

#### **1.4 Tissue Engineering**

Tissue engineering was defined as a science in its own right when Vacanti and Langer published their results in *Science* in 1993 [24]. Among the several definitions, the National Science Foundation defines it as “the application of the basis and methods of engineering and life sciences toward tissue development of biological substitutes to restore, maintain or improve functions” [25]. Regenerative medicine undertakes tissue/organ restoration with three main strategies: cell transplantation, bioartificial tissues and regeneration *in situ* [26]. Tissue engineering deals mainly with bioartificial tissues although some strategies also contribute with alternative plans to regenerate damaged tissue *in situ*.

Many research groups are working on tissue regeneration as well as in repair, by combining engineering, materials and medical technology looking for a guided remodelling of the damaged tissue (Table 1-4). This interdisciplinary science started with bone, cartilage and skin, but currently recent projects have extended this work to more complex tissues such as liver, nerve, gut, pancreas and cardiovascular regeneration.

Cardiac tissue engineering research groups are looking into novel systems which combine different sources of proliferative and differentiated cells as well as novel biomaterials. The focus is on the development of alternative grafts.

REPAIR	Rapid replacement of the damaged, defective, or lost tissue with functional new tissue that resembles, but does not replicate the structure, composition, and function of the native tissue
REGENERATION	Slow restoration of all components of the repair tissue to their original condition such as the new tissue is indistinguishable from normal tissue with respect to structure, composition and functional properties
REMODELLING	Change in tissue structure and composition in response to the local and systemic environmental factors that alter the functional tissue properties

**Table 1-4 Tissue healing models [29]**

These groups also research into suitable environments that encourage rapid cell proliferation and full functionality as well as supporting integration to the surrounding host tissue [27, 28].

#### **1.4.1 Cells for *in vitro* development of cardiac muscle**

Cells used for tissue engineering purposes should be highly proliferative in the early stages for rapid propagation as well as being capable of differentiating to become functional. Recently cardiomyocyte precursor cells were fully established *in vitro*, but before that, a number of different cardiac muscle cell lines were used to develop *in vitro* models of tissue engineering constructs [29]. Although primary cardiac cells remain the main source for cardiac models, availability in large quantities was the main concern for this project. The cell line HL-1 was used as a model to assess biological properties of this novel polymer due to its previous reports as a suitable cardiac model. When cultured under certain conditions this cell line, isolated from mouse tissue, presents a unique property of spontaneous beating and exhibits typical cardiomyocyte morphology. HL-1 cells express most of the cardiac specific proteins such as atrial natriuretic factor, actin, desmin, tropomyosin, Cx43 and myosin heavy chain as well as specific receptors and cardiac electrophysical properties. This cell line is now used as a model cell type for cardiac tissue engineering and to study the effects of drugs on cardiac tissue [30-32].

Cell sources differ when working with *in vitro* systems for research and when developing a graft for clinical applications. Whereas animal cell lines are used for laboratory research, the options for clinical implants are extensive.

Depending on the source, cells may be autogenic (from the patient), allogenic (from the same species) or xenogeneic (from different species). Although the first type is the only one not to elicit rejection without the need of immunosuppressive therapy, the others can be expanded *in vitro* and stored in advance.

As mentioned earlier, stem cells have been suggested as an alternative source of cardiomyocytes; these cells can be embryonic, foetal, neonatal or adult. Availability of foetal and neonatal cells is limited and therefore investigations have concentrated with embryonic and adult stem cell sources. Only recently three cardiac stem cell lines have been reported, all with different levels of cardiac differentiation and protein expression [26].

#### **1.4.2 Biomaterials**

Biomaterials are either synthetic or natural materials used for different applications but aimed to interact with biological systems. Biomaterials are mainly used in medical applications such as implants and surgical aids. However they are also used for other purposes such as *in vitro* cellular studies. These materials include metals, ceramics and polymers. It is also common to combine two or more of these materials to obtain a new material aiming to obtain a composite with better properties than the individual materials [33].

##### **Metals**

Metals are inorganic biomaterials which are generally used as alloys due to their improved properties. Iron, cobalt, chrome, titanium, aluminium,

vanadium, nickel and molybdenum are some of the metallic elements used in modern alloys. The use of these materials in the clinic started when surgeons realised the ability of the human body to keep metallic materials within the body without apparent reaction. Current applications range from dental fillings to orthopaedic use [34].

The main advantage of metallic biomaterials is their mechanical properties, which in general are better for large replacements of hard tissue because of their hardness and resistance to wear and tear. However, these materials do fatigue and issues of their susceptibility to corrosion limit their use; nevertheless these properties can be tailored by adjusting the alloy components to obtain more elastic materials, compatible with a wider range of applications. Metals impede any biological response because of their inorganic nature but by modifying the contact area it is possible to promote a positive reaction from the host environment [35].

### **Ceramics**

Ceramics are inorganic materials constituted by metallic and non-metallic elements bonded by ionic and covalent bonds. Ceramics are catalogued as excellent thermal and electrical isolators as well as possessing resistant to wear even under extreme conditions. These properties make ceramics good biomaterials for implants. The most common ceramics are alumina (Aluminium Oxide), hydroxyapatite and vitro-ceramics (bio-glass), used mainly in bone tissue regeneration. Ceramics are brittle materials also used to repair joints and teeth. Components in the ceramics determine their properties and biological activity; depending on these, ceramics can be classified as inert,

bioactive, or resorbable. The first do not interact at all with the host whereas the second adhere to the tissue. Resorbable ceramics are those intended to be disintegrated and absorbed in the body at the same rate of the new growing tissue [36].

## **Polymers**

Polymers are defined as large, complex compounds formed by any kind of repeated units joined by covalent bonds in a specific spatial arrangement. Polymeric materials can be either inorganic or organic, depending on their carbon content. The inorganic polymers include natural (clays and sands) and synthetic compounds. Polysaccharides and proteins are natural organic polymers, while adhesives, fibres, coatings, plastics and rubbers are synthetic organic polymers [37, 38]. Polymers can be long unbranched, branched or crosslinked chains of repetitive units, or monomers. This structure determines polymer characteristics and therefore the possible applications. Polymers are extensively used not only for medical applications but also in different manufacturing processes in the pharmaceutical, chemical, food, aerospace and automotive industry among others. Table 1.5 summarises the most common polymers in regenerative medicine and their use.

Polymers can also be classified as thermoplastic and thermoset. Thermoplastic polymers are mainly linear polymers that can be modified by heat and pressure whereas thermoset are usually crosslinked-polymers and cannot be re-shaped once they are polymerised. The crystallinity of polymers establishes their behaviour in a thermal environment. Pure crystalline polymers behave as

	EXAMPLES	USE
<b>Synthetic polymers</b>		
Biodegradable	Polyesters (PLLA, PGA, PGLA, PCL)	Biomedical applications, surgical sutures, scaffolds
	Polyurethanes (PU)	Catheters
	Silicones	Implants, facial devices
	Polypropylene (PP)	Sutures, heart valves, finger joints
Non-Biodegradable	Polyethylene (PE)	Artificial arteries, contact lenses
	Poly(ethylene glycol) (PEG)	Hydrogels, drug delivery
	Poly(hydroxyethyl methacrylate) (PHEMA)	Lenses, sutures
<b>Natural polymers (also suitable for hydrogels)</b>		
Proteins	Collagen, gelatine, fibrinogen, albumin, polypeptides	Ligaments, scaffolds, wound healing
Polysaccharides	Hyaluronic acid, alginate, chitosan, chitin, chondroitin	Scaffolds, cell immobilisation and encapsulation, wound healing

**Table 1-5 Synthetic and natural polymers with medical applications [37-39]**

glasses below their glass transition temperature ( $T_g$ ) and as elastomers above it. On the other hand, semi-crystalline polymers have limited mechanical properties and gas/water permeability.

Copolymers are a mixture of two polymers, commonly bifunctional units. When at least one of the monomer units has two or more binding sites, it can bind to two other monomers and cross-links are formed between the different polymer chains, obtaining a single networked molecule with different physical properties.

Elastomers are polymers that can be stretched several times and return to its original shape without permanent deformation; this characteristic is improved when the polymer has been crosslinked. Some elastomers have been used for tissue engineering applications due to their flexible physical profile. Elastomeric scaffolds are suitable for muscle, cartilage and bone culture since it has been shown that tissues maintain better characteristics when cultured under physical stimuli such as stress, compression or stretch.

Optimal monomers for copolymer scaffolds are still to be determined, but natural compounds commonly found in the cell may be useful. Organic acids have been combined with other synthetic materials to obtain a non-toxic copolymer with beneficial effects on tissue culture [39]. Citric acid and 1,8-octanediol were chosen as the monomeric units of a novel copolymer because of their characteristics, as shown in Table 1-6.

	CITRIC ACID	1,8 OCTANEDIOL
Molecular Formula	C <sub>6</sub> H <sub>8</sub> O <sub>7</sub>	C <sub>8</sub> H <sub>18</sub> O <sub>2</sub>
Molecular Weight	192.14	149.23
Melting Point	153-154°C	59-61°C
Boiling Point	Decomposes at 175°C	172°C
Solubility in Water	59.2%	-
Autoignition	1011°C	270°C
Flash Point	100°C	148°C

**Table 1-6 Physical properties of citric acid and 1,8-octanediol [39]**

#### **1.4.2.a.1 Poly-(1,8-octanediol-co-citric acid)**

Poly-(1,8-octanediol-co-citric acid) [POC] is a copolymer suitable for tissue engineering applications as recently reported by Yang and colleagues [40]. This copolymer is formed by condensation and subsequent crosslinking of two monomers: citric acid and 1,8-octanediol.

Citric acid is a colourless crystalline organic compound that can be found in vegetal and animal tissues and fluids and is involved in the Krebs cycle. Citric acid is used in the food industry as flavouring, stabilising agent, preservative or acidulant. This acid is also used in the pharmaceutical and cosmetic industry and in industrial and chemical processing [41].

The chemical 1,8-octanediol is a white crystalline powder commonly used as an intermediate in polymer synthesis because of its two primary hydroxyl groups at terminal locations. This alcohol has other uses in oil refining and in pharmaceutical manufacturing [41]. The polymerisation process of citric acid and 1,8-octanediol to form the copolymer poly-(1,8-octanediol-co-citric acid) is shown in Figure 1-3.

#### **Composites**

Composites are hybrid compounds formed by two or more natural and/or synthetic materials. The blending of different materials allows the targeting of particular characteristics of interest for specific applications. These combinations offer improved mechanical properties and biocompatibility. However not all composites are perfect biomaterials, their mixed composition

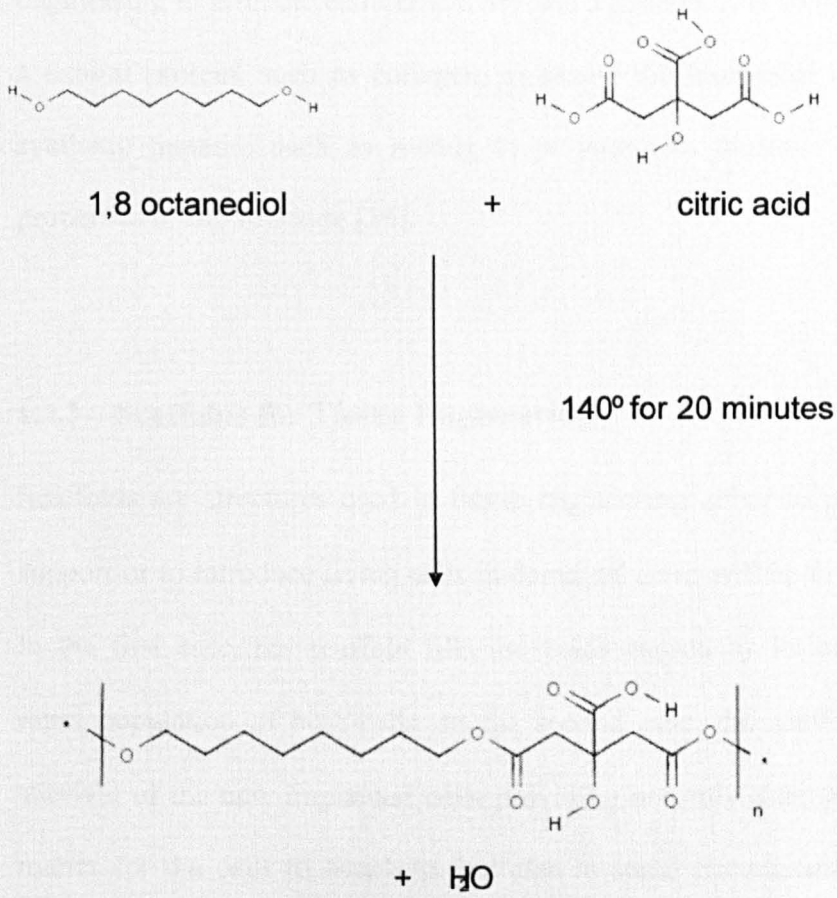


Figure 1-3 Oligomerisation of citric acid and 1,8-octanediol

can make them liable to fractures and cracks, damaging the structure and risking the failure of the construct. Composites have been used in tissue engineering to promote cellular activity and adhesion. It is common to combine a natural protein, such as collagen, to assure the biological response with a synthetic material such as metals or polymers to improve the mechanical properties of the structure [36].

### **1.4.3 Scaffolds for Tissue Engineering**

Scaffolds are structures used in tissue engineering either to provide physical support or to introduce living cells in damaged areas within an organ or tissue. In the first case, the scaffold fills the voids caused by lesions, encouraging rapid population of host cells. In the second case, the scaffold sustains the survival of the new implanted cells providing not only a template of physical matrix for the cells to attach to, but also in some circumstances biochemical factors; this assures their survival and promotes biological responses to encourage the regenerative process within the host. In order to be suitable for tissue engineering applications, scaffolds must meet certain characteristics such as biodegradability, biocompatibility and micro and macrostructure suitable for the cell type and tissue (Table 1-7) [42-44].

Biodegradability levels vary on the specific application of the biomaterial. In certain applications a biomaterial may be required to remain for years without any degradation to substitute tissue loss. However another tissue engineering approach is to provide a temporal support by filling the void and then promote the healing so that the new repaired tissue will be entirely from the host and

Biocompatibility	Non-toxic material
	Surface modified to enhance cell attachment
	Elicit minor or non-immunological/inflammatory response
Biodegradability	Degradation ratio should match removal and tissue regeneration ratio
Macro and micro Structure	Optimum pore size, porosity and interconnectivity
	Must provide a three-dimensional template and ideally should present organised pores to orientate cell attachment
	Must match the mechanical properties of the native tissue

**Table 1-7 Description of the key characteristics in scaffolds design [40-41]**

any residue of the biomaterial will be absorbed and disposed of [45]. Considering this, it is important to control the degradation rate of the material depending on the rate of tissue repair, but also on the rate of degradation product removal in order to decrease undesired host responses. If the degradation is too rapid, this could overwhelm the system and cause graft rejection or failure due to a massive immune response. Degradation products of synthetic materials can be a problem as local pH decreases and prompts a biological reaction [46]. Bio-absorbable materials assure that secondary residues will be discarded through cellular metabolic pathways. Knowing the cellular mechanisms and repair time of the target area defines the biomaterial that can be used. Currently it is possible to vary degradation rates for most of the biomaterials by altering their structure via physical or chemical modifications, such as crosslinking [47]. Biocompatibility concerns the biological response that the biomaterial could trigger in the host. It is important to keep the immunological response to a minimum level so no significant or prolonged reaction is caused and therefore the risk of rejection is reduced. This is a major issue as immunological rejection is one of the main causes of transplantation failure. Biocompatibility can be modified by introducing cells with minor or non antigen recognition such as stem cells or the own patient's cells. Rapid degradation rates can also affect bio-compatibility as discussed earlier. It is vital to use a material that will promote cellular attachment and proliferation in the construct speeding up the remodelling of the area. As synthetic materials do not express natural recognition molecules, tissue engineers frequently use either a combination of natural and synthetic

materials. Another strategy is to chemically modify surfaces to improve cell attachment, proliferation and differentiation to the biomaterial [48].

The structure of a scaffold is defined by the porosity, pore size, interconnectivity of the pores, mechanical properties and the feasibility of processing large amounts in specific shapes and dimensions. Porosity represents the percentage of void spaces within the scaffold. Levels of 60% - 99% porous allow the cells to rapidly populate throughout the scaffold. Pore size is important as pores <100 microns could block the movement or differentiation of cells, whereas pores > 300-500 microns could isolate cells within confined areas and reduce the population expansion pace [49]. Interconnectivity allows the cells to move around the scaffold and to communicate between them by chemical /mechanical /electrical ways. Open porous interconnected structures will facilitate vascularisation and nutrients transport ensuring that not only peripheral cells will survive but also that central cells will be provided with oxygen and nutrients. With cardiomyocytes highly susceptible to ischemia, a porous scaffold could provide increased levels of oxygen and nutrients, as well as different degradation profile and mechanical properties to those of cell sheets. Mechanical properties of biomaterials allow the scaffold to support tissue growth. Hard, inelastic scaffolds are used in applications such as bone regeneration, whereas materials with flexible properties are required for soft tissues such as cartilage and cardiovascular grafts. Tissue engineers have tried to match the mechanical properties of the target tissue to provide a closer match of the artificial graft. Properties such as elasticity, maximum elongation without deformation, force to break and stability are important to characterise a scaffold. It is also

important that the scaffold can be produced in a shape and dimensions that will suit the target tissue. All these characteristics are related and in most of the cases if one is modified at least one other factor will be as well [43]. Currently the most common scaffolds used in tissue engineering are natural polymers such as collagen, alginate and glycosaminoglycan; synthetic polymers such as PLA and PLGA and hydroxyapatite and calcium phosphates ceramics [44].

### **Scaffold Fabrication**

Biomaterials can be processed through different methods to obtain porous structures. Although they offer several advantages, few of these methods are able to control internal structure and homogeneity. New tactics provide a better control of macro and microstructure; yet most of the cases are limited to certain types of biomaterials. The most common approaches to process biomaterials into porous scaffolds are summarised in Table 1-8.

#### **1.4.3.a.1 Solvent Casting and Particulate Leaching (SCPL)**

This method allows the processing of solid biomaterials, soluble in a range of organic solvents, through the incorporation of porogen particles throughout the polymer. Solvent and then porogen are removed to leave a porous structure in the shape of a mould. Porogens used in SCPL include inorganic salts such as NaCl and organic crystals such as glucose. The benefits of this technique include a controlled pore size and porosity and are controlled by the quantity and size of the porogen. Unfortunately structures processed by SCPL cannot be thicker than a couple of millimetres due to the inability to control large

Fabrication Method	Advantages	Limitations
Solvent Casting & Particulate Leaching (SCPL)	High and controlled porosity, crystallinity, pore size, shape and dimensions can be tailored, independent control of porosity and pore size	Limited thickness up to 3 mm, solvent and porogen residues, limited interconnectivity, poor control of internal structure
Phase Separation	Highly porous and interconnected structures, non-compromised activity of biological molecules	Limited to small pore sizes, solvent residues
Fibre bonding	High porosity	Limited range of polymers, mechanical properties mostly suitable for soft tissue applications
Rapid prototyping (Computer Assisted Design/Manufacture)	Three-dimensional matrix, control of macrostructure, independent control of pore size and porosity	Solvent residues, mechanical properties suitable mostly for soft tissue applications, limited interconnectivity
Gas Foaming (High Pressure scCO <sub>2</sub> )	No organic solvents involved	Mostly non porous external surface, low interconnectivity, limited to polymers soluble in supercritical gases
Electro spinning	High porosity, high surface-area-to-volume ratio	Limited to soluble polymers with certain viscosity and conductivity, wide distribution of pore diameter

**Table 1-8 Standard techniques for biomaterial processing into porous scaffolds [33, 41, 50-57]**

structures homogeneously, In addition to the difficulty of manipulating the interconnectivity of the pores or their orientation. The major drawback is that the organic solvent cannot be completely removed and residues could result in cellular toxicity [50-51].

#### **1.4.3.a.2 Phase Separation**

Phase separation is a thermally induced separation of an emulsion formed by a material dissolved in an organic solvent and water. This emulsion is cast in a mould and rapidly frozen and then freeze-dried, or cooled down and vacuum dried so the water and solvent are removed from the emulsion leaving a porous structure. Although these methods are less time consuming than SCPL, porosity nor pore size cannot be controlled and still requires the use of an organic solvent [33].

#### **1.4.3.a.3 Fibre Bonding**

This method uses individual polymer fibres to prepare either knitted or woven 3D structures. Although it generates scaffolds with high porosity values, disadvantages include the difficulty of producing a controlled pore size and the use of solvents and high temperatures. It is difficult to incorporate bioactive molecules and to produce large amounts in a short period of time [52-53].

#### **1.4.3.a.4 Rapid prototyping**

This method, also known as solid free-form fabrication (SFF), is based on structuring layers of biomaterial to engineer a 3D scaffold aided by computer-controlled systems. This technique, used first to model biological structures, provides scaffolds with a defined porosity, interconnectivity, pore size, microstructure and mechanical properties. Current strategies include fuse deposition modelling, stereo lithography (SLA), selective laser sintering, ballistic particle manufacturing and 3D printing [33].

#### **1.4.3.a.5 Gas foaming (super critical CO<sub>2</sub>)**

Carbon Dioxide (CO<sub>2</sub>) is a non-flammable and virtually inert compound that changes into a supercritical phase when it is pressurised and heated to its critical pressure and temperature (1,070 psi and 31°C). In this phase its physical properties are both those of liquid and gas phases, including a lower surface tension than liquids (allowing spreading out along a surface) and the ability to act as a powerful solvent. Once the scCO<sub>2</sub> is dissolved in a material, the release of pressure at a high rate entraps the CO<sub>2</sub> in the material forming bubbles and makes the compound foam when the CO<sub>2</sub> returns to the gaseous phase. This technology is non-toxic, friendly to biological systems, recyclable, and easily scalable [41, 54-56].

scCO<sub>2</sub> technology has been suggested as an effective method to engineer solvent-free biomaterials, such as polymers, which can be foamed to obtain porous scaffolds for biomedical applications [55]. Barry *et al* demonstrated that non-degradable polymer systems can be foamed into highly porous scaffolds with a large percentage of open pores using the scCO<sub>2</sub> process, and that this modification in the structure supports cell culture *in vitro* [57].

#### **1.4.3.a.6 Electrospinning**

This method produces interconnected webs of microfibres, from microns to nanometres, of natural or synthetic polymers creating a high porous scaffold with high surface-area-to-volume ratio and a wide distribution in the pore size. The principle of this technique is to pass a polymer solution through a high-voltage electrostatic field so the solution is ejected due to the surface tension forces. The solvent evaporates and the polymer is left into stretched fibres. The characteristics of these electro-spun scaffolds are defined by the operational parameters of the technique: flow rate, distance between the tip and the collector and applied electric potential.

Although this method produces scaffolds similar to ECM structures, the polymer solutions suitable for this approach are limited by fluid properties such as conductivity, viscosity, dielectric constant, surface tension and boiling point [33].

#### **State of the art of scaffolds for cardiac muscle**

An initial challenge of generating an engineered cardiac patch is the development of the ideal biomaterial for cardiomyocyte culture. Researchers have proposed both synthetic and natural materials to generate a suitable cardiac graft. Bursac *et al.* assessed a 3D spinner flask culture of primary rat heart cells seeded into poly-(glycolic acid) (PGA) fibres. Their results showed that they were able to generate a functional construct within the first 3 days, including normal protein expression of cardiac and muscle markers such as tropomyosin and actin, cell-to-cell connections and spontaneous contractions but this activity decreased in the following 4 days (day 4-7) [58].

Studies not only involving the physical properties of a biomaterial but also its biochemistry have generated useful information. Novel approaches to form a 3D construct have been suggested. Shimizu *et al* used a temperature-responsive polymer to pre-coat culture dishes. Cardiomyocytes were seeded into these plates and once a monolayer was formed, the temperature was decreased to 20° C to detach the cells and the monolayer was placed on top of another cardiomyocyte monolayer and cultured further. Both layers integrated and resulted in a functional culture with cell-to-cell connections between them [59]. McDevitt *et al* cultured cardiomyocytes on a biodegradable, elastomeric polyurethane film. This material, used as a scaffold, allowed the development of spatially organised layers of cardiomyocytes *in vitro*. Biodegradable elastomeric polymeric materials as well as hydrogels are suitable because of their mechanical properties that meet the force-generating demands of the contractile tissue. These segmented polyurethane elastomers were synthesised with the use of a lysine-based diisocyanate, polycaprolactone and a phenylalanine chain extender. The morphology, stability and differentiation of the culture was similar to those cultured on non-elastomeric polystyrene or glass [23]. The use of elastomers to process porous scaffolds has been limited due to their lack of biodegradability.

Natural polymers have been used for cardiovascular engineering. Sodian *et al* reported that poly-(hydroxyalkanoate) (PHA) is a useful material for cardiovascular engineering. This bacterial-derived polymer is thermoplastic and can be moulded into almost any shape. For example, in cardiac valve engineering, this polymer showed high elasticity and mechanical strength appropriate for this application [60].

Polonchuk *et al* tried a novel approach for cardiomyocyte culture. Titanium dioxide ceramics were used as this material mimics cell surface topography and promotes vinculin expression, a protein that defines cell shape. This molecular stabilisation maintained the cardiomyocyte differentiated phenotype for nine days [61].

Another innovative method is the one published by Shin *et al*. They fabricated a nanofibrous mesh of polycaprolactone by electrospinning and seeded it with neonatal rat cardiomyocytes. After culturing these under static conditions, contractile constructs were obtained with more accurate cardiac protein expression and good cellular attachment [62].

Schmidt *et al* believe that synthetic materials should not be used as scaffolds because of the residual cellular components and undesired effects such as calcification and immunological recognition. Natural sources are suitable for cardiovascular remodelling but cross-linking is needed for mechanical compliance [63]. An example is the work reported by Qing Ye *et al* using fibrin gels. They found that these were suitable for 3D engineered structures because of the lack of toxic degradation or inflammatory responses that is seen with synthetic materials [64].

Collagen scaffolds are commonly used for tissue engineering. Kim *et al* demonstrated its elastic properties during cyclic strain. They also assessed elastin content on smooth muscle cell culture and found higher levels than those cultured in PGA. Elastin is important due to its role in the regulation of proliferation and organisation of cells [65]. Costa *et al* reported that the culture of cardiomyocytes in collagen showed normal mechanical and electrical behaviour. They exposed the collagen system to tension by clamping two

ends of the gel to a stretch device to assess the effect on the alignment of the cells. The results confirmed that the gel orientation is parallel to free boundaries rather than to lines of tension, and independent to the geometry of the construct [66]. However other results have shown that collagen exhibited limited mechanical properties and batch-to-batch variation [67] and Radisic and Vunjak-Novakovic stated that collagen is not a candidate for cardiac scaffolds because of its “poor structural integrity” [68].

Three-dimensional scaffolds have been produced as well as 2D. Evans *et al* have worked on the development of a novel model to obtain a better understanding of cardiomyocyte differentiation. The system is a 3D tubular scaffold made from aligned type I collagen strands that appeared to induce a switch in the cellular growth from a hyperplastic to a quiescent phenotype. The authors also concluded that the system promoted myofibrillogenesis as well as cell-to-cell connections. Moreover the constructs showed an aligned phenotype along the tube [69].

Collagen-based scaffolds have been combined with other materials. Radisic *et al* worked on the hypothesis that a rapid gel-seeding with media perfusion would improve the rate, yield, viability and uniformity of cell seeding. Neonatal rat cardiomyocytes and the c2c12 cell line were seeded in collagen sponges, with Matrigel as the vehicle, in either perfusion cartridges or in orbitally mixed Petri dishes. Results showed that cell viability was higher in perfusion cartridges than in mixed dishes. Perfusion conditions encouraged spatial cell distribution as well as proliferation and differentiation, confirmed by synchronous contractions of constructs under electrical stimulation [70].

Kofidis *et al* built a bioartificial myocardial tissue by seeding neonatal rat cardiomyocytes in a novel scaffold, a bovine collagen type I-based matrix that has been used as a hemostaticum (patches used to stop bleeding) in surgery. This “tissue fleece” patch has a similar elasticity curve to that of the myocardium and supported contractile grafts with normal cardiac protein expression for 12 weeks [71].

Alginate has also been used in several studies. Dar *et al* used porous alginate scaffolds to seed cardiomyocytes and obtain 3D high cell density constructs with a uniform distribution. The centrifugal force applied during the seeding allowed a uniform cell distribution throughout the alginate scaffold. Although the seeded cellular density was high the cardiomyocytes did not differentiate in this system [72].

Surface modifications are also used to improve the rate of cell binding to the biomaterial. Hubbell *et al* have conjugated growth factors and peptide sequences namely RGD from fibronectin and YIGSR from laminin on a collagen matrix via a polyethyleneglycol (PEG) spacer. This technique allowed a better attachment of cells to the surface [73]. Zisch *et al* worked with a vascular endothelial growth factor (VEGF)-modified fibrin injectable matrix that gels under physiological conditions in a single-step reaction. It has been proposed that this matrix could be used for multiple clinical applications such as an angiogenic response inducer in ischemic regions or implants [74]. These works are summarised in table 1.9.

PAPADAKI <i>ET AL.</i>	Cardiomyocytes in both spinner flasks and rotating vessels. Results showed that cardiomyocytes cultured on PGA disks (non-coated or coated with laminin) in a rotating bioreactor possessed enhanced viability, electrical coupling and differentiation because of the laminar flow conditions of the rotating vessel compared to the turbulent environment of the spinner flask.
AKHYARI <i>ET AL.</i>	Cardiac constructs, cultured whilst being stretched, exhibited an increased amount of collagen in the matrix compared to those cultured statically.
CARRIER <i>ET AL.</i>	Constructs cultured at an oxygen pressure of 160 mm Hg expressed higher protein and deoxyribonucleic acid (DNA) levels than those cultured at 60 mm Hg.
SODIAN <i>ET AL.</i>	The stroke volume, rate and the inspiration/expiration time of the ventilator of the perfusion system was adjusted to achieve a biomechanical stimulus in the perfusion system through different pulsatile flows and pressures.
CARRIER <i>ET AL.</i>	A perfused system provided homogenous conditions showing a uniform cell distribution across the entire construct.
CARRIER <i>ET AL.</i>	A minimal cell seeding density of $4-8 \times 10^6$ cells/disk was required to preserve the construct structural density over a two week culture period. Rotating culture increased the quality of the constructs possibly due to the higher supply of oxygen.
SOLAN <i>ET AL.</i>	A stirred bioreactor provided mechanical stimulation via a media pulsatile system which induced increased levels of collagen deposition in the constructs
RUWHOE <i>ET AL.</i>	Mechanical stress is a key factor for the development of haemodynamic overload-induced cardiac hypertrophy and therefore in the developing cardiac constructs.
KADA <i>ET AL.</i>	The effect on myofibril orientation was assessed by changing the duration of the stretching to 120% in length at 30 cycles/min. The stimulus induced a parallel orientation of fibrils to the force when the culture was stretched in early stages of development meanwhile stretching in the later stages induced a perpendicular orientation of the myofibrils

**Table 1-9 State of the art in stimulated cardiac systems [75-84]**

#### **1.4.4 Bioreactors**

A bioreactor is a system that provides a controlled environment for cell growth (Figure 1-4). A bioreactor was first used for large scale fermentation processes including fermented beverages and antibiotics. Recently bioreactors have evolved into specialised specific systems for high technology applications such as recombinant proteins and tissue engineering. Because of the wide range of applications, bioreactors vary from simple agitated tanks to complex electronically operated devices.

Nutrient availability is the major concern for 3D culture as mass transport between constructs and media is carried out by convection, whereas within the constructs is only by diffusion. Tissue engineering dynamic bioreactors aims to improve this mass transfer by laminar shear to assure that all the cells within the constructs receive the same levels of nutrients, gases and in some cases to assure the removal of waste or secondary metabolites [33].

In addition to the mass transfer, bioreactors allow the tissue engineers to mimic the environment of the host tissue stimulating the constructs by electrical or mechanical forces. Mechanical stimulation during cell culture has been shown as an effective method to promote cell growth, rapid differentiation and protein expression compared to static culture. This mechanical stimulus can be either via flow-mediated shear stress, uniaxial/biaxial strain or hydrostatic pressures.

There are three main types of general bioreactors: batch, fed-batch and continuous. Batch bioreactors, such as spinner flasks or rotary cell bioreactors, are sealed vessels where the constructs are cultured with media circulating at a

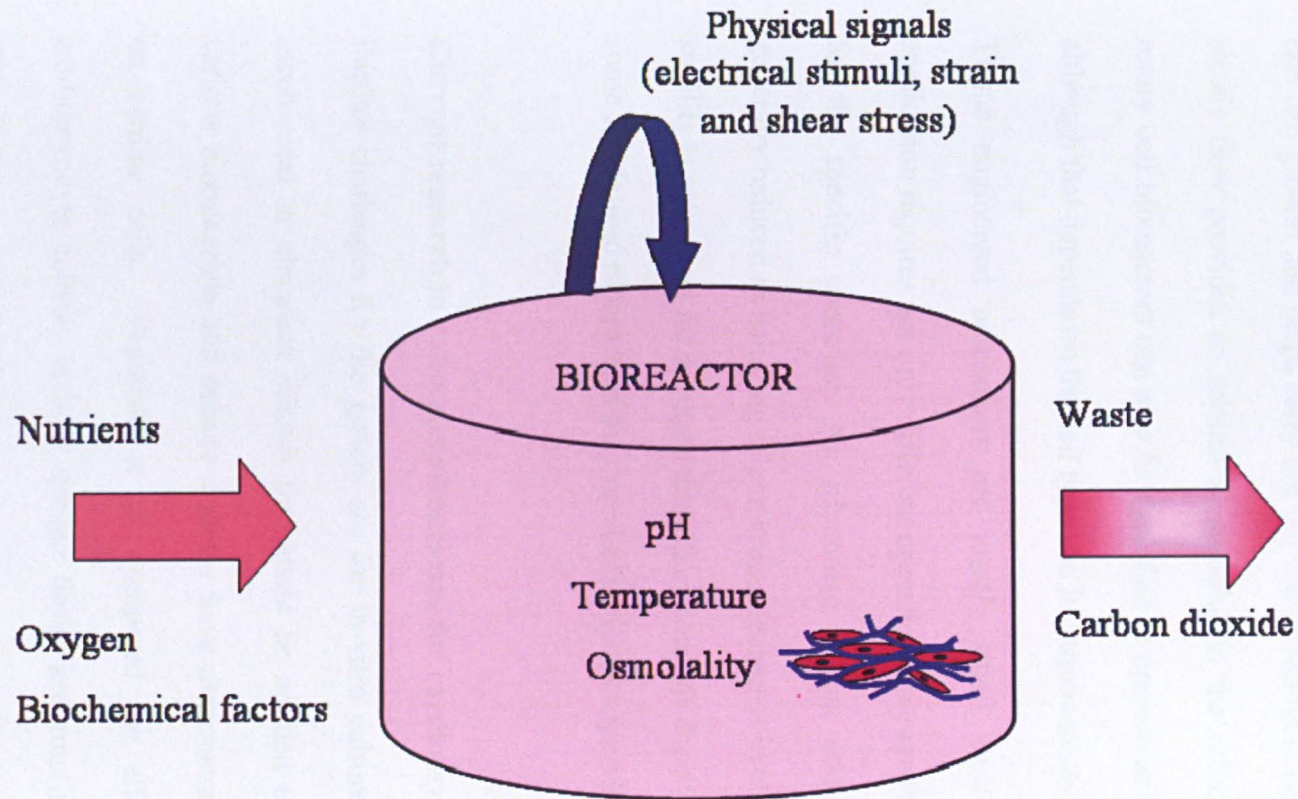


Figure 1-4 Principle of a bioreactor

controlled speed for a determined time. Fed-batch is the same principle with the exception that nutrients are added when needed, so the final volume of media is greater than the initial. Continuous bioreactors, such as perfusion or pulsatile, have a constant flow of media that improves the nutrient exchange and cell growth and helps carry out the waste. Media is never depleted and the steady flow provides an additional stimulus to the cells. Spinner flasks and rotary cell bioreactors can also be modified to operate as a continuous system although that depends on the cell type and its requirements [29].

Tissue engineered bioreactors are mostly small custom-designs as each application requires not only different operational parameters and conformation for the specific construct. An advantage is that contamination risks are generally reduced as handling of constructs decreases in closed systems and the sterility is preserved for a longer time; however this depends on each system as some specialised bioreactors may need continuous supervision.

### **Current research in culture environments for cardiomyocyte culture**

Further challenges for the system are the in-vitro culture conditions such as mechanical or electrical stimuli that could be applied to it. Studies using various biomaterials and culture systems have demonstrated different effects on cardiac cells. Papadaki *et al.* compared the effect and quality of cardiomyocyte culture, in both spinner flasks and rotating vessels, on PGA disks that were non-coated or coated with laminin. Following a period of time in culture, the constructs were assessed for protein expression connexin43 (Cx43), myosin heavy chain (MHC) and creatine kinase MM (CK-MM) as

well as electrophysical properties under stimulation. They showed that cardiomyocytes cultured in a rotating bioreactor possessed enhanced viability, electrical coupling and differentiation because of the laminar flow conditions of the rotating vessel compared to the turbulent environment of the spinner flask [75]. Different mechanical-stimulated culture systems have been shown to influence the proliferation, protein expression and morphology of the cultured cells and to impact directly on the resultant structure and properties of cardiac constructs. Also, Akhyari *et al.* concluded that a mechanical regimen could improve the formation of 3D tissue engineered cardiac graft by promoting the proliferation and distribution of cardiac cells and by stimulating organised matrix formation. They showed that cardiac constructs cultured whilst being stretched exhibited an increased amount of collagen in the matrix compared to those cultured statically [75].

A direct perfusion culture system has been used to culture PGA scaffolds seeded with cardiomyocytes. Different concentrations of oxygen were used in the system to investigate the effects on the resulting constructs. Constructs cultured at an oxygen pressure of 160 mm Hg expressed higher protein and deoxyribonucleic acid (DNA) levels than those cultured at 60 mm Hg. This work also demonstrated that serially connected constructs enhance spatial uniformity by eliminating diffusional transport over large distances [77].

Sodian *et al* also worked with perfusion systems for cardiomyocyte culture. They adjusted the stroke volume, the stroke rate and the inspiration/expiration time of the ventilator to achieve a biomechanical stimulus in the perfusion system through different pulsatile flows and pressures [78].

Carrier *et al* have been working with cardiomyocyte cultures in a perfused environment. This system provided homogenous conditions showing a uniform cell distribution across the entire construct. However, the cardiomyocytes exhibited a rounded phenotype which may have been the result of shear stress from the media flow [79]. The same group conducted experiments with PGA disk-shaped, non woven meshes (5 mm diameter x 2 mm thick) seeded with either rat or chick embryo ventricular cardiomyocytes at different cell concentrations. They cultured the seeded dishes using different parameters including static culture, dynamic culture in a spinner flask (60, 90 rpm) and two rotating microgravity simulating bioreactors: high aspect ratio vessel (HARV) and slow turning lateral vessel (STLV). Their results showed that a minimal cell seeding density of  $4-8 \times 10^6$  cells/disk was required to preserve the construct structural density over a two week culture period. Rotating culture increased the quality of the constructs possibly due to the higher supply of oxygen. A morphological improvement was observed as the rotated constructs showed a more uniform distribution of cells throughout the scaffold [80].

Other mechanical changes such as pulsatile stimuli have been investigated. Solan *et al* worked with a tubular PGA scaffold in a stirred bioreactor that provided mechanical stimulation via a media pulsatile system which induced increased levels of collagen deposition in the constructs [81].

Another approach to improve cardiac muscle regeneration is to subject the construct to physical activity (stress or strain) during culture. Sugden *et al* reported the main differences between stress and strain in cardiac tissue. They also discussed mechanotransduction conditions of the heart pump [82]. Ruwhof

*et al* described how the effect of mechanical stress is a key factor for the development of haemodynamic overload-induced cardiac hypertrophy and therefore in the developing cardiac constructs. This team used the Flexercell Strain culture system to culture monolayer cardiomyocytes under cyclic stretch conditions to analyze growth factor and hormone release as a response to the mechanical force. Cardiomyocytes secreted high levels of Transforming Growth Factor beta (TGF $\beta$ ) and Atrial Natriuretic Factor (ANF) when subjected to this kind of forces [83].

Silicone dishes used to cyclically stretch cardiomyocytes cultures were used by Kada *et al*. They assessed the effect on myofibril orientation by changing the duration of the stretching to 120% in length at 30 cycles/min. The stimulus induced a parallel orientation of fibrils to the force when the culture was stretched in early stages of development meanwhile stretching in the later stages induced a perpendicular orientation of the myofibrils [84].

Several strategies have been developed to generate a clinically viable cardiac graft but there are still some unresolved issues. Reffelman *et al* reported that long-term in vitro culture of cardiomyocyte grafts results in the cells dedifferentiating and developing hypertrophic growth patterns. Mechanical and electrical integration is not completed because the graft is commonly surrounded by collagen and scar tissue. Cardiomyocyte grafts have benefits on the cardiac tissue but the muscle can not be remodelled [85]. In order to overcome these problems it will be needed to optimise the cell source and differentiation stage and the *in vitro* culture time.

## **1.5 Aims of the Study**

The first aim of this work was to generate a flexible scaffold using POC to mimic the elements in cardiac tissue. This work looked into the physical and mechanical properties of this POC scaffold as well as cellular compatibility in 2D and 3D systems. The effect of mechanical forces applied during *in vitro* culture was then assessed to determine if they assisted in the maintenance of a cardiomyocyte cell line and tissue formation.

This polyester, previously described by Yang *et al* [33], is a novel elastomeric biomaterial that can be processed into porous scaffolds with optimum pore size of pore and porosity for cardiomyocyte infiltration and growth. Physical characterisation of this flexible scaffold as well as modifications to improve cell viability and attachment were assessed. A stretching bioreactor was used to mimic the cardiac mechanical stimuli to determine whether this could have any beneficial impact on the development of the cardiac construct.

### **1.5.1 Objectives**

The specific objectives of this work were:

1. Synthesise a novel flexible biomaterial (POC) and process it into porous scaffolds suitable for cardiac muscle tissue engineering.
2. Characterise these POC scaffolds with respect to mechanical properties, degradation and structure.

3. Assess cardiomyocyte cell adhesion to the POC and evaluate the modification of the material surface with ECM proteins to improve cell adhesion.
4. Assess different seeding methods to establish an efficient method to seed cells into POC scaffolds.
5. Compare cell survival, morphology and gene expression of constructs of cardiomyocytes seeded into POC scaffolds cultured in a controlled environment under the effect of mechanical stimuli to those cultured without it.

## **2 General Materials and Methods**

## **2.1 Polymer Preparation, Processing and Characterisation**

### **2.1.1 Polymer synthesis**

Equimolar quantities of 1,8-octanediol (Sigma, UK) and citric acid (Sigma, UK) were added to a round-bottomed flask. The mixture was melted by stirring at 160°C in a paraffin bath after which the temperature was lowered to 140°C. The stirring conditions and temperature were held for a further 20 minutes [41]. The pre-polymer solution was allowed to cool to room temperature (RT) and then dissolved in acetone (Sigma, UK) at 33.3% (w/v) solution and stirred for 48 h to decrease the viscosity. The pre-polymer solution was poured into a poly-(tetrafluoroethylene) [TEFLON] mould to obtain either discs (10 mm diameter) or rectangular scaffolds (56 mm x 24 mm x 2.5 mm) and the solvent was allowed to evaporate overnight. Moulds were transfer to an oven and cross-linked at 80°C and atmospheric pressure for two weeks to obtain POC films.

### **2.1.2 Scaffold manufacture**

#### **Gas foaming processing (scCO<sub>2</sub>)**

Foaming was attempted as follows: the copolymer was placed into the scCO<sub>2</sub> pressure system (Figure 2-1) and then the autoclave was clamped and tightened. The temperature was measured and controlled using a temperature controller and monitor, while the pressure was controlled by a back pressure regulator (BPR) and a computer software program (Flowplot V3.04). The program used for these experiments involved filling the chamber with food

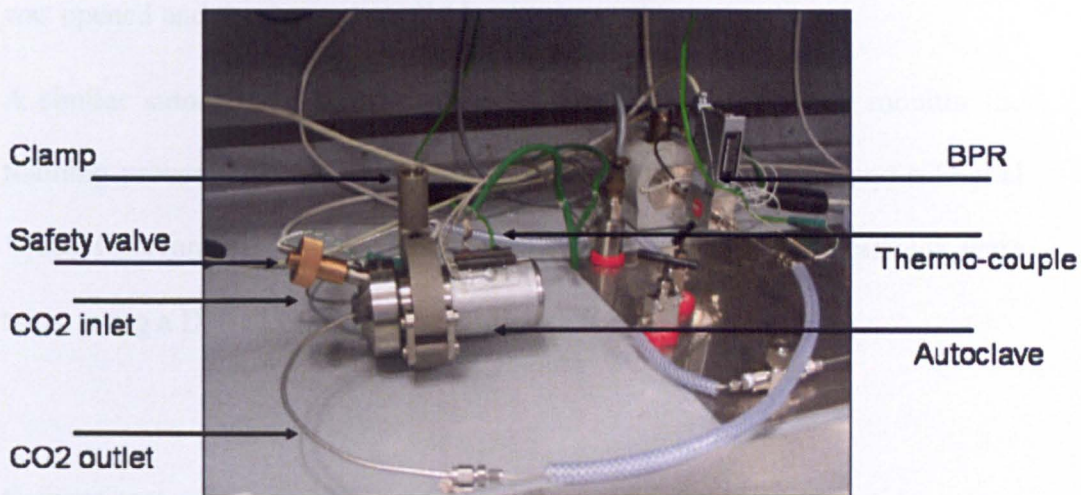


**Figure 2-1** Digital image of the supercritical Carbon Dioxide (scCO<sub>2</sub>) system

grade CO<sub>2</sub> (Cryoservice, UK) up to 207 bar for 20 min, the system was held at 207 bar (soak time) and then vented over 1 hour. Soaking time ranged from 1 to 12 hours. Once the system was at atmospheric conditions, the chamber was opened and the foamed scaffold was removed.

A similar autoclave but with a sapphire view cell was used to monitor the foaming process using a Rigid Borescope (Olympus Ind., UK) and a Digital Video Camcorder MV450 (Canon, UK). Photographs of the scaffolds were taken using a Digital Camera A60 (Canon, UK)

### **Solvent cast**

POC was processed by this method to obtain porous structures. Briefly the POC pre-polymer/acetone solution was poured into a Teflon mould (disc or rectangular shape, as in 2.1.1) containing sieved sodium chloride of particle size greater than 212 microns (Sigma, UK) and covered to allow the salt to soak for 30 minutes. The acetone was allowed to evaporate off for 24 hours at room temperature after which the samples were transferred to an oven for the crosslinking stage for two weeks at 80°C. The scaffolds were cast out and washed several times in distilled water for three days to remove all the salt particles. The monomer residues were then washed out in PBS to adjust the pH to physiological levels. The material was either oven dried at 80°C for 2 hours and stored at room temperature or stored at -20°C and freeze-dried overnight before use. The porosity was tailored by an increment or decrement of the salt content to obtain a final theoretical porosity of 60%, 70% or 80%.

### **2.1.3 Polymer Characterisation**

#### **SEM**

The pore morphologies of the foamed samples were investigated using a JEOL JSM 6060 microscope. The samples were analysed in triplicate, briefly scaffolds were sputter coated with gold at an Argon pressure of 13 Pa for 3 minutes at a current rate of 14 mA. Samples were imaged at an accelerating voltage of 10 and at a spot size of 40.

Random areas were selected to evaluate pore size. The pore diameter was determined by measuring the distance across the pores using JEOL software. A minimum sample size of 50 pores in each of 5 scaffolds was counted. Pore size distribution was determined as well as mean pore diameter.

#### **Microtomography (microCT)**

A micro-CT system ( $\mu$ CT 40, Scanco Medical, Bassersdorf, Switzerland) was used to non-destructively image and visualise the three dimensional micro-morphology as previously described (Figure 2-2) [44]. Scaffolds were mounted on a stage within the imaging system and subsequently scanned at a voltage of 55 kV and a current of 143 mA. Specimens were scanned at a 30 $\mu$ m resolution with an integration time of 300 ms to produce 3D images. Raw 2D images were thresholded to remove background values (threshold value = 70). From this analysis porosity and pore size was calculated using the Scanco software.

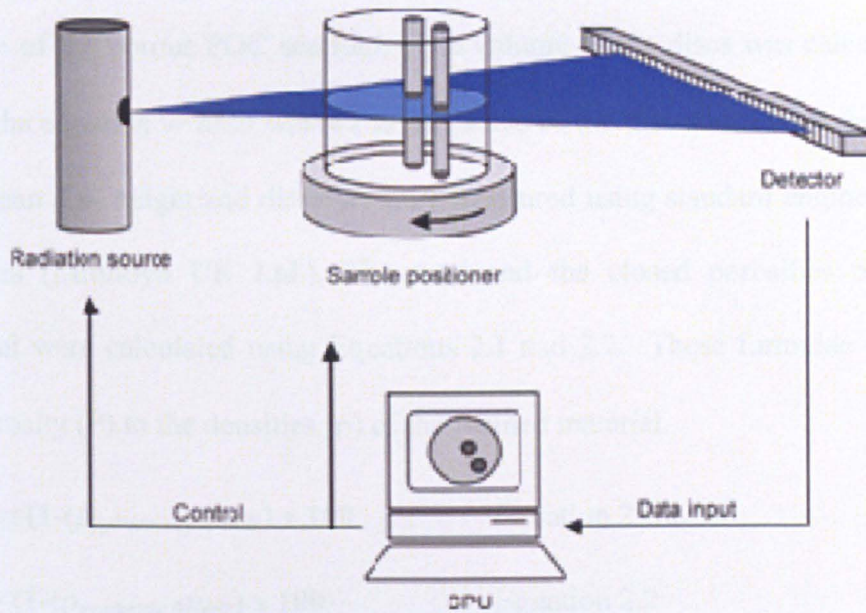


**Figure 2-2 Schematic diagram of a cone beam X-ray microtomography system [86]**

## Helium pycnometry

A Micromeritics AccuPyc 1330 Pycnometer (Figure 6-3) was used to evaluate the density of the scaffolds ( $\rho$ ) testing three different scaffolds for each porosity. Gross measurements and weight were used to calculate the geometric density  $\rho_{\text{geometric}}$ .  $\rho_{\text{geometric}} = m/v$ , where  $m$  is the mass and  $v$  is the volume of the porous POC scaffold. The volume of the discs was calculated using the equation  $v = \pi r^2 h$  where  $r$  is the radius of the disc and  $h$  is the height. The mean disc height and diameter were measured using standard engineering callipers (Mitutoyo UK Ltd.). The total and the closed porosities of the material were calculated using Equations 2.1 and 2.2. These formulae relate the porosity ( $P$ ) to the densities ( $\rho$ ) of the foamed material.

$$P_{\text{closed}} = (1 - (\rho_{\text{pycnometry}} / \rho_{\text{bulk}})) \times 100 \quad \text{Equation 2.1}$$

$$P_{\text{total}} = (1 - (\rho_{\text{geometric}} / \rho_{\text{bulk}})) \times 100 \quad \text{Equation 2.2}$$

## Mechanical properties

Tensile tests were conducted in triplicate on a TA.XTplus Texture Analyser (Stable Micro Systems ®) with a load cell of 5 kg, using pneumatic clamps to secure the samples. A minimum of three scaffolds (8 mm x 54 mm x 2.5 mm, length x width x thickness) were tested at four different rates: 18 mm/min, 180 mm/min, 300 mm/min and 500 mm/min. Strain, stress, maximum elongation and the engineering Young's modulus values were obtained using the package Texture Exponent 32® (Stable Micro Systems). The same texture analyser was used to evaluate in triplicate the fatigue of the porous material over 1000 cycles at 300mm/min, 60% strain and at a frequency of 0.27 Hz.

## **Degradation**

In-vitro degradation was evaluated by weighing dry POC scaffold samples (8 mm x 54 mm x 2.5 mm, length x width x thickness), placing them in a container with 20 ml of PBS and incubating them at 37°C for up to 6 months. Specimens were washed as required to maintain a pH of 7.5. After incubation, samples were oven-dried and weighed to assess the loss of dry-weight. [87-88]

## **2.2 Cell culture methods**

### **2.2.1 Culture of HL-1 cardiomyocytes**

The mouse cardiac myocyte cell line HL-1 was a kind gift from Dr. Claycomb (Louisiana State University - Health Sciences Center, USA) and was grown at 37°C in a humidified atmosphere 5% CO<sub>2</sub> in air in medium: Claycomb Medium (JRH Biosciences) supplemented with 10% (v/v) foetal bovine serum (JRH Biosciences, USA), 0.1 mM norepinephrine (Sigma, Poole, UK), 2 mM glutamine (Sigma, Poole, UK) and 100 U/ml: 100 µg/ml Penicillin/Streptomycin (Sigma, Poole UK). HL-1 cells were seeded into gelatine (DIFCO, UK)/fibronectin (Sigma, Poole, UK) pre-coated 25 and 75 cm<sup>2</sup> cell culture flasks as described by the supplier [30]. The medium was changed every 24 h. Serial passages were made by trypsination, centrifugation and re-suspension of pellets of sub-confluent monolayers and then re-plated at a dilution of 1:3.

## **2.2.2 Culture of c2c12 myocytes**

The mouse myoblast cell line c2c12 were obtained from the ECCAC and cultured in 25 and 75 cm<sup>2</sup> cell culture flasks at 37°C in a humidified atmosphere 5% CO<sub>2</sub> in air in medium: DMEM media (Gibco, UK) supplemented with 10% (v/v) foetal bovine serum, 2 mM glutamine (Sigma, Poole, UK) and 100 U/ml penicillin, 100 µg/ml streptomycin and 0.25 µg/ml amphotericin B (Sigma, Poole UK). C2c12 cells were plated into T-25 and T-75 cell culture flasks as described by the supplier. The medium was changed every 48 h. Serial passages were made by trypsination, centrifugation and re-suspension of pellets of sub-confluent monolayers and then re-plated at a dilution of 1:6 or 1:10.

## **2.3 Culture of cell seeded scaffolds**

### **2.3.1 Preparation of POC films and scaffolds**

Non porous POC films were cut into squares (0.70 cm<sup>2</sup>) whereas POC scaffolds were cut in small rectangular pieces of 1 x 3 cm. POC structures were sterilised by incubation in a solution of 10% (v/v) antibiotics/antimycotics (100 U/ml penicillin, 100 µg/ml streptomycin and 0.25 µg/ml amphotericin B) for 1 hour, washed with sterile PBS, then incubated in 70% (v/v) ethanol for 30 min, washed again and finally by ultraviolet (UV) light exposure for 15 minutes each side. Sterile POC films and materials were stored at RT until use. Prior to seeding POC structures were washed in PBS to remove acidic residues, incubated in non-supplemented DMEM at 4°C for 24

hours, washed again in sterile PBS and modified with an ECM protein as required (Section 2.3.2).

### **2.3.2 Modification of POC surface with ECM proteins**

Collagen, laminin and fibronectin were chosen to modify the nature of the polymer as they constitute the majority of the cardiac ECM. Due to the high temperatures used to synthesise the elastomer, these proteins could not be incorporated into the material. Hence POC surface was modified by passive adsorption even though there was a risk of protein detachment. For adhesion studies, POC films were incubated in a fibronectin (Sigma, Poole UK) at 400  $\mu\text{g}/\text{cm}^2$ , 40  $\mu\text{g}/\text{cm}^2$  and 4  $\mu\text{g}/\text{cm}^2$ , collagen (Sigma, Poole UK) at 10  $\mu\text{g}/\text{cm}^2$ , 1  $\mu\text{g}/\text{cm}^2$  and 0.1  $\mu\text{g}/\text{cm}^2$  or laminin (Sigma, Poole UK) at 2  $\mu\text{g}/\text{cm}^2$ , 0.2  $\mu\text{g}/\text{cm}^2$  and 0.002  $\mu\text{g}/\text{cm}^2$  solution overnight at 4°C and washed three times in PBS prior to incubation with cells [30, 89-91]. After the results of the adhesion studies, POC scaffolds for Tencell experiments were then coated at the higher concentration of fibronectin.

### **2.3.3 Seeding cells into non-porous POC films**

Myocytes were detached from the monolayer culture by enzymatic digestion with trypsin EDTA in PBS. This cell suspension was then centrifuged for 7 minutes at 1,000 rpm (200 g, MSE Mistral 1000, Sanyo Biomedical Co. Ltd) and diluted in supplemented media to a concentration of  $2 \times 10^6$  cells per mL. For the ECM protein study, coated POC films were seeded with  $1 \times 10^6$  HL-1 cells/ $\text{cm}^2$ , and incubated for 18 hours. After this time, films were washed three times in PBS for 5 minutes and analysed for survival using Live/Dead stain.

#### **2.3.4 Seeding cells into porous POC scaffolds**

Myocyte concentrated cell suspensions of  $320 \times 10^3$  and  $2.2 \times 10^6$  cells per mL were prepared as described in Section 2.3.3. Coated POC scaffolds were seeded with either  $160 \times 10^3$  for the seeding studies or  $0.55 \times 10^6$  and  $1.1 \times 10^6$  HL-1 cells for the Tencell studies. These constructs were placed in 6-well or 8-well non-tissue culture treated plates or directly into Tencell bioreactor chambers. Constructs were incubated for 1 or 7 days. Afterwards, constructs were removed and analysed with Alamar Blue, processed for quantitative RT-PCR (qRT-PCR) analysis and treated to be imaged by Stereo, Confocal and SEM.

##### **Static seeding**

For static seeding 500  $\mu$ L of the concentrated cell suspension was pipetted through each scaffold three times and allowed to incubate in a humidified incubator (37°C, 5% CO<sub>2</sub> in air) for 20 hours before imaging and analysing for survival.

##### **Centrifugal seeding**

POC scaffolds were placed at the bottom of 15 mL Falcon centrifuge tubes, one per tube, and 500  $\mu$ L of the concentrated cell suspension in 5 mL of supplemented media was added. Constructs were centrifuged at 1,000 rpm (200 g) for 7 minutes. Supernatant was discarded and constructs were transferred to 6-well non-tissue culture treated plates and incubated in a humidified incubator (37°C, 5% CO<sub>2</sub> in air) for 20 hours.

### **Dynamic seeding**

For dynamic seeding, 500  $\mu$ L of the concentrated cell suspension was pipetted through each scaffold three times and transferred to an orbital shaker, in a humidified incubator (37°C, 5% CO<sub>2</sub> in air), to agitate at 100, 200 or 300 rpm for 20 hours.

### **2.3.5 Static culture**

Seeded scaffolds were transferred to either 8-well non-tissue culture treated plates or to Tencell static chambers. One scaffold was placed in each well or chamber containing 6 mL medium. Media was replenished everyday with fresh culture medium. Constructs were cultured for 20 hours or 1 week in either a humidified incubator or in the Tencell.

### **2.3.6 Tencell culture**

The Tencell bioreactor was chosen to perform the dynamic culture due to its multi-station capacity and chamber geometry (Figure 2-3). Tencell was designed and custom-built at the Leeds University to culture constructs under uni-axial strain [92] (Leeds, UK). The work carried out in the Tencell was possible thanks to the collaboration of Professor Ingham and Joanne Ingram, from Leeds University, who kindly provided the device and the training, respectively. Briefly, the Tencell bioreactor was sanitised and then sterilised by UV light exposition whilst chambers and other components were sterilised by dry heat. Seeded scaffolds were mounted into the 16 chambers and assembled

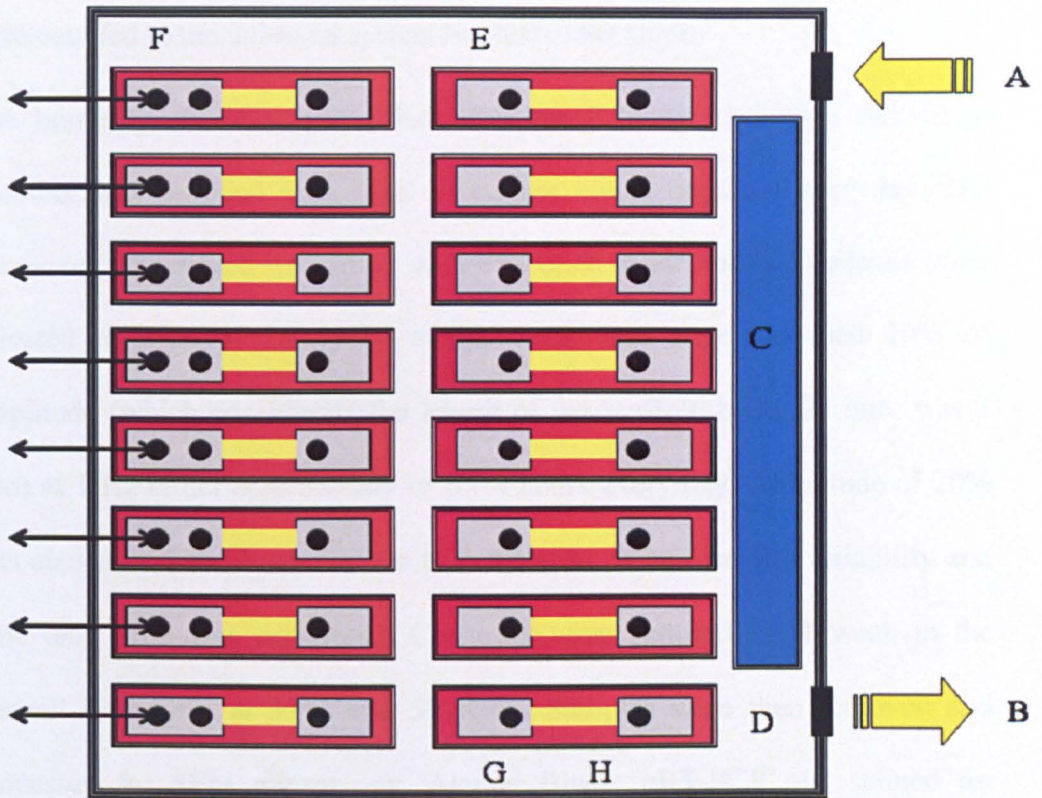


Figure 2-3 Diagram of the Tencell bioreactor

Bioreactor includes (A) Air/CO<sub>2</sub> mix inlet (B) air/CO<sub>2</sub> mix outlet, (C) sterile water bath, (D) hotplate, (E) static/control group, (F) Mechanical stimulated group with coupling to adjust stretching at 10% and 1 Hz. Clamps (G) and constructs (H) are also shown.

in the stations. Stations 1 to 8 were kept static as control while stations 9 to 16 were coupled to the uni-axial system to control the strain.

The humidity chamber was filled with sterile water and each individual chamber was supplied with 6 ml of culture media, replaced everyday. The bioreactor was sealed and filled with 5% CO<sub>2</sub> in air and the controls were adjusted to provide the cyclic strain. Constructs were stretched 10% of amplitude (which considering the length of the scaffold being 30 mm, was 3 mm) at 1 Hz either continuously or for 4 hours every day. Amplitude of 20% was also considered however due to constraints of equipment availability and time only 10% was performed. Construct were cultured for 1 week in the Tencell bioreactor at 37°C and 5% CO<sub>2</sub>. Samples were then removed and processed for SEM microscopy, Alamar Blue, qRT-PCR and stained for Live/Dead imaging.

## **2.4 Biochemical and Molecular assays**

### **2.4.1 Alamar Blue**

The Alamar blue assay is a simple, sensitive, rapid and safe method to measure metabolic activity of mammalian cells and other organisms. This method can be used for cell suspensions or attached cells. This assay is based in the reduction of resazurin or Alamar blue (blue, non-fluorescent) into resorufin (pink, fluorescent), by metabolic cellular activity. The chemical reduction is quantified by either colorimetric or fluorescent evaluation. The medium was removed from the culture plate and the cells were washed with PBS. 1 ml of Alamar Blue working solution was added to the attached cells and incubated

for 90 min at 37°C protected from light. Alamar working solution was prepared by diluting 1:10 the 10x stock solution of Alamar Blue (Serotech). After incubation, 100 µl of the solution was transferred to a 96-well plate (Falcon) by triplicate per each of the three samples and read on the fluorescence plate reader (Cytofluor, Perceptive Biosystems) at 530nm excitation, 590nm emission. After Alamar blue assay, samples were washed in PBS and used for further analysis [93]. Cell number was calculated using the calibration curve for each cell type.

#### **2.4.2 Quantitative RT-PCR**

First  $\alpha$ -actin,  $\beta$ -MHC and ANF were defined as the proteins of interest. Primers for the corresponding genes (*actc1*, *myh6* and *nppa*, respectively) were designed for qRT-PCR as follows: the gene sequence was obtained from the NCBI Gene Bank. Because the SybrGreen technique employed for qRT-PCR is not selective for a specific DNA sequence, particular care had to be taken when designing primers for gene amplification. The forward primer was specifically located on an intron-exon boundary, so that the 5' half of the primer binds to one exon, and the 3' to the following exon. This resulted in the lack of binding to genomic DNA during PCR and thus in a selective amplification of cDNA. Primers were designed using the software "Primer3" [94-95]. This software calculates all the possible options and sort them out depending on the optimal primer length, melting temperature, specificity, absence of self-complementarity, G/C content, G/C and A/T distribution and

Gene	Oligo primer	MW	Efficiency	Tm	Sequence 5'-3'
<i>myh6</i>	Forward	5895.8	NA	65.4	AGTGCAGGCGGAACAAGAC
	Reverse	6034.8		63.5	GGTCATCTCCTTCACCTTGG
<i>actc1</i>	Forward	6731.2	0.961	62.1	CTTTCATTGGTATGAATCTGC
	Reverse	6461.1		63.7	GCATACAGGTCTTTGCGGATA
<i>nppa</i>	Forward	7047.5	0.959	63.2	TGGATTTCAAGAACCTGCTAGA
	Reverse	5970.7		64.3	CCTGCTTCCTCAGTCTGCTC
<i>hprt1</i>	Forward	6133	0.974	64.1	AGTCCCAGCGTCGTGATTAG
	Reverse	7584		63.0	GGAATAAACACTTTTTCCAAATCCT
<i>rpl32</i>	Forward	6077	0.96	63.9	GCAAGTTCCTGGTCCACAAT
	Reverse	6101		63.3	TTGTGAGCAATCTCAGCACA

**Table 2-1 qRT-PCR primer sequences designed for mouse cells**

the 3'-end sequence[94-95]. The primers were based on a target size of 80-100 bp. Table 2-1 present the primer sequences for the qRT-PCR.

Tencell samples were preserved in RNAlater at -80°C until analysis. Constructs were thawed and trypsinised prior to mRNA extraction carried out with the mRNA isolation kit (Miltenyi, UK) and then processed using the cDNA synthesis kit (Miltenyi, UK) to obtain the cDNA. This cDNA was mixed with 2 µM primer solution (reverse and forward), SYBR green mix (Bio-rad, USA) and water. Samples were processed in triplicate in the iCycler Real-Time PCR Detection System (Bio-rad, USA). Samples were evaluated using *hprt1* and *rpl32* as housekeeper genes. Relative expression levels were calculated using the results and the associated software REST 2005 [96-97].

## **2.5 Imaging of cells**

### **2.5.1 Evaluation of Cell Morphology and Contraction Rate.**

The morphology of the cells adherent to the surface was imaged using a LEICA microscope. A minimum of 100 cells from different passages were randomly chosen and photographed at high magnification (20x). Myocyte cross-sectional areas, length and width were measured by using an image analysis software package (Leica QWin, UK).

For survival area, a number of live cells in a randomly delimited area were analysed by triplicate using the same image analysis package to calculate cell area coverage. For contraction rate, 25 cells from 10 T-25 flasks were randomly chosen and visually assessed with a chronometer.

### **2.5.2 Video recording of HL-1 cells**

Contractile HL-1 cells were video recorded using either a Canon Powershot S1 camera (Canon, USA) or a UEye hi-speed camera (Micro-enterprises Inc, USA). Videos were edited and analysed using Windows Media Player and Windows Movie Maker (Microsoft Corp, USA).

### **2.5.3 Immunofluorescence staining for sarcomeric-actin**

Immunofluorescence is a method used to visualise proteins by a specific immunological reaction between the protein or antigen and a conjugate. This technique can be used for fixed cells or tissue sections and is based on the use of fluorescent conjugates that will bind and stain the protein using a fluorescent microscope. Cells were washed in PBS and fixed in 4% PFA/PBS (Sigma, Poole, UK) for 10min, washed again and then permeabilised for 5 min with 0.1% Triton X-100 in PBS. Cells were washed before incubation in 4% normal goat serum (Dako, UK) for one hour.

Samples were incubated overnight at 4°C with monoclonal goat anti-mouse anti- $\alpha$ -actin (Sigma, Poole, UK) diluted 1:50. Samples were washed in 0.05% (v/v) Tween 20 in PBS and incubated with the secondary antibody, conjugated rabbit-anti-goat IgG-FITC diluted 1:100 for an hour and then washed again with 0.05% (v/v) Tween 20 in PBS. Cells were washed with dH<sub>2</sub>O before mounting and visualising them under UV at ex/em 560/620 nm in a Leica DMBRI Fluorescence microscope (Leica, Microsystems Ltd., Bensheim, Germany) [98].

#### **2.5.4 Live/Dead assay for Stereo and Confocal microscopy**

This assay is a two-colour fluorescence method that measures cell viability by simultaneously determining the number of live and dead cells. Live cells are coloured as intracellular esterases convert to fluorescent green the calcein acetoxymethyl (calcein AM) permeated into the cell through intact membranes. Dead cells are recognised as damaged membranes allow the reaction of ethidium homodimer-1 and nucleic acids resulting in an intense fluorescent red colour. This method can be used to quantify live and dead cells or to visualise them under a fluorescent microscope [99]. Films or scaffolds were incubated for 30 minutes with 1.05  $\mu\text{mol/L}$  calcein AM and 4.0  $\mu\text{mol/L}$  ethidium homodimer (Live/Dead stain, Molecular Probes, UK) and then visualised under a fluorescent stereo and confocal microscope. POC films and scaffolds incubated in PBS were used as controls to assess the auto-fluorescence of the material.

#### **2.5.5 SEM**

For SEM, biological samples are usually prepared to preserve the *in vivo* characteristics by dehydration and drying before being sputter-coated with gold [100]. POC constructs containing cells were processed prior to imaging under SEM. Polymer constructs were fixed in 3 ml of 3% glutaraldehyde and stored at 4°C in a sealed container. Glutaraldehyde was then removed and samples were washed in PBS. Constructs were covered with a 1% (v/v) osmium tetroxide solution and incubated at RT for 2 h before washing with  $\text{dH}_2\text{O}$ .

Samples were then serially dehydrated through ethanol solutions of 25%, 50%, 70%, 90%, 95% and 100% (v/v) before incubating with HMDS and then allowed to dry at room temperature. Samples were sputter-coated as previously indicated in 2.1.3.1. The constructs were imaged in a JEOL JSM 6060 with an accelerating voltage of 10 and at a spot size of 40.

## **2.6 Statistical analysis**

Normal distribution was confirmed by visual assessment, validating the use of parametric tests. For all data, except the qRT-PCR gene expression, the mean, standard error of the mean, variance and t-test of two tails, considering equal variances, were performed using Microsoft Excel 2002 (Microsoft Corporation, USA).

For the qRT-PCR data, the software REST 2005 was used to generate the relative expression of the gene normalised with the reference gene as well as to calculate the standard error, the 95% confidence interval and the value of the probability of alternate hypothesis, difference between sample and control groups, was due only to chance (p) [97].

### **3 Processing, Characterisation and Mechanical Properties of Poly-(1,8 Octanediol-Co-Citric Acid) [POC] Porous Scaffolds for Cardiac Muscle Tissue Engineering**

*This chapter presents the synthesis of the elastomer POC and the efforts to process it into porous scaffolds for cardiac tissue engineering. The results of the subsequent characterization, including the macro and microstructure, are also discussed. Special emphasis is given to the mechanical properties and the biodegradability.*

### **3.1 Processing Biomaterials into Scaffolds**

Several research groups are developing elastic biocompatible scaffolds for cardiovascular applications and for cartilage regeneration [101-102]. These elastomeric scaffolds are of special interest due to the need to mimic native conditions *in vitro* by applying external forces. Matching the mechanical properties of the host tissue has also been a concern and so new flexible materials have been developed.

#### **3.1.1 Polymers and elastomers**

Monomers are assembled sequentially through chemical reactions to produce large chains called polymers. Polymers are also classified depending on the reactions by which they were formed. Addition polymers are those obtained by addition reactions of free radicals where all atoms in the monomer become part of the chain. Monomers with two reactive groups continue extending the chain whereas monomers with only one terminal group usually result in low molecular weight polymers. Condensation polymers are synthesised in chemical reactions in which small by-products are released, usually water or methanol [34]. These polymers are formed by monomers with two different groups of atoms, capable of forming ester or amide bonds, resulting in polyesters or polyamides.

Monomers with more than two reactive groups can link non-linearly, giving a three-dimensional structure. Cross-linked polymers often contain monomers with hydroxyl groups that covalently bonds to free ionised hydrogen atoms, triggered by high temperature or pressure. These polymers do not have

crystalline regions and therefore exhibit restricted molecular mobility. Copolymers, those with two or more monomers, are generally designed to modify the properties of the material to match a particular application. This is of fundamental importance in tissue engineering especially when the purpose is to work with cells in a mechanical environment to try to mimic the biological setting.

Biopolymers are polymers that contain monomers found in biological processes and therefore can be degraded by metabolic pathways. Biopolymers are not only biocompatible to some tissues but can also display specific secondary or tertiary architecture to give spatial cues to cells [103]. As previously explained, elastomers are polymers with elastic properties that makes them useful for applications in the remodelling of tissues subject to mechanical activity. POC is one of the crosslinked elastic biopolymers reported with potential applications in tissue engineering. The processing of this material to obtain porous structures and their characterisation are the subject of interest in this chapter.

### **3.1.2 Processing polymers into porous scaffolds**

Solid polymers are processed into different shapes and structures to specific needs. The complete range of methods used to modify polymers is described in the first chapter of this work. The methods used to process poly(1,8-octanediol-co-citric acid) into porous scaffolds will be discussed here.

## **Gas foaming**

Gas foaming is also called supercritical fluid technology because it involves the use of a gas under supercritical conditions. Once a gas reaches above the critical point of temperature and pressure, the material no longer behaves as a fluid or as a gas but as both, with the density and solvating properties of liquids and the diffusivity and viscosity of gases. Supercritical fluids are solvents that have been used in extractions for different applications such as pharmaceutical and food processes, dry cleaning, chemical waste disposal and more recently as polymerisation catalysts. These fluids act as plasticisers modifying the viscosity, the glass transition temperature ( $T_g$ ) or elastic modulus of the polymer without bonding permanently to it [102].

Carbon dioxide ( $\text{CO}_2$ ) has been used in several supercritical applications because its low toxicity, flammability, cost, high availability and stability and low critical point conditions (304.1°K/31.1°C and 73.8 bar/7.38 MPa).  $\text{CO}_2$  dioxide is one of the gases used as porogen to process polymers because it acts as a “clean” solvent on the material, replacing the need of an organic solvent [105-107]. When the pressure is released in the  $\text{CO}_2$  supercritical system to reach ambient conditions, the diffused  $\text{CO}_2$  dissipates through the polymer, “foaming” the material leading to a porous structure [108-110].

The creation of pores occurs in two stages, the first is the nucleation. Pores are formed because of the sudden pressure change modifying the solubility of  $\text{CO}_2$ . During the nucleation, the diffusion of the gas defines the pore size; rapid release will produce homogenous pores as diffusion is minimal whereas slow release will induce a mix of large and small pores caused by the greater diffusion effect on the material [111]. After the pore formation, the

vitrification is caused by the change in the  $T_g$  securing the pores and stabilising the structure [106,108-112].

The gas foaming method has been used and modified by several authors to produce porous structures. These alterations include the combination of gas foaming and salt leaching of NaCl particles to increase interconnectivity and avoid using high temperatures as Harris *et al* described in 1998 [113]. Several groups have been working towards the inclusion of bioactive molecules in scaffolds using supercritical fluids. Richardson *et al* reported the use of this technique as a method to integrate growth factors; Vascular Endothelial Growth Factor (VEGF) and Platelet-Derived Growth Factor (PDGF) were processed into scaffolds without losing the biological activity [114]. Kanczler *et al* incorporated VEGF to poly(DL-lactic acid) (PLA) scaffolds and showed that after being exposed to supercritical conditions, this growth factor retained its angiogenic activity *in vitro* as well as *ex vivo* in an animal model [115]. Furthermore this method has been combined with a water-in-oil emulsion method, by Hile *et al*, to include the basic fibroblast growth factor (bFGF). This group used the supercritical fluid to extract the organic solvent phase and to create the porous scaffold, although it was reported that the bFGF was deactivated by this process [116]. Proteins such as ribonuclease A and catalase were included in supercritical processed scaffolds by Howdle *et al*; results showed that protein structure and function were maintained and that the incorporation of thermo-labile molecules was possible by their novel process [117]. Supercritical scaffolds have also been exploited as a vehicle to deliver either cells or DNA to target tissues. Ginty *et al* reported the inclusion of mammalian cells such as C2C12 myoblasts, 3T3 fibroblasts, chondrocytes and

hepatocytes into the supercritical process to create porous scaffolds. The constructs were created using either supercritical carbon dioxide or nitrogen; both methods resulted in scaffolds with viable cells. Although the cell survival did depend on the cell type, Ginty *et al* demonstrated that there was a maximum time that cells could be exposed to supercritical conditions before losing metabolic activity [118]. Heyde *et al* combined DNA and P<sub>DLLA</sub> to develop a non-viral DNA release system for tissue engineering applications. An aqueous solution of polymer/DNA complex was placed on top of P<sub>DLLA</sub> powder and freeze-dried the mix for 48 hours prior to processing it in scCO<sub>2</sub>. Even if transfection ratios varied depending on the DNA cryoprotectant, they were superior to those of commercial DNA release products. This method offered the benefit of a slow and continuous delivery of DNA in a localised area due to the DNA being encapsulated in the scaffold during the scCO<sub>2</sub> process [119].

ScCO<sub>2</sub> was used to foam POC under different conditions as described in the Materials and Methods section.

### **Solvent casting / Particle leaching**

The particle leaching method has been widely used to fabricate porous three-dimensional scaffolds from biodegradable polymers. In this work sodium chloride, of a minimal diameter of 312 µm, was used as a porogen and it was added to a solution of POC/acetone. After the solvent was evaporated, the mixture of polymer and porogen was allowed to crosslink overtime. Once the polymer was crosslinked, this structure is immersed in water to leach out the salt, leaving the porous matrix to be used as a scaffold. Salt leaching produces

scaffold with high porous ratio and good interconnectivity; however the polymers processed by this procedure are restricted because of the solvent phase [120].

Different alterations of the general method have been adapted including solvent merging/ particle leaching and salt fusion. Liao *et al* utilised a cylindrical Teflon mould with a leach that allowed the use of negative pressure to wash the organic solvent after dissolving the NaCl/PLA mix. This configuration also permitted the pass of a non-solvent to precipitate the matrix, and of distilled water to leach out the salt and create the porous structure. This technique was reported to be quicker and easier than the conventional approach. In addition to this, it was possible to carve different structures from the large porous scaffolds depending on the application [121]. Murphy *et al* modified the method forcing crystal fusion by exposing the porogen, NaCl, to 95% humidity for 0-24 hours prior to solvent casting. This change resulted in a highly interconnected matrix with internal bridges between pores and increased pore diameter and sphericity. These results also showed that the compressive modulus is increased for those scaffolds with exposed humidity of 24 hours [122].

### **3.1.3 Methods for scaffold characterisation**

#### **Micro-computed tomography (microCT)**

Micro-computed tomography is a method that uses X-rays to recreate virtual 2D and 3D models of specimens. This technology does not damage the original sample nor requires prior preparation, and therefore can be used in

living and inert models. MicroCT is a variation of the original tomography equipment designed for medical scans, but the resolution is higher as micro refers to the precision of the technique.

The device used for this technique, the Scanco  $\mu$ CT40, is a closed x-ray system with a cone-beam imaging system of 2D x-ray detector, or still cameras, and one electronic x-ray source that creates and collects the cross sections images that can be reconstructed later into static or dynamic 3D models [123].

Microtomography has been used to evaluate and characterise the structure of materials and polymeric scaffolds in tissue engineering but also to monitor morphological changes of constructs and its micro-architecture [124-125].

### **Scanning Electron Microscopy (SEM)**

Scanning electron microscopy has been used to characterise materials. Macro and microstructure can be determined as it is not only possible to analyse shape and porosity but also pore size and interconnectivity. SEM is a standard technique to analyse surface morphology because it enables the characterisation of solid materials as well as porous structures. In the case of scaffolds, it is a concern that the biological performance may be altered by the material characteristics and so this information allows to modify the material to adapt for the needed response. As this type of microscopy requires a dried and metal coated sample, it must be considered that this technique may alter the morphology, especially on materials that undergo changes in hydrated conditions [126-127].

## Pycnometry

Helium pycnometry is a non-destructive technique that allows the quantitative analysis of porosity through the measurement of volume and true density of the samples; these are calculated using the Archimedes principle of fluid displacement and the Boyle's law. In this instance the displaced helium can infiltrate the porous material giving the true volume and then comparing this to the geometrical volume [128].

Equations 3.1 and 3.2 were used to calculate the density ( $\rho_{pycnometry}$ ) determined by pycnometry and the density ( $\rho_{geometric}$ ) determined by geometric (weight/volume) analyses using a micrometer screw gauge and scales [31].

$$\rho_{total} = (1 - \rho_{geometric} / \rho_{bulk}) \times 100 \quad \text{Equation 3.1}$$

$$\rho_{closed} = (1 - (\rho_{pycnometry} / \rho_{bulk})) \times 100 \quad \text{Equation 3.2}$$

### 3.1.4 Mechanical properties of scaffolds

The mechanical properties of a material define its behaviour under a load and refer to the type of forces or stress that the material can resist. These properties include the strength, hardness, toughness, brittleness, ductility, malleability, elasticity and plasticity of the material. The mechanical properties of scaffolds are relevant not only in constructs that will be subject to dynamic culture systems but also for structures in static systems. These are important as the constructs will be implanted into living beings and therefore need to support the natural strain of the native tissue and surroundings. Tissue

engineering scaffolds must withstand types of stress such as tension, compression, impact, fatigue and in some cases shear and torsion.

Because a cardiac implant will need to meet the stretching physiology of cardiomyocytes, the most important mechanical characteristics of a cardiac scaffold are the fatigue and elasticity. Fatigue is the property that enables the material to resist continuous stresses and is assessed by the number of cycles that the material can resist this stress. Elasticity is the ability to return to its original shape without permanent deformation once the stress has been removed. This is evaluated by measuring the tensile stress that the material can bear before reaching the limit of load of permanent deformation. Elasticity is determined by parameters such as maximum elongation and Young's modulus. Maximum elongation is the greatest deformation of the specimen before failure. The Young's modulus or elastic modulus,  $E$ , is a constant that quantify the stiffness of the material and is defined as the ratio of change of small stress to strain as described in the equation 3.3.

$$E = \frac{F * L_0}{A_0 * \Delta L} \quad \text{Equation 3.3}$$

Where  $E$  is the Young's modulus or elastic modulus,  $F$  is the force applied to the object,  $L_0$  is the initial length of the material before the load is applied,  $A_0$  is the original cross-sectional area through which the force is applied and  $\Delta L$  is the change of length once the stress was applied. In his project, the scaffolds were tested by applying a tensile load uniaxially and measuring the elongation of the elastomers. The engineering Young's modulus was calculated in all the

cases with software based on the previous equation, which also can be described as

$$E = \frac{\sigma}{\varepsilon} \quad \text{Equation 3.4}$$

where  $\sigma$  is the stress or load per unit of area and strain ( $\varepsilon$ ) is the change of length divided by the original length. As stress is a pressure, its international units are Newtons per square meter ( $\text{N/m}^2$ ) or Pascal (Pa); whereas the strain is dimensionless [34]. The physical state of a material defines its elasticity. Materials in a glassy state are stiffer and therefore E ranges in the thousands of MPa whilst rubbery materials have a lower E, between 0.1 and 10 MPa [129].

Elastomeric polymers, as most of the rubbers, present an unusual behaviour as seen in Figure 3-1. Contrary to other polymers that exhibit different regions in the stress/strain curve including a linear portion, elastomers display a large flat section which means that after an initial elongation there is region of stretching which occurs without increasing strain.

Mechanical properties of porous materials vary widely from those of the solids as they depend on the porosity and pore size. However, when designing a scaffold it is required to guarantee mechanical strength as well as high porosity. Pores weaken the structural strength in a non-linear proportion depending on the density of the structure, for this reason, homogeneity of pore size is important to maintain a high density and not negatively affect the mechanical strength [130].

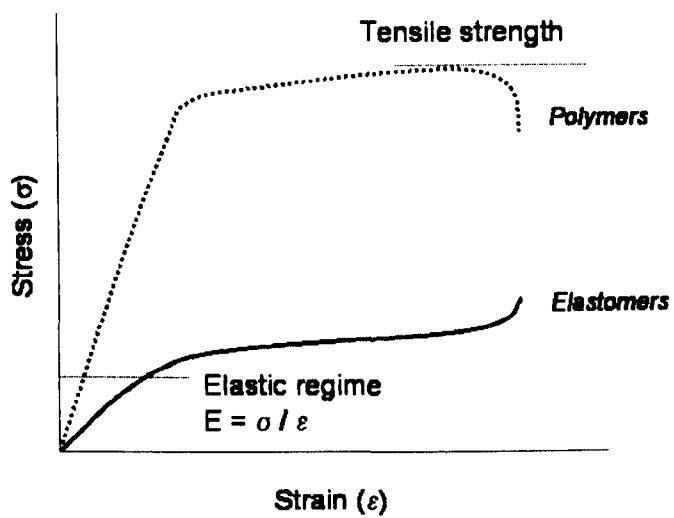


Figure 3-1 Elastic behaviour of polymers and elastomers [119]

Several equations have been used to empirically assess the relationship between the elastic modulus of a solid material and the one of its porous structure as can be seen in Equation 3.5.

$$E = E_0 * (1 - p/p_c)^f \quad \text{Equation 3.5}$$

where  $E$  is the Young's modulus of the porous material with porosity  $p$ ,  $E_0$  is Young's modulus of the solid material,  $p_c$  is the porosity at which the effective Young's modulus becomes zero and  $f$  is the parameter dependent on pore geometry (pore size and closed pores) and grain morphology (grain size and cracks) of the material. The value of  $p_c$  is often considered as 1, while the value of  $f$  in linearised models is one [131]

When materials are cyclically stressed at the same point over a long period of time, they frequently fail on conditions below their maximum load or tension. This fatigue, along with the fracture and failure of porous materials are influenced by imperfection and internal flaws in the structure such as cracks, notches and large pores [130, 132-133].

Mechanical properties such as strength can be altered by combining other materials. Cellulose has been reported as a biodegradable polymer suitable for scaffold fabrication for hard and soft tissue engineering, including cartilage [134-136]. Still the major challenge of a homogeneous biodegradable elastomeric composite with optimum biological and mechanical properties is unresolved.

### **3.1.5 Degradation**

Polymer degradation is defined as the deteriorative change of properties in a material caused by physical (heat, light and radiation), biological, chemical (including pollutants, oxidation and hydrolysis) or mechanical stress. Oxygen, hydrolysis and biological action are the most common causes of degradation of scaffolds. Degradation is desired in some biological systems as the release of monomers allows the reduction of molecular weight and facilitates the disposal by biological pathways [137]. However, degradation of a scaffold also means that the mechanical properties may be compromised. The challenge when designing a polymer is to obtain a polymer that will last enough to support the remodelling of the area but will eventually degrade and disappear from the host.

When implant materials interact with biological surroundings, either the material loses molecules to the environment (leaching) or takes up foreign fluid into its structure (swelling). This diffusion phenomenon affects the mechanical properties of the material. Swelling limits the elasticity and speeds up the failure whilst leaching can diminish the elasticity due to the voids but also has a major impact, as degradation products can trigger local and systemic responses from the biological host [138]. Because of this, it is of major importance to characterise the degradation profile of the materials used in tissue engineering. There are few reports of the degradation of POC in-vivo and in-vitro and therefore this work also focused part of this chapter to that.

### **3.1.6 Aims of this study**

The aims of this study were to find a suitable method to process POC into porous structures. The mechanical properties of the resultant 60%, 70% and 80% porous POC and POC-cellulose films were investigated after different storage conditions. The elastic modulus as well as the maximum elongation and force at break were evaluated with the stress/strain curves resulting from tensile tests.

## **3.2 Materials and methods**

### **3.2.1 Synthesis of POC**

The POC was synthesised as described in 2.1.1. Briefly 10 g of citric acid powder were mixed with 7.61 g of 1,8-octanediol in a round-bottom flask. The stirring mixture was melted at 160°C and then polymerised at 140°C. The resulting polymer was cast into moulds and allowed to cool down before being crosslinked at different times. Alternatively POC was dissolved in acetone to 30% (v polymer/v solvent) to prepare the polymer solution needed for the salt leaching method.

### **3.2.2 Gas foaming of POC**

The POC discs (10 mm diameter, 8 mm thick) were placed into high pressure vessels and foamed as described in section 2.1.2.1

### **3.2.3 Salt leaching of POC**

The POC polymer solution was mixed with NaCl, in proportion to the porosity required and cast into a mould. After the solvent was evaporated the polymer mix was crosslinked as described in 2.1.2.2 for 2 weeks and washed in PBS for 3 days to dissolve the porogen and create the porous structure.

### **3.2.4 Characterisation of POC scaffolds**

Scanning electron microscopy was used to observe the cross-sectional pore morphology of the scaffolds and to determine pore size. Samples were mounted on an aluminium stub and sputter-coated with gold. SEM observations were carried out at 20 kV as described in 2.1.3.1.

MicroCT was used to determine pore size and porosity as detailed in 2.1.3.2. Porosity was evaluated by helium pycnometry using equation 2.1 and 2.2 as explained in section 2.1.3.3.

The tensile tests to generate the mechanical data for the specimens were carried out as described in 2.1.3.4 and the degradation studies followed the method specified in 2.1.3.5.

## **3.3 Results and Discussion**

POC was processed into porous scaffolds using two methods. Results were analysed in order to select the most advantageous method for a rapid manufacture of POC scaffolds. These structures were then analysed for pore

size, porosity and mechanical properties under different composition and storage conditions.

### **3.3.1 POC processing**

POC was synthesised as previously described in 3.2.1 according to a previous published work; the physical characteristics of the material were determined by the crosslinking time. Crosslinking times of 3 and 7 days and temperatures of 80°C and 120°C were compared. When POC was crosslinked for only 3 days at moderate temperature, the polymer was not crosslinked enough to solidify and the elastomer remained a transparent viscous slurry. However, when POC was crosslinked at higher temperatures for the same period of time, it resulted in slightly stiff yellow discs. POC crosslinked for a longer period of time, 7 days, at moderate temperature (80°C) resulted in elastic discs, whilst higher temperature (120°C) produced “over-crosslinked” stiffer orange discs. The resulting solid discs can be seen in Figure 3-2.

The higher the level of crosslinking, the stiffer a polymer becomes. Previously it has been reported that crosslink density affects the strain-hardening. Yamaguchi *et al* found that an increased crosslink density restrained the chain stretching and therefore affected the strain hardening and other rheological properties [139].

### **Supercritical Carbon Dioxide Processing**

Once the polymer was synthesised, supercritical foaming was chosen as a processing method to obtain porous scaffolds. Previous work has demonstrated

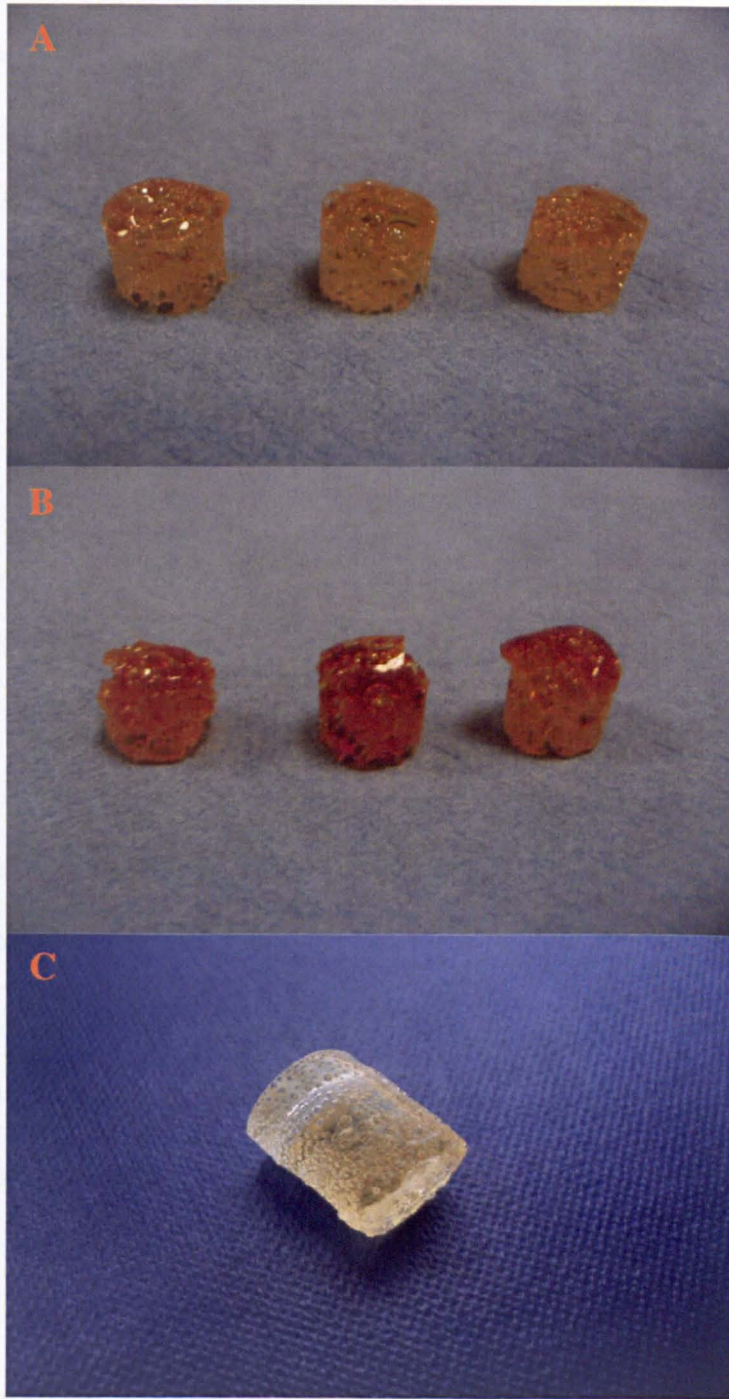


**Figure 3-2**Digital images of POC discs crosslinked for (A) 3 days at 120°C, (B) 7 days at 120°C and (C) 7 days at 80°C

that supercritical technology can produce highly open porous structures when applied to certain polymers [105-113]. As POC is a relatively new polymer, there is no prior experience of this material processed in scCO<sub>2</sub> and therefore the two main parameters of the system, venting and soaking time, were modified to produce a porous scaffold. POC was placed in TEFLON moulds to control the shape of the resulting scaffold and then located in the pressure vessel. Venting time was maintained short to create homogeneous porous structures whereas the soaking time was increased starting from 15 minutes to 30 minutes, 2, 4, 6, 8, 12 and 16 hours. POC processed for less than 8 hours showed a slightly foamed exterior in the top of the disc but no change at all in the internal structure as can be seen in Figure 3-3. When time was increased to 8 hours, the core of the polymer cylinder was partially foamed but. It was decided to increase the soaking time to obtain a total porous structure. POC processed for 16 hours in the supercritical CO<sub>2</sub> system resulted in a foamed scaffold as can be seen in Figure 3-4.

One of the advantages of using scCO<sub>2</sub> is the short exposure times to foam a polymer (just five minutes), which allows incorporating live cells and thermo-labile bio-molecules [117-119]. In order to understand why POC needed 16 hours to be foamed thoroughly, both monomers were subjected to scCO<sub>2</sub> separately; it was found that none of these were soluble in CO<sub>2</sub>. It has been previously discussed that only high amorphous and non-crystalline polymers dissolve in supercritical fluids and therefore foam when the pressure is released. Also, high molecular weight polymers with long chains resist expansion during foaming [112, 140].

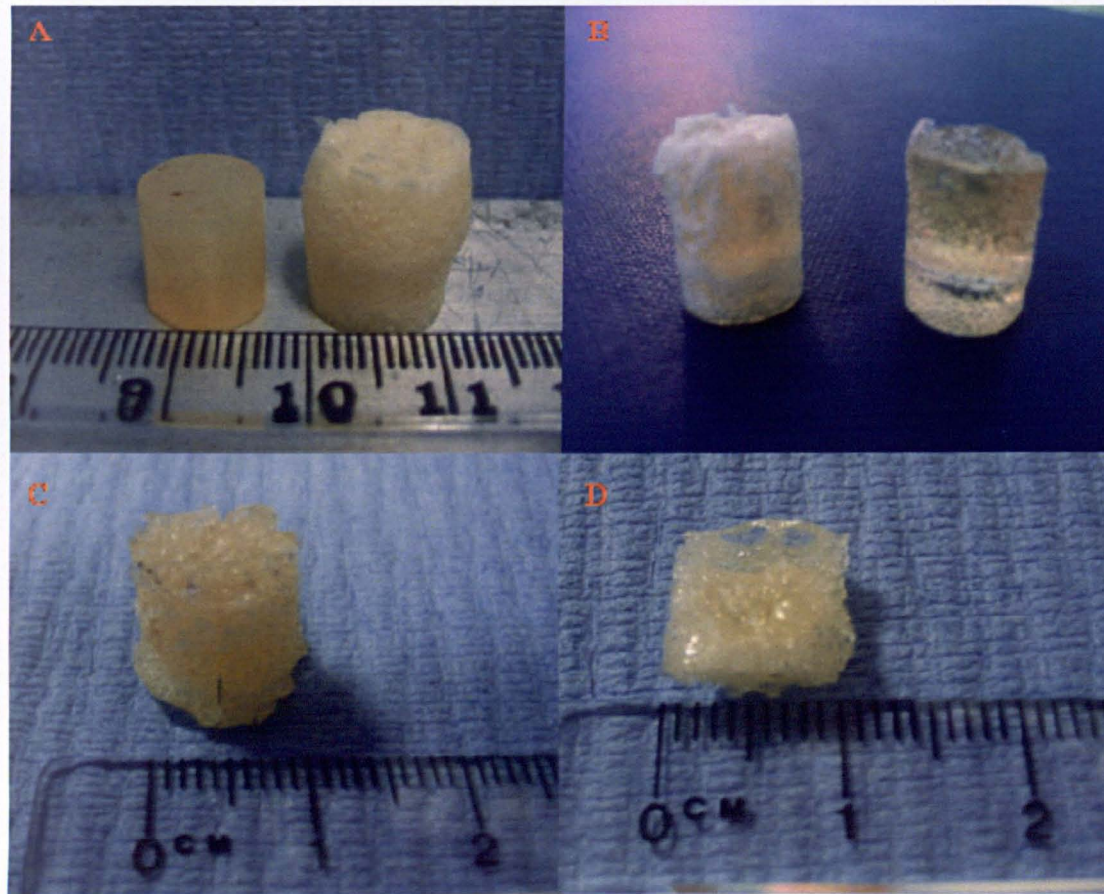


**Figure 3-3**Digital images of (A) non processed POC disc compared to porous POC structures processed by scCO<sub>2</sub> for 2 hours, foamed only in the superior part of the disc. (B) POC processed for 4 hours compared to an untreated disc and (C-D) fully foamed POC discs after 16 hours of supercritical processing.

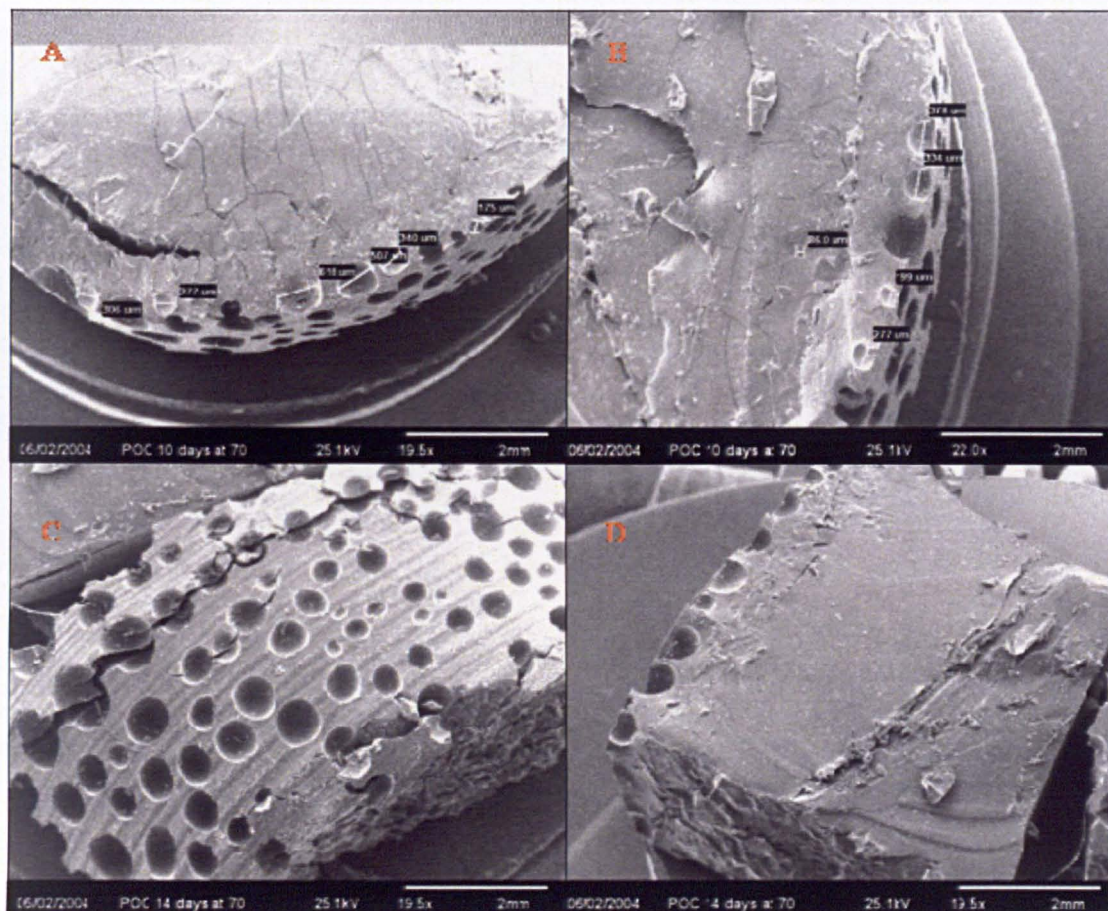


**Figure 3-4 SEM images of (A-B) POC discs crosslinked for 10 days and processed with scCO<sub>2</sub> for 6 hours showing solid internal structure with pores only in the surface. (C-D) POC crosslinked for 14 days and then foamed for 6 hours showed the same effect with a resultant solid core.**

In addition to the long hours needed to treat POC discs, the supercritical method is carried out in a pressure vessel which limits the number and shape of Teflon moulds used.

Mechanical conditioning of POC scaffolds requires a rectangular shape rather than cylindrical scaffolds. In addition, processing POC with scCO<sub>2</sub> would mean that only one scaffold was produced every 24 hours. Although supercritical fluid is a solvent free technology used to create porous structures, unfortunately in the case of POC, this was not a suitable method and was not a cost/time-efficient method. Furthermore the limitation of shape, size and number of scaffolds created per batch made the gas foaming technique not adequate for this project.

### **Salt leaching**

Salt leaching was tested as an alternative method to scCO<sub>2</sub> foaming to produce porous scaffolds. This method is an easy technique restricted only by polymer solubility. Due to the concern of residual solvent toxicity, solvents are best avoided when processing scaffolds for clinical applications. As the use of solvents is indispensable in this case, a mild toxic solvent, acetone, was used. Polymer was crosslinked for 2 weeks, with 20%, 30% or 40% salt and then washed out in subsequent washes with dH<sub>2</sub>O for 4 days.

Salt leaching produced highly porous POC discs as can be seen in Figure 3-5; porosity and pore size was confirmed using SEM as described with more detail in section 3.3.2. This method allowed the fabrication of different forms and sizes, as the final morphology depended on the mould used to cast the scaffold.

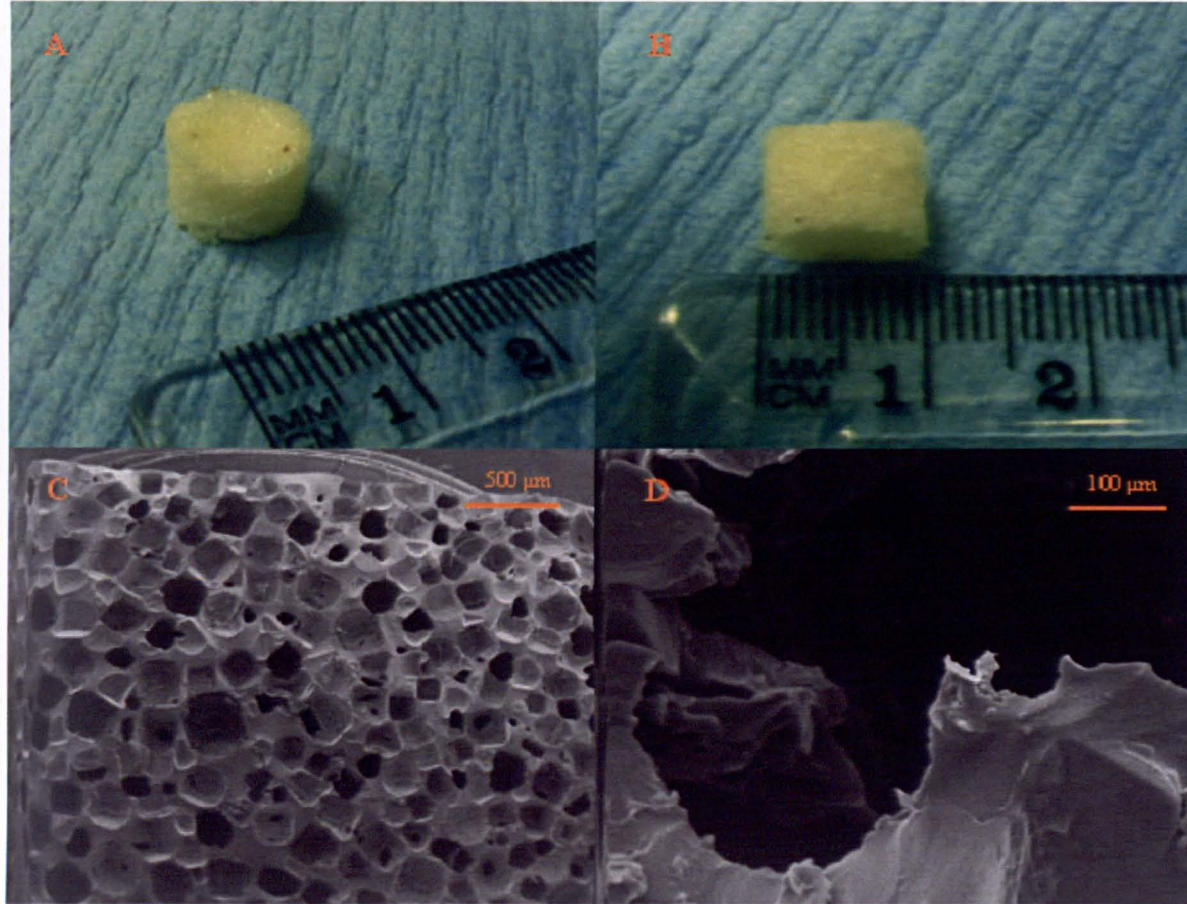


Figure 3-5 Digital images of (A-B) salt leached POC discs of 10 mm diameter and 8 mm thick. Magnified images of (C) pores shaped like the porogen and (D) interconnected pores

Teflon moulds were customised to assure the rectangular shape needed for the stretching bioreactor (Figure 3-6). Whereas POC discs were highly porous and homogenous, POC rectangular films proved to be heterogeneous with porosities greater than 80%. An initial effort to fabricate POC porous films of 90 and 95% porous demonstrated that they were not homogeneous because of the large open area in the mould. Previously it was reported that scaffolds for tissue engineering ideally should be 90% porous or more. However in the case of POC large films this was difficult to achieve and the scaffold was mechanically compromised due to its shape and hence could not sustain the strain intended for this application. Three different porosities were designed for the films: 60, 70 and 80%. The weight/volume of the porogen was considered in order to assure the porosity intended for films and confirmed after porosity analysis.

This technique produced well interconnected porous scaffolds as was confirmed by SEM and microCT (Figure 3-7 and table 1-).

Due to the concern of achieving the required mechanical strength, it was considered to incorporate cellulose to strengthen the films. Entcheva *et al* reported the use of cellulose acetate fibres to culture cardiac cells. Cellulose is considered as a biomaterial due to its biodegradability although a non-mammalian enzyme, cellulase, is needed to break it down to glucose. Results showed that cellulose supported cardiomyocyte growth and physiology [136]. An initial approach of incorporating 10% (w/w) of cellulose was used in the same salt leaching technique to produce 60%, 70% and 80% scaffolds.

It was found that water vapour bubbles were created and trapped within the polymer during crosslinking. These bubbles did not completely escape from

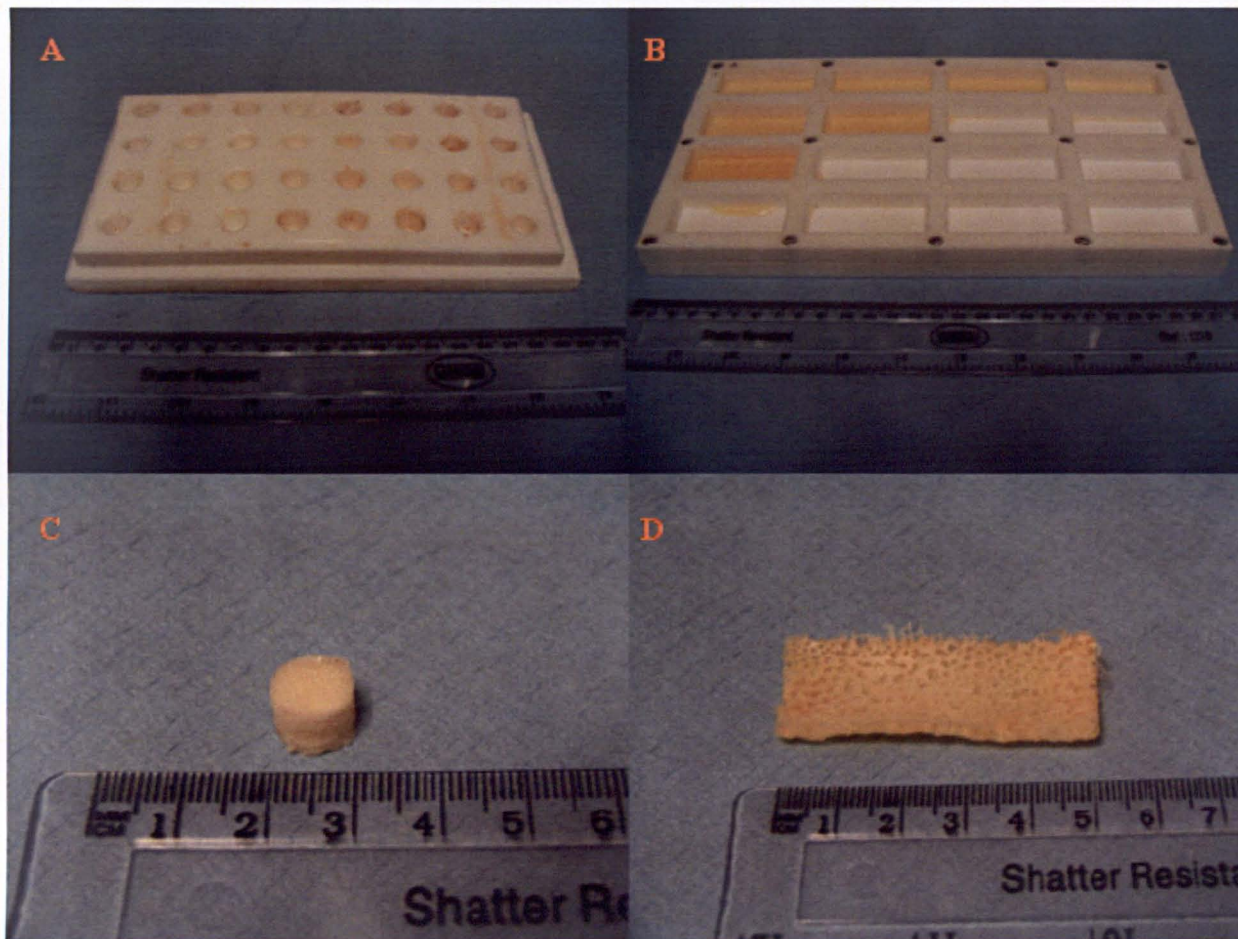


Figure 3-6 Digital images of Teflon moulds and the resultant POC discs and rectangular films after solvent casting process

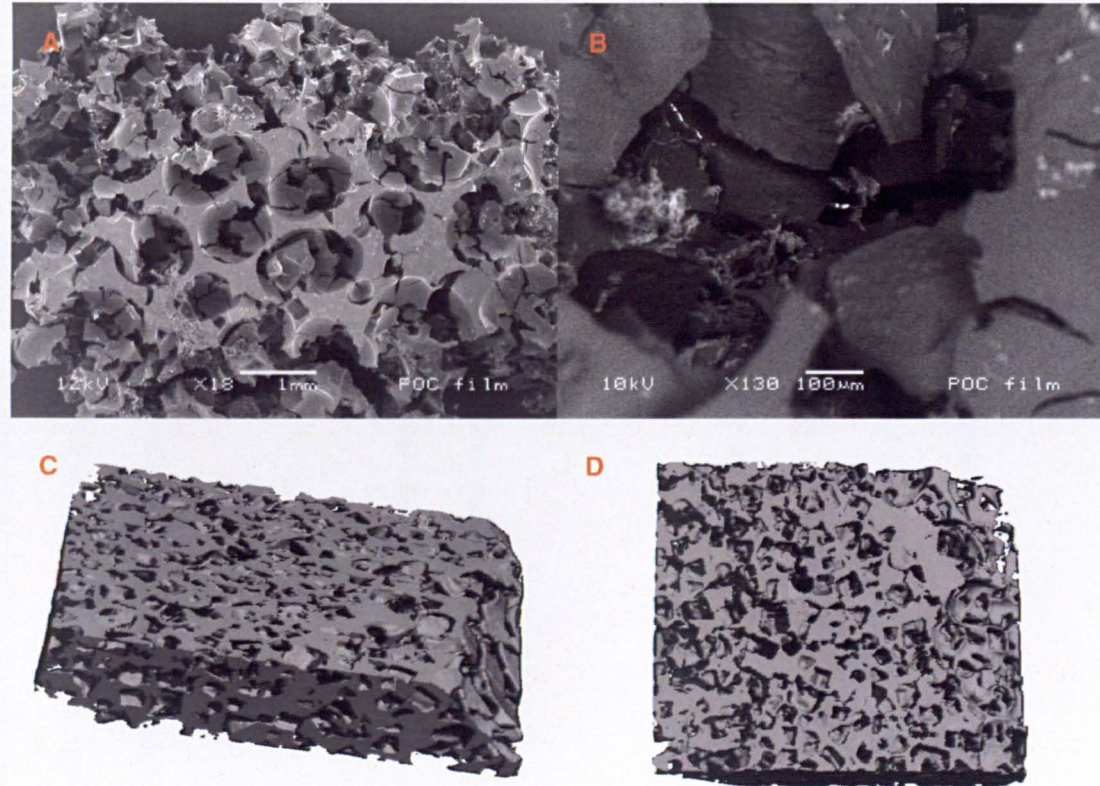


Figure 3-7 (A-B) SEM and (C-D) microCT images of salt leached POC 70% porous scaffolds confirming full porous structure and interconnectivity

the structure and therefore the surface was left with large holes on the upper side. In an attempt to avoid this, the acetone was cooled to slow down the evaporation process but the end result was the same. Although these apertures could weaken the scaffold mechanically, it was hypothesised that at the same time they could facilitate cell seeding and mass transfer once in culture.

### **3.3.2 POC scaffold characterisation**

POC scaffolds were characterised to establish the suitability of these structures for cardiac culture. Morphology, porosity, pore size, pH in aqueous media, mechanical properties and degradation were assessed as reported below.

#### **Morphology**

Scaffold morphology of POC films matched that of the mould in which they were cast: 56 mm of length, 24 mm of width and 2.5 mm of thickness.

#### **Porosity**

The weight/volume of the porogen was considered in order to assure the final desired porosity for films. This calculated porosity was confirmed by microCT and helium pycnometry. As discussed before it was used three different porosities, 60, 70 and 80%. These porosity values may influence cell attachment and proliferation, as the porosity increases the cells have more space to spread and to improve diffusion of nutrients and oxygen. In contrast, the less porous the structure, the more difficult it is for cells to infiltrate and populate the construct; although that would offer better mechanical properties.

Therefore a compromise had to be reached. Porosity of POC and POC/cellulose scaffolds stored at room temperature and at -20°C was assessed. Analysis of microCT images (Figure 3-8) showed that there was a minimal variation between the real and the theoretical porosity. Porous scaffold with theoretical porosity of 60% reported a porosity of  $61.06 \pm 1.20\%$  when analysed by microCT and of  $61.04 \pm 5.42\%$  when pycnometry was used. Insignificant differences were also found in 70 and 80% porous scaffolds as can be seen in Table 3-1. This table also shows the results of Helium pycnometry which confirms the porosity of the scaffolds. SEM showed that the scaffolds are not totally open-porous but with a porous structure that will be able to host the cardiac cells (Figure 3-9).

### **Pore size**

Characteristic distribution of pore size in these scaffolds showed a peak around the value of the porogen size. Larger pore sizes were due to the creation of bubbles in the structure. The mean pore size of 70% porous scaffold, as determined by microCT, of 365 microns was greater than the average of 242 microns found with the SEM (Table 3-2). Mean pore size varies between microCT and SEM analysis, mainly because SEM only considered random transversal images of the microscopic pores whereas the microCT evaluation includes the average of the void fraction, offering a thoroughly analysis. Typical distribution of pore size for 60%, 70% and 80% porous POC scaffolds stored at room temperature are shown in Figure 3-10 whereas those stored at -20°C are in Figure 3-12. The same microCT analysis was performed for POC/cellulose scaffolds (Figure 3-12).

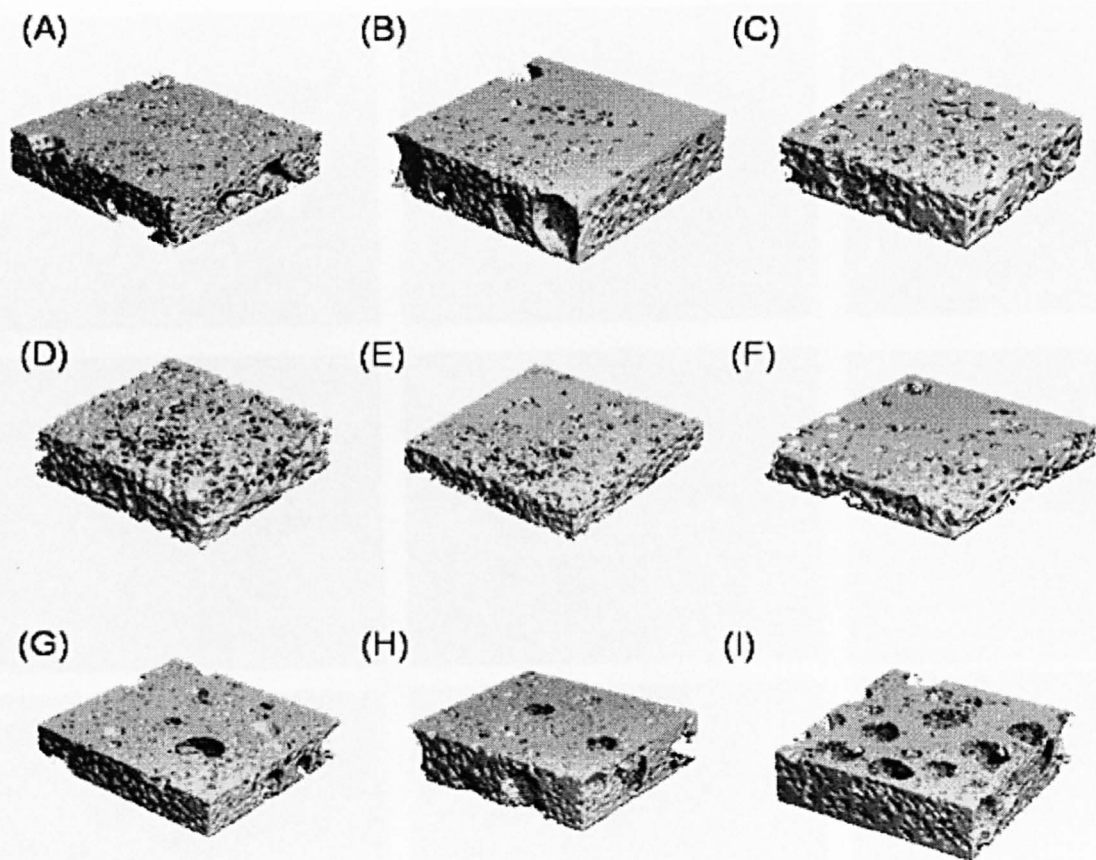


**Figure 3-8** MicroCT images from sections of (A) 60%, (B) 70% and (C) 80% porous POC scaffolds stored at room temperature; (D) 60%, (E) 70% and (F) 80% POC porous scaffolds stored at -20°C and of (G) 60%, (H) 70% and (I) 80% POC/cellulose scaffolds stored at room te

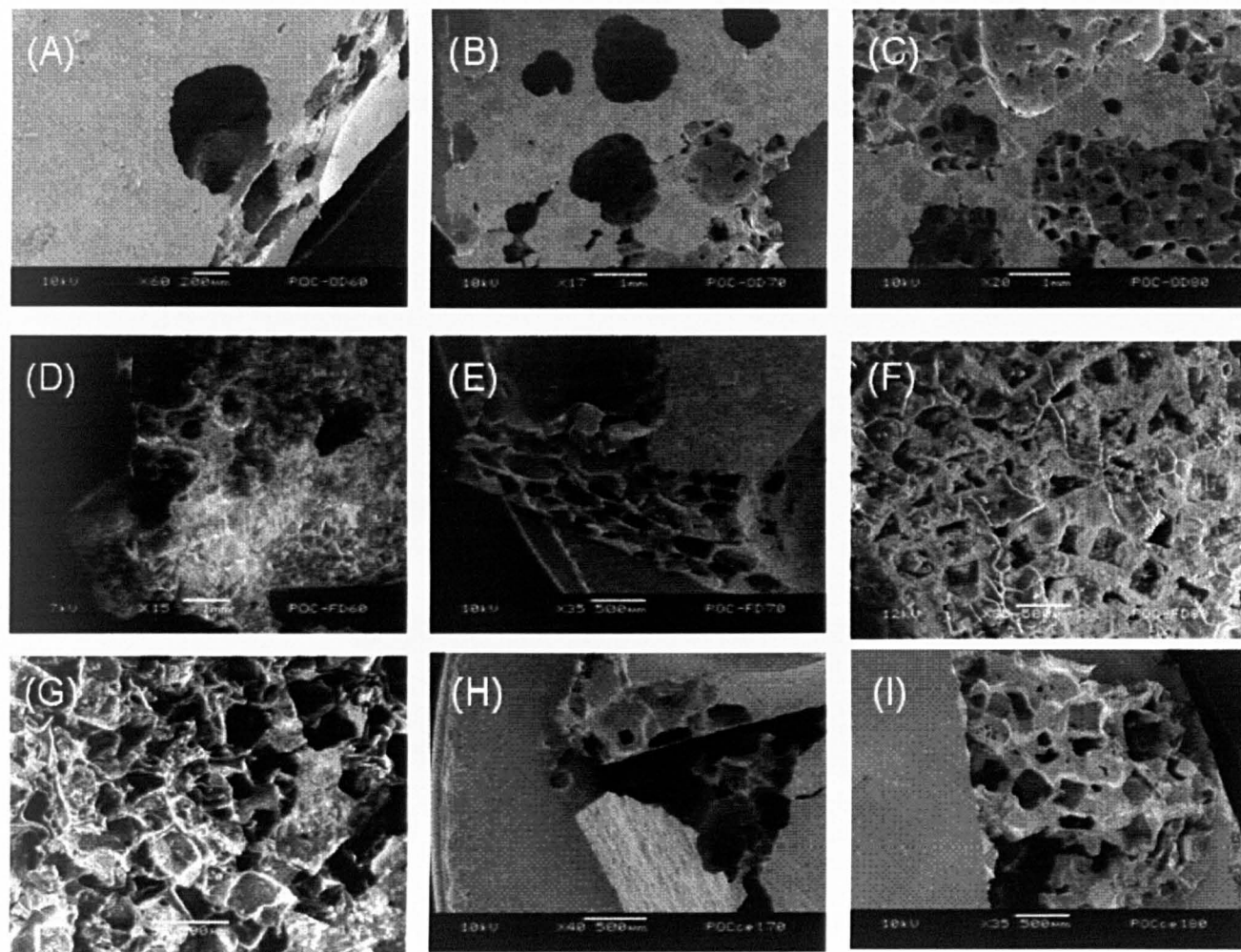


Figure 3-9 SEM images from sections of (A) 60%, (B) 70% and (C) 80% porous POC scaffolds stored at room temperature; (D) 60%, (E) 70% and (F) 80% POC porous scaffolds stored at -20°C and of (G) 60%, (H) 70% and (I) 80% POC/cellulose scaffolds stored at room temperature

THEORETICAL POROSITY	POROSITY	POROSITY
	MICROCT	HE PYCNOMETRY
60%	61.06 ( $\pm$ 1.20) %	61.04 ( $\pm$ 5.42) %
70%	69.56 ( $\pm$ 2.59) %	71.67 ( $\pm$ 1.04) %
80%	80.80 ( $\pm$ 1.17) %	79.33 ( $\pm$ 0.81) %

**Table 3-1 Porosity of POC scaffolds (n=3 for microCT; n=9 for He pycnometry)**

MEAN PORE SIZE	MEAN PORE SIZE
ACCORDING TO MICROCT	ACCORDING TO SEM
365.66 ( $\pm$ 16.25)	242.33 ( $\pm$ 41.54)

**Table 3-2 Mean Pore size (StDev) of POC scaffolds (n=3 for microCT; n=9 for He pycnometry)**

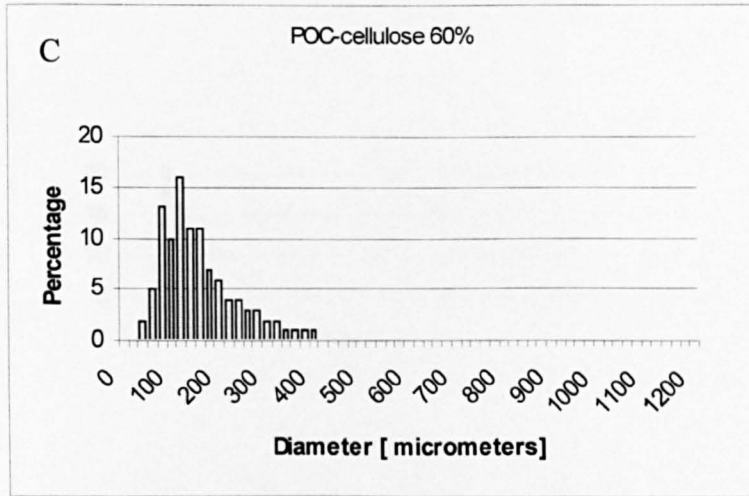
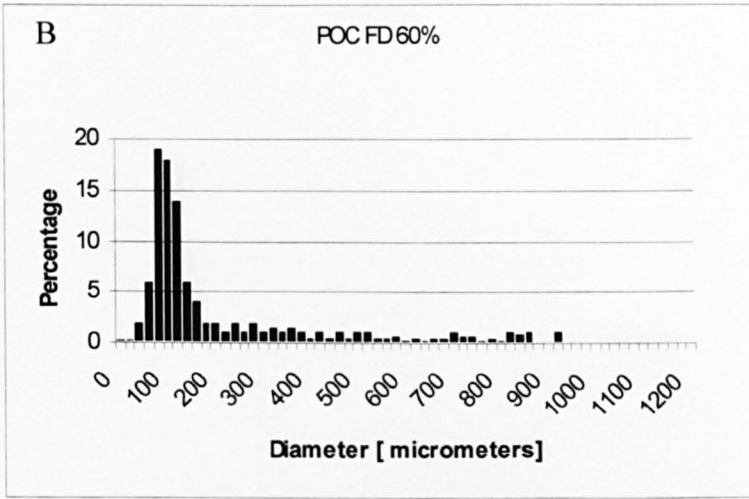
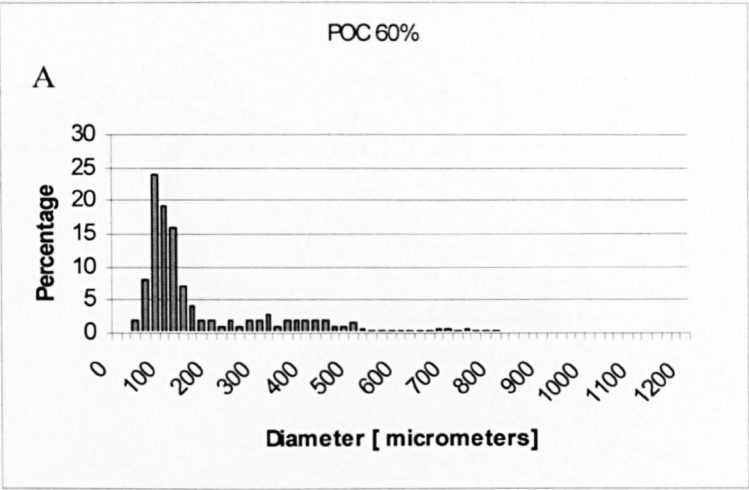


**Figure 3** Histograms of pore size distribution of (A) POC scaffolds, (B) POC freeze-dried and (C) POC/cellulose. Data obtained from microCT analysis of POC scaffolds 60% porous.

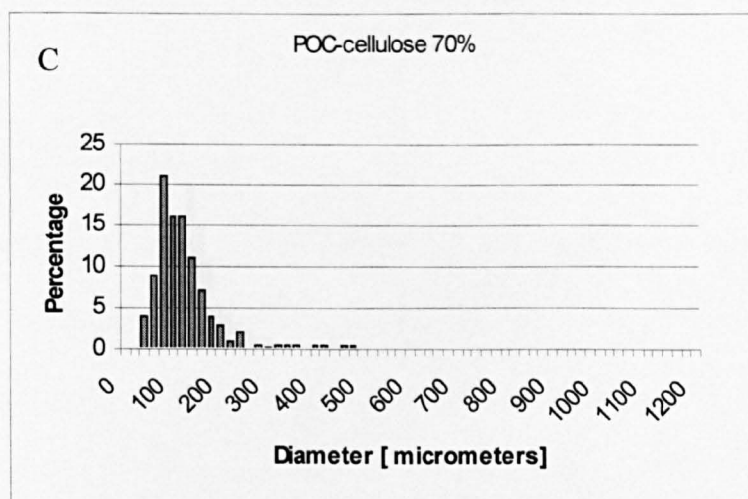
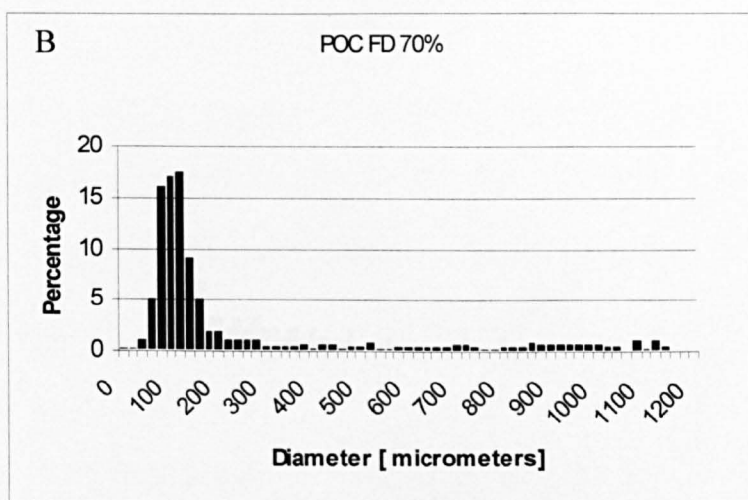
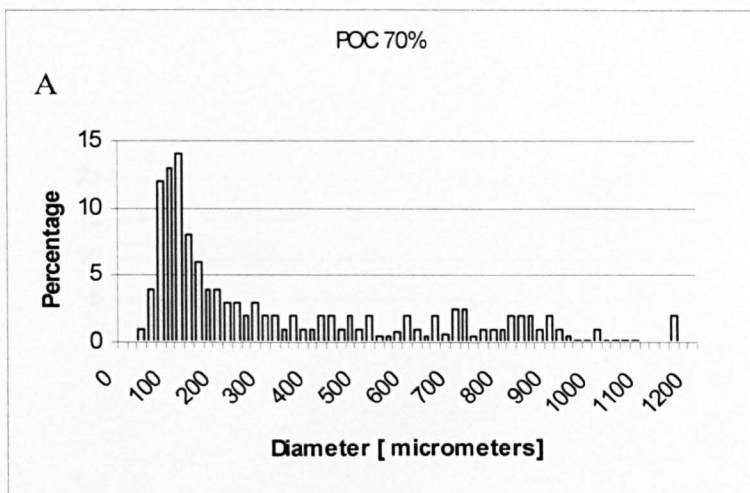


**Figure 3-11** Histograms of pore size distribution of (A) POC scaffolds, (B) POC freeze-dried and (C) POC/cellulose. Data obtained from microCT analysis of POC scaffolds 70% porous.

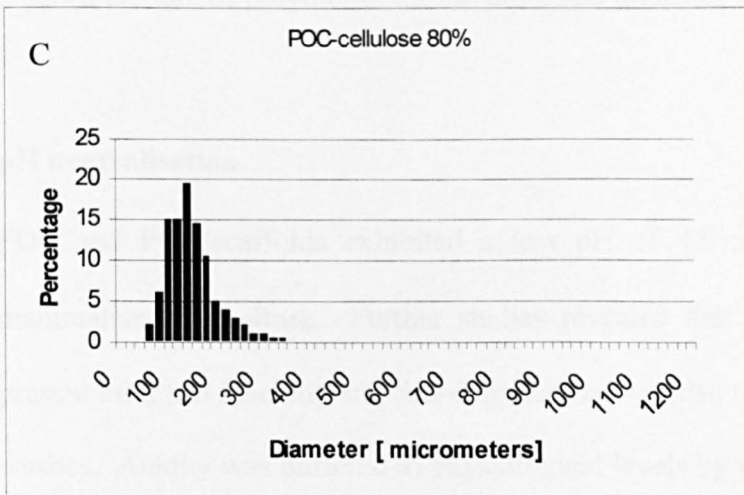
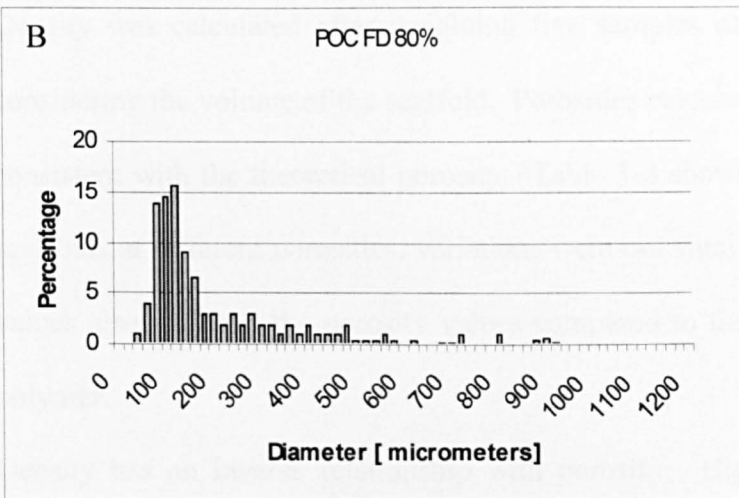
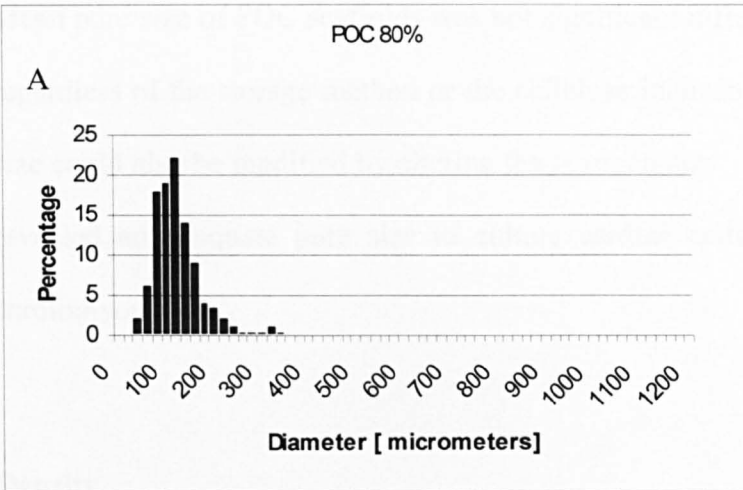


**Figure 3-12** Histograms of pore size distribution of (A) POC scaffolds, (B) POC freeze-dried and (C) POC/cellulose. Data obtained from microCT analysis of POC scaffolds 80% porous.

Mean pore size of POC scaffolds was not significantly different from each other regardless of the storage method or the cellulose inclusion (Table 3-3). Pore size could also be modified by altering the porogen size. In that case the SEM revealed an adequate pore size to culture cardiac cells due to the size of cardiomyocytes.

### **Density**

Density was calculated after weighting five samples of each randomly and considering the volume of the scaffold. Porosities calculated by the density are consistent with the theoretical porosity. Table 3-4 shows the density of POC scaffolds at different porosities, variations were not significant. These density values also matched the porosity values compared to the solid density of the polymer.

Density has an inverse relationship with porosity. High porosities mean a reduced amount of polymer in the structure and therefore a lower density.

### **pH neutralisation**

POC and POC/scaffolds exhibited a low pH of  $4.0 \pm 0.4$ , unsuitable for mammalian cell culture. Further studies revealed that acidic residues were present after salt leaching and that degradation was also triggered by the dH<sub>2</sub>O washes. Acidity was buffered to physiological levels by washing subsequently with PBS. The pH neutralisation in small volumes of buffer washes, 100 ml per scaffold, took more time than when washed in large PBS volumes, 4 litres,

CONDITION	PORE SIZE (StDEV)
Stored at room temperature	242.33 ± 41.54
Stored at -20°C	269.33 ± 9.50
POC/10% cellulose scaffolds	255 ± 38.43

**Table 3-3 Pore size between RT, -20, + cellulose (microCT) (n=3 for microCT; n=9 for He pycnometry)**

	DENSITY [g/cm <sup>3</sup> ]	POROSITY
Solid POC	1.2469 ± 0.0147	
60%	0.4746 ± 0.01929	61.94%
70%	0.3781 ± 0.0079	69.68%
80%	0.2582 ± 0.0050	79.27%

**Table 3-4 Density of POC scaffolds at different porosity values (mean values ± SD, n=3)**

as is presented in Figure 3-13. After stabilising the pH, scaffolds were freeze dried and stored, either at -20°C or at room temperature. Another approach to clear the acidic remains of the polymerisation include the use of supercritical fluids to wash the undesirable residual monomers; unfortunately, as mentioned before, both monomers were not soluble in scCO<sub>2</sub> and therefore this method was ineffective (Figure 3-14).

### **Degradation profile**

The construct was designed to be used as an implant and therefore it is required to study the degradation profile, how long will it last inside a host and how long will it support the seeded cells. It is also important to see if there was an excess of by-products that could trigger immunological responses.

POC scaffold are hydrophilic and when placed in aqueous solution they absorbed water and swelled, increasing their volume up to 30%. This large swelling degree is comparable to collagen as reported by Radisic *et al* [70]. Initial leaching out and pH buffering washed the remaining acidic residues in a process that is not considered as degradation.

Rapid degradation by hydrolysis was observed as scaffolds lost around 25% of their weight in the first four weeks. Degradation slowed down on the second and third month losing 10% in average; however the final stage of degradation was rapid again from the fourth month, when only 18-28% of the scaffold remained. The majority of the scaffolds were a thin jelly-like film by the 22<sup>nd</sup> week, whereas by the 25<sup>th</sup> week most of them were totally degraded.

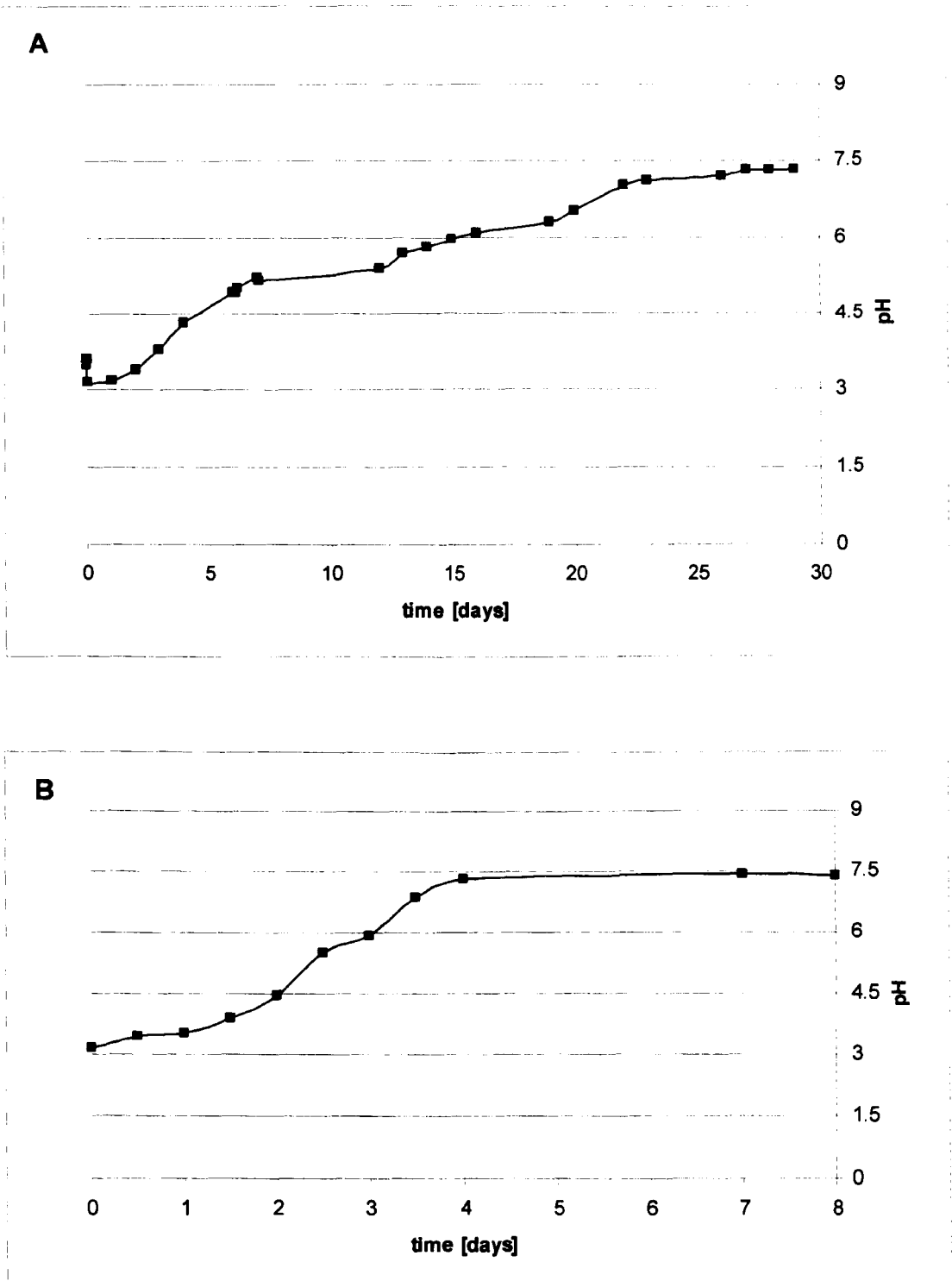


**Figure 3-10** pH neutralisation of a POC scaffold washed in (A) 100 ml and (B) 4,000 ml of PBS

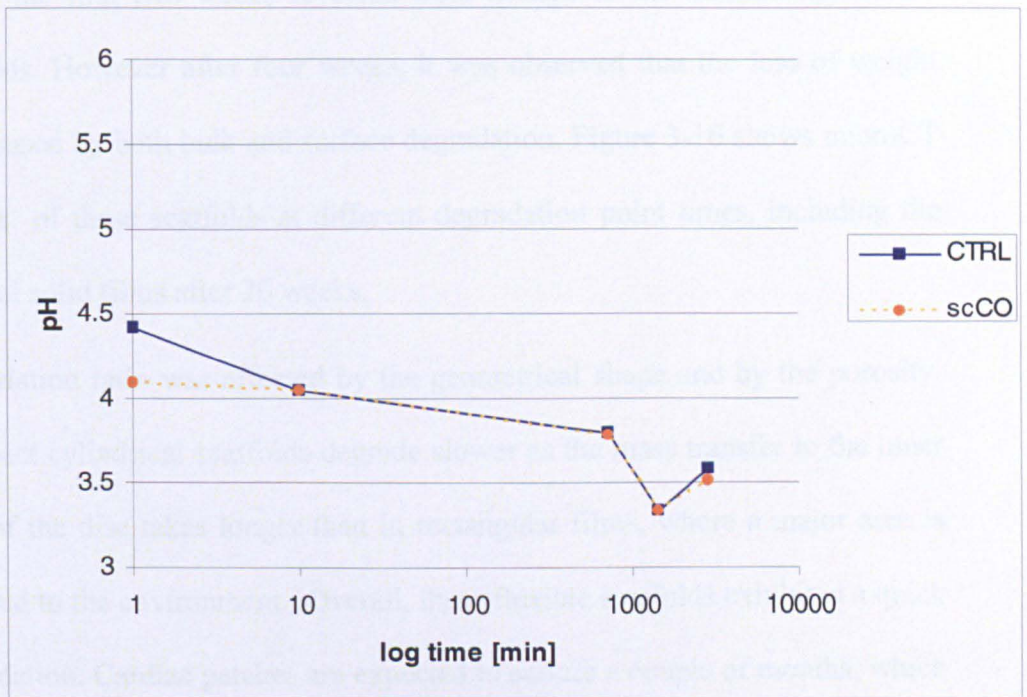


**Figure 3-11 pH variation of POC scaffolds washed in scCO<sub>2</sub> compared to untreated POC scaffolds overtime**

Also, as can be seen in Figure 3-15, 80% porous POC scaffolds showed a slightly faster degradation profile than 60% and 70% porous scaffolds, although no significant difference was observed. MicroCT analysis of samples during the first two weeks revealed little change in the morphology of the scaffolds. However after four weeks, it was observed that the loss of weight was caused by both bulk and surface degradation. Figure 3-16 shows microCT images of these scaffolds at different degradation point times, including the residual solid films after 26 weeks.

Degradation ratio was affected by the geometrical shape and by the porosity. Compact cylindrical scaffolds degrade slower as the mass transfer to the inner core of the disc takes longer than in rectangular films, where a major area is exposed to the environment. Overall, these flexible scaffolds exhibited a quick degradation. Cardiac patches are expected to endure a couple of months, which in addition to the previous weeks, when the material was processed and conditioned, it would be expected to maintain its integrity for at least three months. A slower degradation profile could be tailored by increasing the crosslinking of the polymer.

### **Mechanical properties**

Previous works on the mechanical properties of non-porous POC films reported that the elastomer has an ultimate elongation of 260% and a Young's modulus of 2.6 MPa [41]. However scaffolds fabricated with POC for soft tissue application showed a decreased elongation of less than 100% and a Young's modulus of 0.5 MPa [141].

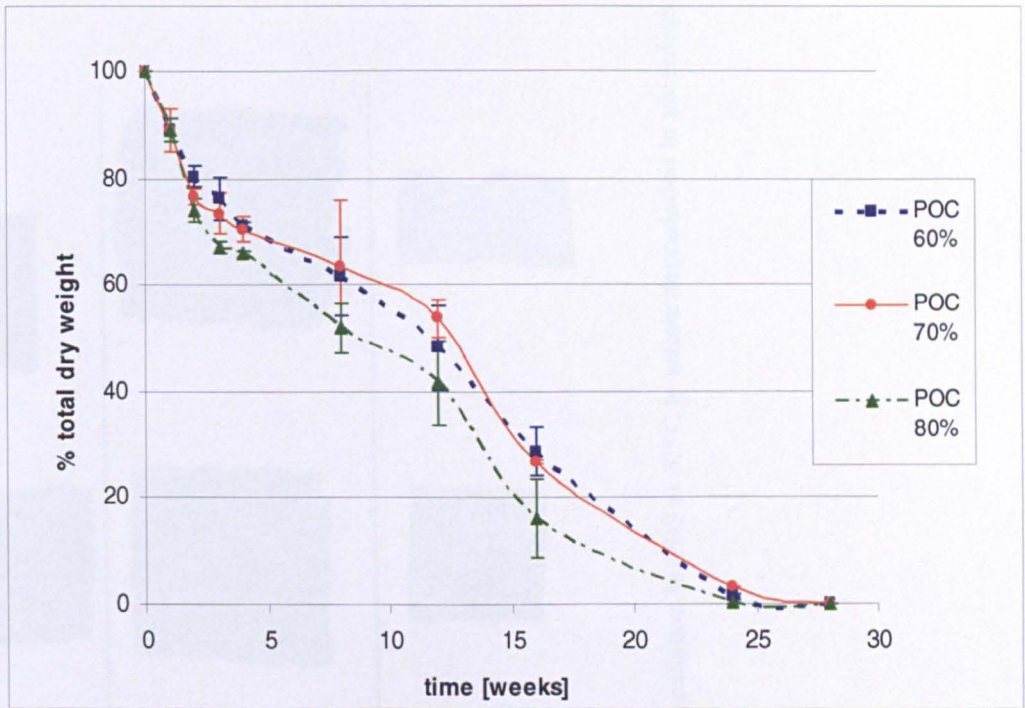


**Figure 3-12** Degradation overtime of POC films incubated in PBS at 37°C (mean values  $\pm$  SD, n=3)

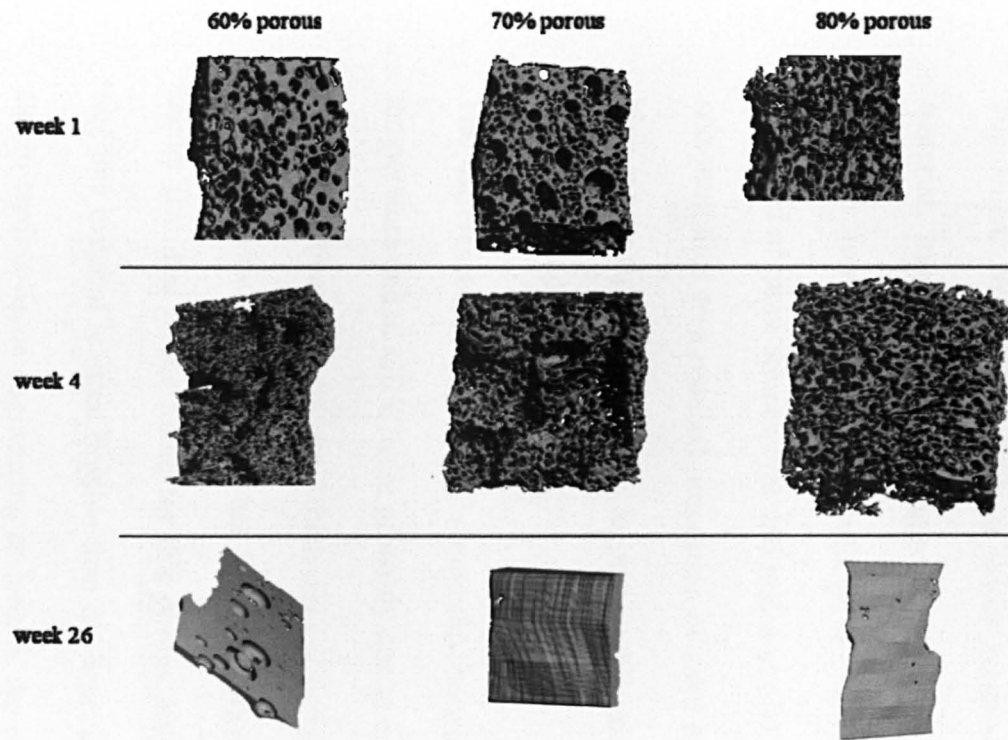
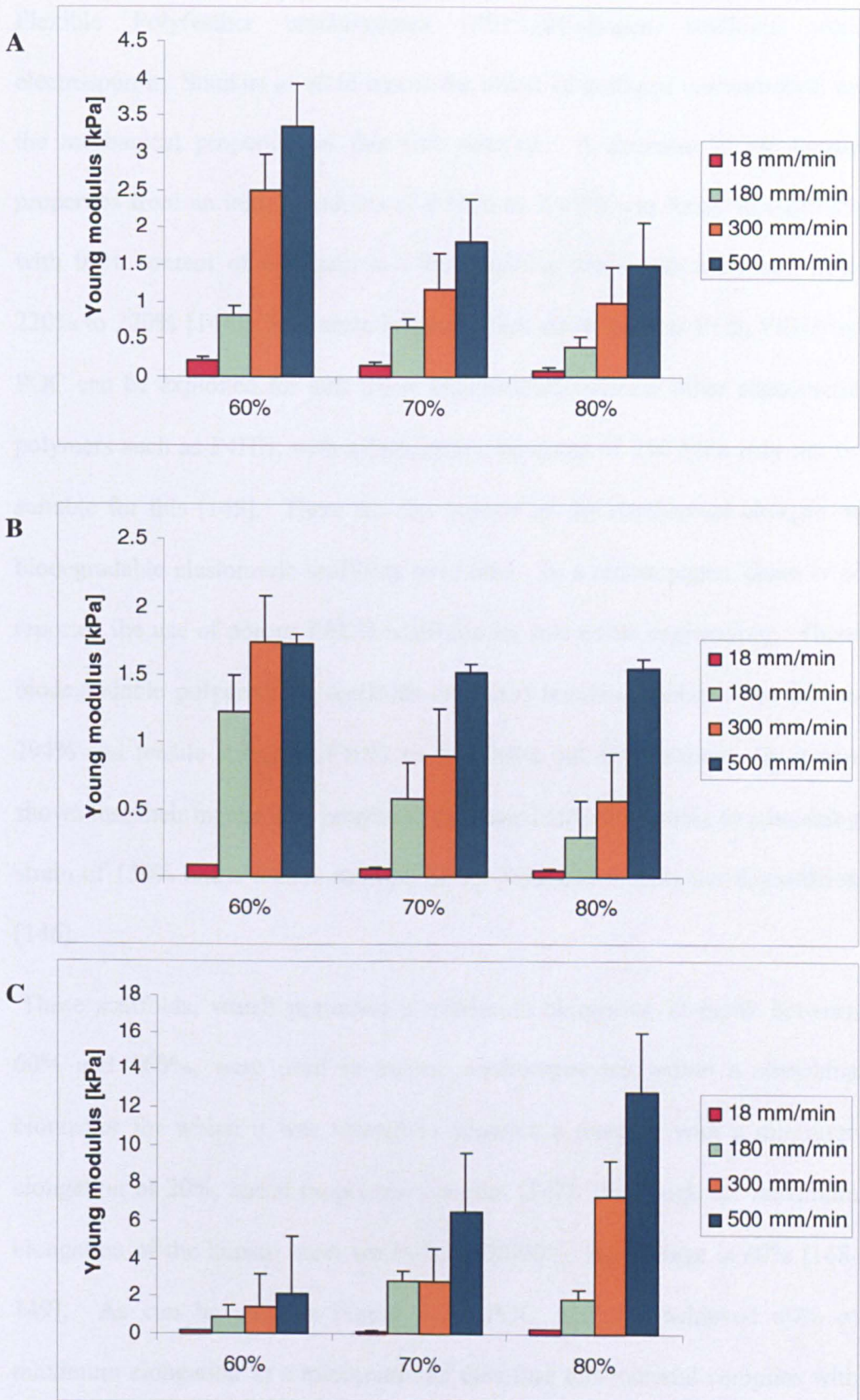


Figure 3-13 MicroCT images of 60, 70 and 80% porous scaffolds after incubation in PBS at 37°C to mimic degradation in physiological conditions. Scaffolds after 26 weeks were solid POC films

It was found that after processing, the mechanical properties of these scaffolds were weakened by the presence of pores, POC films exhibited a Young's modulus that ranged from 1.5 to 3.3 kPa. Alterations in the Young's modulus were observed when the strain rate and the porosity were modified. An increment of the strain rate during the tests exhibited an increased Young's modulus in all the specimens. This is congruent with this elastomer, as an augmented strain rate equals a lower temperature and therefore a stiffer material. In addition, the Young's modulus decreased in scaffolds with higher porosity, from 3.5 KPa – 1.5 kPa for 60% - 80% porous scaffolds respectively, all stored at room temperature and tested at 500 mm/min (Figure 3-17). This was attributed to a reduced proportion of solid material in the scaffolds and a high percentage of voids due to pores weakening the mechanical properties resulting in less stiff structures.

The differences in the Young's modulus between scaffolds stored at room temperature and at -20°C were probably due to continued cross-linking during storage at room temperature, which did not occur at -20°C. The stiffness of the left ventricle of the heart has been calculated at 31 kPa [142], which is higher than the values found for this porous polymer scaffold. This suggests that this material is more flexible than the heart and that could be suitable for use in cardiac tissue engineering as long as the maximum elongation and the fatigue values matches those of the native tissue. Studies using other biodegradable elastomers have reported similar mechanical properties to proteins found in human tissues. Wang *et al.* synthesised a biocompatible biodegradable-elastomer, poly(glycerol-sebacate) (PGS), that exhibited a low Young's modulus of 0.28 MPa and a minimum elongation of 267% [143].



**Figure 3-14** Young's modulus of POC scaffolds stored (A) at room temperature, (B) at -20°C and (C) POC/cellulose scaffolds strained at 18, 180, 300 and 500 mm/min. (mean value  $\pm$  SD, n=3)

Flexible Poly(ester urethane)urea (PEUU)/Collagen scaffolds were electrospun by Stankus *et al.* to assess the effect of collagen concentration on the mechanical properties of this soft material. A decrease in the tensile properties from an initial modulus of 8 MPa to 2 MPa was found in scaffolds with 90% content of collagen, but the breaking strain was increased from 220% to 270% [144]. Soft materials with high strain such as PGS, PEUU or POC can be exploited for soft tissue applications, whereas other elastomeric polymers such as P4HB, with a high elastic modulus of 250 MPa may not be suitable for this [145]. There are few reports on the mechanical changes of biodegradable elastomeric scaffolds over time. In a recent paper, Guan *et al* reported the use of porous PEUU scaffolds for soft tissue engineering. These biodegradable polyurethane scaffolds exhibited breaking strains from 214 to 294% and tensile strength of 0.97 to 1.64 MPa but most importantly it was shown that their mechanical properties decreased after two weeks to a breaking strain of 150% and a tensile strength of 0.8 MPa due to polymer degradation [146].

These scaffolds, which presented a maximum elongation at break between 60% and 160%, were used to culture cardiomyocytes within a stretching bioreactor for which it was wanted to generate a material with a minimum elongation of 20%, based on previous studies [147]. Although the maximum elongation of the human heart varies from 20-90%, the average is 60% [148-149]. As can be seen in Figure 3-18, POC scaffolds achieved 60% of maximum elongation as a minimum and therefore this material complies with the physiological parameters required for cardiac tissue engineering.

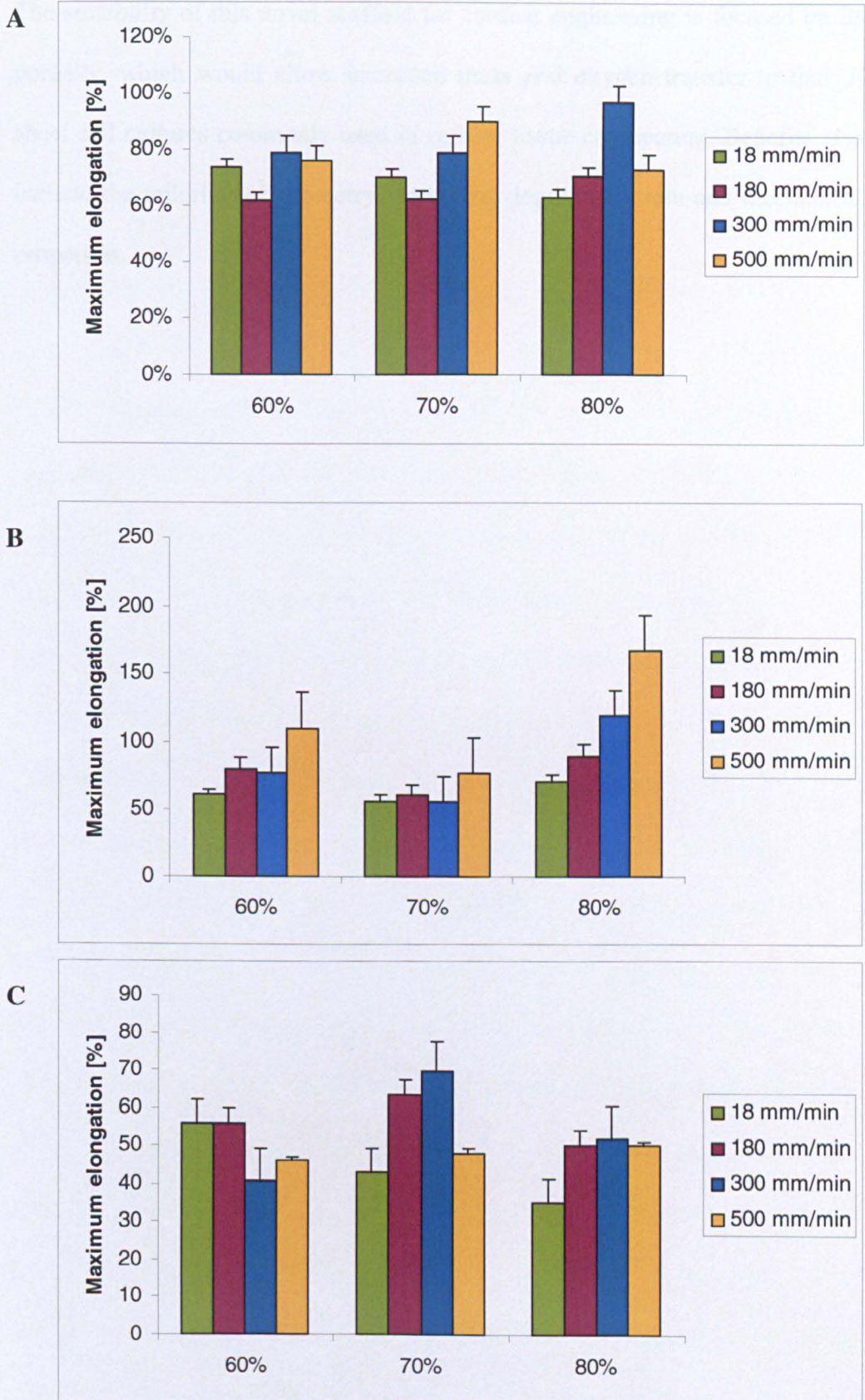


**Figure 3-15** Maximum elongation of POC scaffolds stored (A) at room temperature, (B) at  $-20^{\circ}\text{C}$  and (C) POC/cellulose scaffolds strained at 18, 180, 300 and 500 mm/min. (mean value  $\pm$  SD,  $n=3$ )

The suitability of this novel scaffold for cardiac engineering is focused on its porosity, which would allow increased mass and oxygen transfer to that of sheet cell cultures commonly used in cardiac tissue engineering. Benefits also include the tailoring of geometry, pore size, degradation rate and mechanical properties.

### 3.4 Conclusions

Physical and mechanical characteristics of a tissue engineering scaffold are of major importance as it must withstand the environmental stresses and strains that the native tissue undergo. These must be true to normal conditions but also during healing and remodelling processes. This chapter presents the processing of POC into porous structures to fabricate elastic scaffolds using two different methods. Table 3-3 shows the advantages and disadvantage of these methods. POC is a novel polymer which can be processed into porous structures to host mammalian cells. The micro-architecture of such scaffolds can be tailored in accordance to the target tissue. High porosities can be achieved in cylindrical scaffolds whereas films are restricted to porosities no higher than 80% in order to guarantee its mechanical strength. Pore size does depend on the processing method. In the case of salt leaching, porogen size and morphology determined pore size distribution. The rectangular films designed to match the dynamic bioreactor were easily produced and differences between batches were not significant. Although the elastic modulus was lower than expected at each porosity, the elongation was superior than anticipated in all the cases. Altogether the mechanical properties exhibited, allowed the use of these scaffolds for cardiac culture in a stretching bioreactor. The degradation profile revealed that the constructs must last until the regenerated tissue populate and take on its structural role. It is expected that the mechanical properties of the construct will decreased more rapidly overtime when it is subjected to cyclic strain than during static culture as observed by Boublik *et al* [150].

	ADVANTAGES	DISADVANTAGES
Supercritical carbon dioxide	<ul style="list-style-type: none"> <li>- Clean technology (no use of solvents)</li> <li>- Allows incorporation of bio-molecules and cells</li> </ul>	<ul style="list-style-type: none"> <li>- Limited materials suitable</li> <li>- Restricted geometry</li> <li>- Small production batches</li> </ul>
Salt leaching	<ul style="list-style-type: none"> <li>- Easy to process</li> <li>- Allows pore size, porosity and mechanical properties tailoring</li> </ul>	<ul style="list-style-type: none"> <li>- Use of solvents is required</li> <li>- Heterogeneous structures in large pieces</li> </ul>

**Table 3-3 Advantages and disadvantages of methods used to process POC**

#### **4 Optimisation of seeding conditions for myocytes in Poly (1,8-octanediol-co-citric acid) films and scaffolds**

*This chapter presents the results obtained after seeding myocytes in two and three-dimensional models. Scaffold morphology and surface chemistry modification as well as different seeding strategies were explored with the intention of setting the operational parameters for cardiomyocyte culture in a dynamic bioreactor.*

## 4.1 Introduction

### 4.1.1 Cardiomyocyte culture

Cardiac cell lines are difficult to establish as they do not retain their electromechanical characteristics for long periods. Cardiac research has been based on the use of primary cells either from rat or mouse; however these cells are obtained after a difficult multi-step procedure. For the isolation of cardiac primary cells, a freshly removed heart must be perfused to remove all the blood and then digested before dissociating the ventricles to obtain a cell suspension. After purifying the cell suspension, the cells are ready to be plated and cultured [151]. Cardiac ECM is a complex network composed of structural proteins (collagen and elastin), adhesive proteins (laminin, fibronectin and type IV collagen), anti-adhesive proteins (tenascin, thrombospondin and osteopontin), proteoglycans, several growth factors and hormones. In addition to this, cardiomyocyte requirement for nutrients is elevated and they are highly susceptible to ischemia [152].

As alternatives to functional cardiac primary cells, smooth muscle and skeletal myoblast cell lines have been proposed as muscle models; C2c12 and h9c2 have generally been used lines for basic research. C2c12 is a mouse skeletal muscle cell line that differentiates rapidly and forms myotubes. This cell line can be shifted from myoblastic to osteoblastic by supplementing the media with bone morphogenic protein 2 (BMP-2). H9c2 is a rat heart myoblastic cell line that also forms myotubes and has been reported as an *in vitro* cell line model to screen drugs [153]. It was not until ten years ago that a mouse cardiac muscle cell line, HL-1, was derived. This cell line can be serially

passaged and still preserve their morphology and physiology, including electromechanical coupling. HL-1 cells have been used in several studies of cardiomyocyte physiology and metabolic activity [30, 154-159].

It is known that when culturing cells, different parameters may be needed to promote either proliferation or differentiation. Selective switching between proliferation and differentiation in cell populations is achieved by combining different culture media with biochemical factors and microstructures [160]. In the case of HL-1 cells, it is recommended to incubate the culture surface with fibronectin/gelatine before plating the cells; additionally the media is supplemented with nor-epinephrine to retain their electrophysiological properties [30].

#### **4.1.2 Cell adhesion**

Anchorage-dependent cells rely not only on physical substrates, such as glass or plastic, for attachment and differentiation, but mainly on proteins. Cell spreading, proliferation and repair pathways are influenced by this and by biochemical adhesion factors on the surface. Biochemical signals may result from the presence of peptides, proteins, carbohydrates and other molecules soluble in the cellular environment [151].

In order to mimic the biological processes during wound healing and tissue remodelling, tissue engineering considers the use of extracellular matrix (ECM) components as a key factor in tissue repair. ECM provides not only the structural support of cells but also the biochemical cues to moderate cell physiology and phenotype. Surface receptors in the cell recognise and translate

these signals into the indicated response. Cell adhesion regulates proliferation and differentiation and involves several receptors. Some receptors mediate adhesion to other cells (leading to assembly of 3D structures), and others adhesion to a physical surface to establish cellular orientation and spatial organisation.

Cell adhesion onto a biomaterial can be either specific, with cell receptor recognition and binding to proteins or peptides, or non-specific, by non-covalent attractive forces between cells and the biomaterial. Both improve cell adhesion and proliferation but in the case of non-specific adsorption, higher concentrations of coating are needed to achieve the same effect that in specific adhesion.

Cell-to-cell adhesion regulates anchor (support cells), filtration and barriers, polarity, migration, metabolism, differentiation and proliferation. The main ECM molecules involved in this are collagen IV and laminin, although collagen XV, XVIII, and glycoproteins also intervene.

### **Surface modification of a biomaterial to improve cell attachment**

Biomaterials should either include or promote ECM production with the aim to mimic cellular environment. By integrating a material with ECM components, cells are able to maintain a stronger interaction with the biomaterial and with adjacent cells.

The first strategy is to biochemically modify material surfaces by adsorption of ECM proteins. A chemical approach involves ion-exchange reactions, dissolutions, and degradation to immobilise and attach compounds to surfaces.

Covalent coupling is also possible either by enzymatic attachment or during matrix formation. Bioactive surfaces incorporate proteins to elicit particular cell responses. Peptides are also used as these are recognisable sequences of ECM proteins such as RGD, present in fibronectin and YIGSR from laminin. Peptides do not exhibit differences in cell adhesion to that achieved with their native proteins; however it has been shown that they do not promote the same signalling for cellular physiology [161].

For cell to surface adhesion, ECM proteins are also used in addition to different compounds such as matrigel and serum, which contain adhesion factors such as fibronectin and vitronectin. Although most of them are well characterised, some compounds, such as serum have the disadvantage of being unreliable caused by its animal origin and the unpredictability of unknown components [162].

Collagen is the most common compound used to modify surfaces as it represents nearly one third of all proteins in the human body. Cardiac connective tissue is composed of fibronectin, laminin and elastin in addition to the collagen. Collagen is the major component of cardiac tissue, comprising 85% of it and acting as the structural support for electro-mechanical contraction [163]. It has been observed that changes in the load affect the ECM, which changes in response to this. After myocardial injury, remodelling of the tissue starts with collagen fibre degradation followed by further development of type III collagen accumulation which prevents dilatation of the infarcted area. However when an excessive deposition of collagen occurs, collagen production leads to fibrosis, which accounts for stiffer muscle, arrhythmias and decreased cardiac function. This process is regulated by

antifibrotic factors such as Atrial Natriuretic Peptide (ANP) and Brain Natriuretic Peptide (BNP) [164-166].

Besides the other main ECM proteins laminin and fibronectin, fibrin glues, hyaluronic acid and alginates are also used for clinical applications, including the coating of implants. Table 4-1 shows the three main ECM proteins, their location and their function. Coatings are also used to direct cell growth into specific patterns. Precise configurations are achieved by polymer lithography, photo-lithography, deposition or printing of concentration gradients. These differences in surface structure prompt distinctive responses at different times. These techniques also allow for specific cell distribution and mixed cultures [43].

### **Morphological modification of a biomaterial to improve cell attachment**

Scaffold morphology has been shown to affect cellular proliferation and differentiation. Porosity and pore size can induce different cellular responses with changes in morphology and phenotypic expression, fluctuating considerably with cell type and biomaterial.

Scaffold porosity affects the availability of nutrients and oxygen. Higher porosity provide low resistance to mass transfer and therefore the supply of nutrients and waste exchange is less restricted than in scaffolds having a lower porosity. However, in the case where mechanical stability can be jeopardised by high porosity, it may be considered to compromise on a lower porosity to

PROTEIN	LOCATION
type I Collagen	Connective tissue, wound healing
type II Collagen	Cartilage
type IV Collagen	Basement membrane
type VII Collagen	Skin and Mucosa
type VIII Collagen	Endothelial, support endostatin formation
type X Collagen	Hypertrophic cartilage
Fibronectin	Plasma, connective tissue & basement membrane, binds cell surfaces and ECM. Control of migration, wound healing, proliferation and blood coagulation
Laminin	Basement membrane, regulate migration, embryonic development and neural system

**Table 4-1 Principal ECM proteins used in surface modification of biomaterials for cell adhesion [161-163]**

assure the mechanical stability of the construct. Van Tienen *et al.* reported that in scaffolds with low values of porosity and pore size, degradation began before the material was populated by the cells. However, they also reported that even in scaffolds with greater porosity and pore size, ingrowth was completed in the construct but the mechanical properties were also compromised by degradation [167].

Pore size affects cellular orientation and spatial organisation by facilitating cell to cell contact, metabolic activity, adhesion and migration into the structure. Although large pores may facilitate other processes, certain cells are not capable of bridging pores greater than their own diameter. Zeltinger *et al* evaluated the effect of porosity and pore size in fibroblasts, myocytes and epithelial cells and found that the minimal acceptable value to influence the cellular response in a positive way was a porosity of 90% and a pore size no greater than 38 $\mu\text{m}$  [168]. O'Brien *et al.* compared the cell adhesion of 3T3 cells in collagen-glycosaminoglycan (CG) scaffolds having four different porosities, between 95 and 150  $\mu\text{m}$ . They found that for these cells attachment decreased as the pore size increased [169]. According to the literature cell adhesion and proliferation is promoted by the size of the pores and by the type of porogen used to process the scaffolds when endothelial cells were used [170].

#### **4.1.3 Seeding strategies for scaffolds**

The techniques used to seed cells into scaffolds can be classified into static and dynamic methods. Static seeding consists of either repipetting concentrated

cell suspensions into a three-dimensional scaffold or dripping the suspension and allowing it to passively infiltrate the matrices by gravity.

Dynamic seeding includes dispersion by agitation, filtration, seeding on continuous/pulsatile perfusion chambers or seeding enhanced by vacuum, centrifugal or magnetic forces [43, 171-174]. Radisic *et al* compared two dynamic set-ups, an orbital shaker at 25 rpm and a perfusion cartridge at 0.5 mL/min and found that cell viability and live cell yield decreased in dishes [175]. Shimizu *et al* reported high seeding efficiency of smooth muscle cells and fibroblasts into *ex vivo* scaffolds when using “Mag-seeding”. This novel method labels cells with magnetic composites whilst a magnet is incorporated into the scaffold. The magnet-scaffold is then submerged in the labelled-cell suspension where cells are attracted to the scaffold. This procedure also allows the use of mixed population of cells in one scaffold [176].

Immobilisation and encapsulation of cells guarantee high concentration of cells in the scaffold but limit cell migration and mass transfer, leading to cell death in the core of the structure [173]. Seeding efficiencies of static and dynamic methods vary depending on the cell type and biomaterial architecture.

#### **4.1.4 Aims**

The aim of this chapter was to optimise myocyte culture for three-dimensional myocyte culture in POC scaffolds using 2D POC film models. The first objective was to assess the effect of modifications in the biomaterial surface and architecture. The hypothesis was that the adsorption of cardiac ECM proteins to the POC surface would improve cell adhesion and survival. In

addition to this it was expected that higher porosities should promote increased survival when compared to lower porosities.

The second objective was to analyse different seeding techniques to determine the most favourable seeding conditions. The hypothesis was that dynamic seeding would promote a more homogeneous cell distribution and attachment whilst static seeding would confine cells to limited areas, influencing viability and phenotype as a consequence. Dynamic seeding techniques result in constructs with increased cellular density and ECM production when compared to static strategies [167]. Nevertheless dynamic seeding could also impair cell adhesion for some cells and so it was relevant for the project to evaluate the effect of high agitation rates for these cells and this material.

## **4.2 Materials and methods**

### **4.2.1 Manufacture of POC films**

The POC films were manufactured as in section 2.4. Briefly 10 g of powdered citric acid was added to 7.61 g of powder 1,8-octanediol and melted at high temperature. POC pre-polymer solution (POC in acetone) was then placed in PTFE moulds to cure at 80°C for two weeks.

### **4.2.2 Casting of POC scaffolds**

POC scaffolds were processed as previously described in Section 2.1.2.2. POC pre-polymer solution was dissolved in acetone at 33.3% (w/v) before being added to a PTFE mould containing sodium chloride. The mixture was allowed to

polymerise for two weeks and was then washed in distilled water to remove the porogen particles.

### **4.2.3 Cell culture**

HL-1 cardiomyocytes were obtained from Dr. Claycomb ((Louisiana State University - Health Sciences Center, USA) and cultured as described in Section 2.2.1. HL-1 cells used in the studies discussed in this chapter were between passages 61-75. C2c12 myocytes were obtained from the ECCAC and cultured as detailed in Section 2.2.2. C2c12 cells used for seeding experiments were between passages 40-58.

### **4.2.4 Seeding cells into scaffolds**

Scaffolds were prepared for cell culture as described in section 2.2.3. Scaffolds were conditioned for cell culture and sterilised before being seeded either with HL-1 cells or with c2c12 cells as described in section 2.2.5. Briefly, cells were trypsinised and re-suspended in cell culture medium to a concentration of  $3.2 \times 10^5$  cells per mL. For static and dynamic seeding techniques, 250  $\mu$ L of the cell suspension was pipetted through each scaffold in a 6-well non-tissue culture treated plate and allowed to incubate for 30 minutes before adding 5 mL of media. Static seeded constructs were incubated for 24 hours before analysing cell survival. Dynamic seeded constructs were immediately agitated in an orbital shaker at 100, 200 and 300 rpm for 24 hours.

Scaffolds were seeded in triplicate for cell viability assays and image analysis and were assessed after 24 hours.

Centrifugation seeding was achieved by placing a conditioned scaffold in a 15 mL Falcon tube containing 5 mL of a  $16 \times 10^3$  cells/mL cell suspension. The tube was centrifuged at 7000 rpm (13,000 x g) for 7 minutes. Supernatant was discarded and the resultant construct was incubated at 37°C for 24 hours before being analysed for cell survival.

#### **4.2.5 Surface modification**

The POC film surface was modified as described in Section 2.3.2. Protein suspensions were prepared for fibronectin, collagen and laminin at their optimum concentration for myocyte culture and then serially diluted to assess the effect of the concentration on cell survival.

#### **4.2.6 Analysis of cell viability**

Relative cellular viability was assessed by the Alamar blue assay as described in Section 2.4.1. Briefly, the constructs were transferred to a 24-well plate and washed three times with PBS. Samples were incubated with 1 mL Alamar blue working solution for 90 minutes at 37°C. Samples were shaken for 15 minutes and then analysed in a fluorescence plate reader at excitation and emission wavelengths of 530 nm and 590 nm respectively. The number of cells was calculate using the calibration curve for the cells.

Scaffolds conditioned for cell culture but not seeded were used as controls; these were also incubated and analysed for Alamar blue after 24 hours.

#### **4.2.7 Inverted microscopy and total area**

Images of c2c12 and HL-1 monolayer culture were taken as described in section 2.5.1. Briefly random images were taken at high magnification (20x) and then analysed for area coverage using Leica QWin software associated with the microscope.

#### **4.2.8 Imaging of cells on scaffolds**

POC scaffolds and constructs were analysed by light microscopy and SEM as described in Sections 2.5.4 and 2.5.5. In brief, samples were fixed and stored at 4°C. Before processing samples in osmium tetroxide they were washed and dehydrated. After treatment specimens were sputter-coated in gold before using a field emission scanning electron microscope Jeol.

#### **4.2.9 Statistical analysis**

Data was analysed for mean values and standard deviation using Microsoft Excel 2002 as described in Section 2.6.

## **4.3 Results and Discussion**

### **4.3.1 Monolayer culture of c2c12 and HL-1 cells**

The c2c12 line is a mouse myoblast cell line widely used for myogenesis research. These cells proliferate rapidly and provide a model for studies involving a large numbers of cells such as the seeding experiment. HL-1 is a cardiomyocyte cell line which takes longer to proliferate, however this is the only cardiac cell line characterised for cellular biology. It was considered to assess both, a myoblast cell line and a cardiomyocyte cell line to investigate the compatibility of muscle cells to the flexible biomaterial. Although the target application was cardiac tissue engineering, it was considered that evaluating the material with another muscle line could provide valuable information. C2c12 cells were also thought as a surrogate cells for experiments that require large amount of cells in the case that HL-1 cells did not reach the quantity required. C2c12 cells and HL-1 cells inspected visually with an inverted microscope did not display conspicuous morphological changes when cultured as monolayers on tissue culture plastic (TCP) flasks. Moreover both cell lines behaved as expected and exhibited elongated phenotype as can be seen in Figure 4-1. C2c12s organised more rapidly into myofibres than HL-1s. However, HL-1 cells exhibited contraction when confluence was greater than 70%; normal contraction ratios were observed with some areas of synchronic beating when confluence was higher than 80%. Myocytes were seeded on POC films to assess the biocompatibility of the material with these cells. SEM images of monolayer culture of c2c12 cells on POC were analysed for cell coverage, showing poor attachment to the surface of uncoated films when compared to area coverage in untreated TCP (Figure 4.1A and B). HL-1 cells

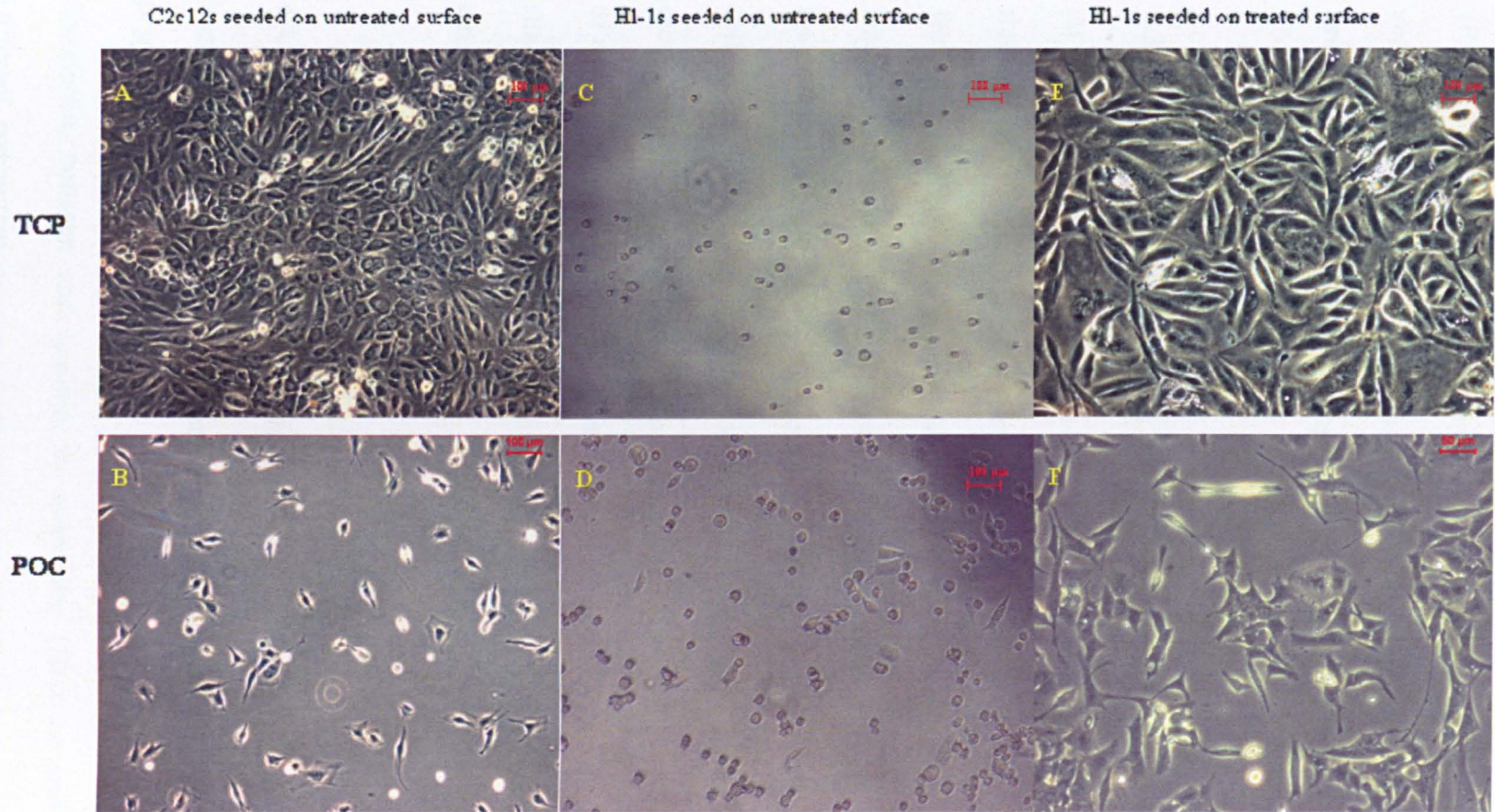


Figure 4-1 Images of c2c12 myocytes cultured on untreated (A) TCP and (B) POC film and HL-1 cardiomyocyte monolayer cultures on (C) untreated TCP, (D) untreated POC, (E) treated TCP and (F) treated POC. TCP images are on day 3 while in POC are on day 1.

displayed the same attachment levels in POC as in TCP flasks, minimal adhesion on untreated surfaces whilst good attachment on treated materials (Figure 4-1 C - F). This difference in cell attachment was caused by the surface modification which was pre-coated with gelatine/fibronectin for HL-1s as previously recommended by the supplier.

### **4.3.2 3D culture of c2c12 and HL-1 in POC scaffolds**

At the same time C2c12 and HL-1 cells were cultured in POC scaffolds in three-dimensional structures. Figure 4.2 shows scanning electron micrographs for both cell lines with minimal adhesion. Myotube formation did not occur when the cells were seeded on POC scaffolds and allowed to incubate for 24 hours. SEM revealed no real presence of cells in the scaffold. Low levels of cell adhesion were thought to be caused by a low affinity of the cell surface receptors to POC ligands, the absence of anchoring proteins and the presence of acidic monomers. These two factors were further investigated in subsequent studies to improve cell attachment and proliferation before conducting long term culture studies.

### **4.3.3 Surface coating with Extracellular Matrix (ECM) Proteins**

Surface modification was used to improve cell attachment on POC scaffolds. POC scaffolds were coated by adsorption with three ECM proteins: fibronectin, collagen and laminin, to assess the effect on cell adhesion. Different concentrations were used starting with the optimum reported for

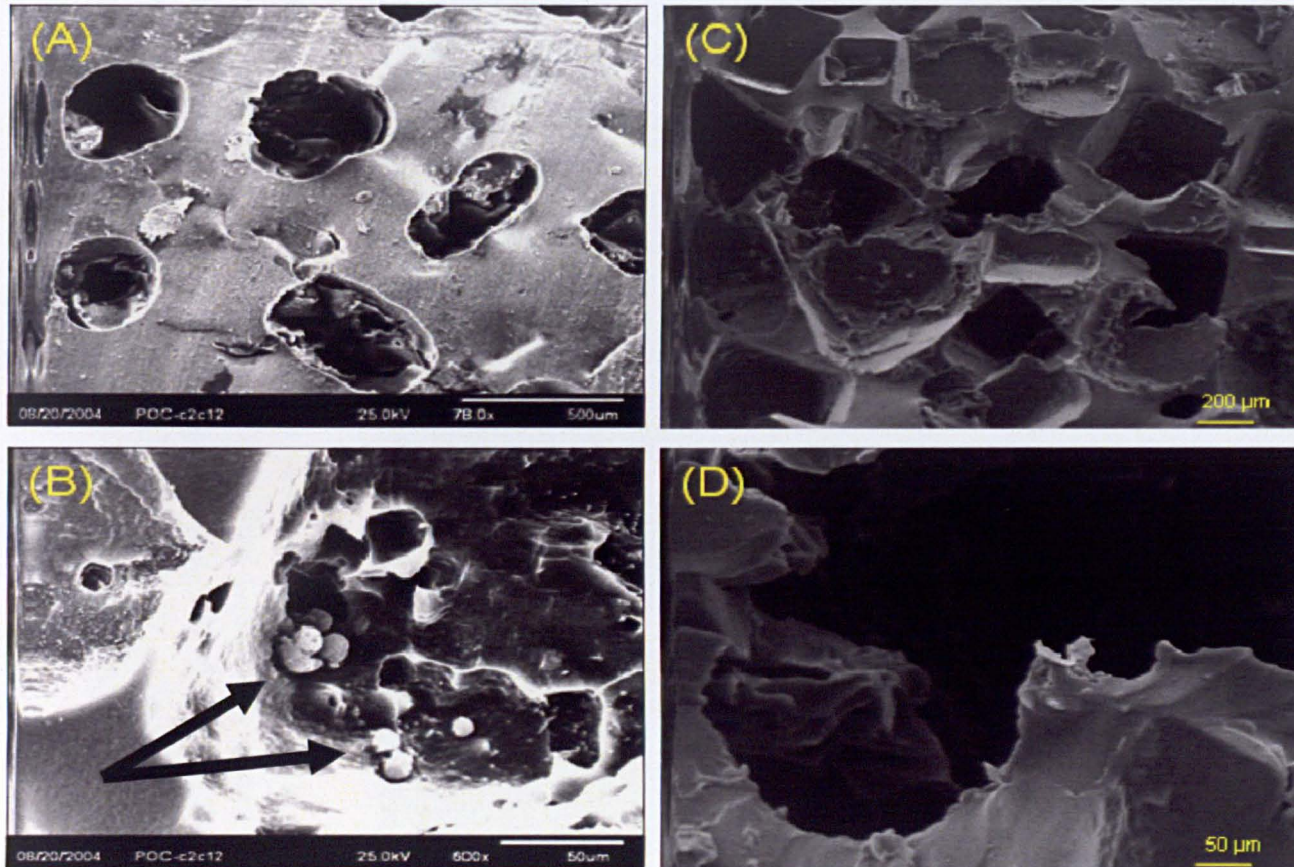
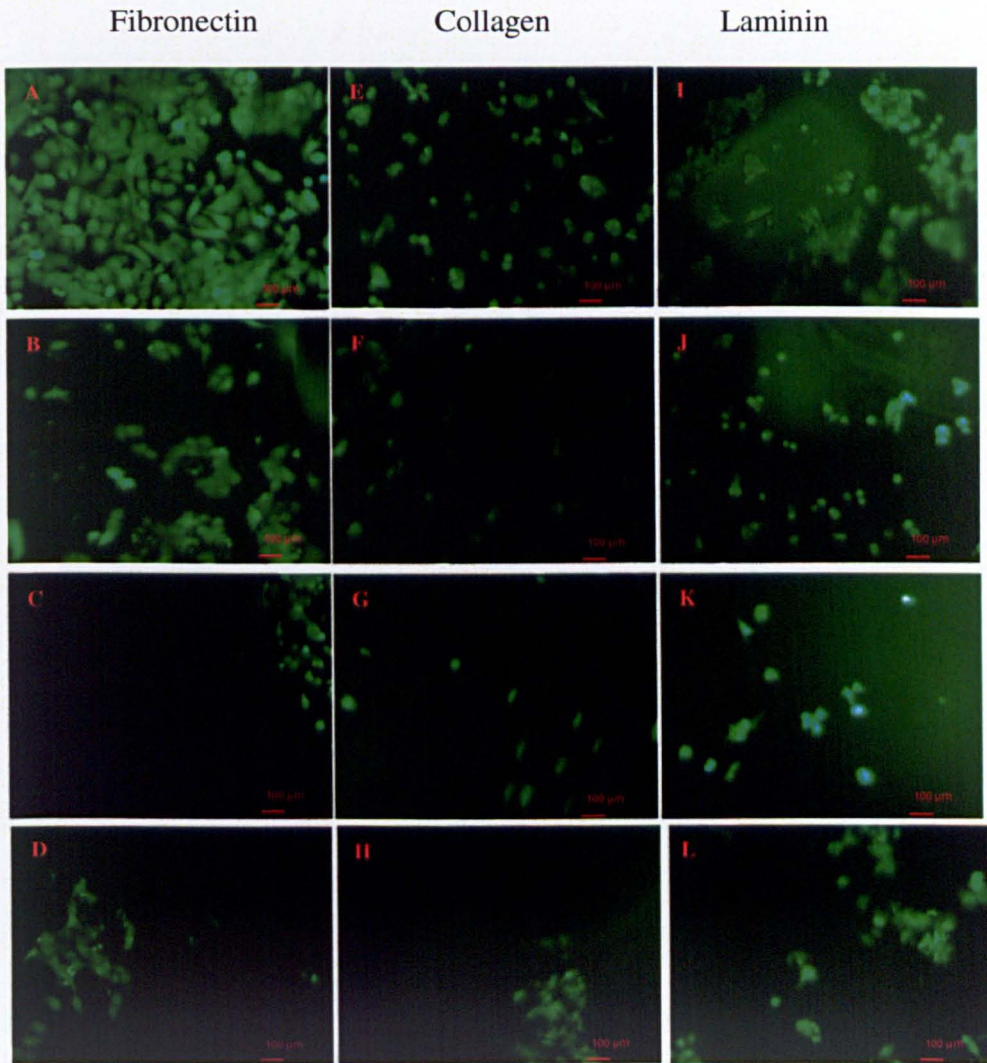


Figure 4-2 Images at low and high magnification of (A-B) c2c12 cells and (C-D) HL-1 cells cultured on un-conditioned POC scaffolds for 24 hours. Poor attachment is caused by the low affinity of the cell surface receptors to POC ligands, absence of proteins on the surface and acidic conditions. Arrows show dead cells.



**Figure 4-3** Representative images of area coverage of HL-1 cells after 18 hours cultured on poly(1,8-octanediol-co-citric acid) [POC] films coated with proteins at different concentrations: Fibronectin (A) 400  $\mu\text{g}/\text{cm}^2$  (B) 40  $\mu\text{g}/\text{cm}^2$ , (C) 4  $\mu\text{g}/\text{cm}^2$  and (D) control-PBS; Collagen (E) 10  $\mu\text{g}/\text{cm}^2$ , (F) 1  $\mu\text{g}/\text{cm}^2$ , (G) 0.1  $\mu\text{g}/\text{cm}^2$ , and (H) control-PBS; Laminin (I) 2  $\mu\text{g}/\text{cm}^2$ , (J) 0.2  $\mu\text{g}/\text{cm}^2$ , (K) 0.02  $\mu\text{g}/\text{cm}^2$  and (L) control-PBS.

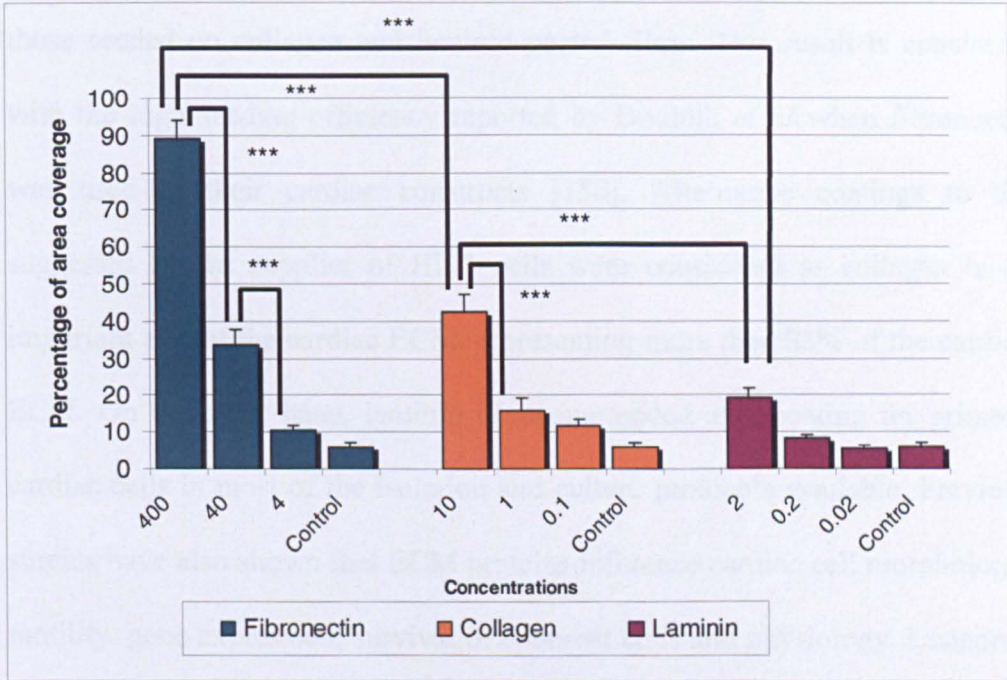


Figure 4-4 Total area coverage of HL-1 cells after 18 hours of culture on poly (1,8-octanediol-co-citric acid) [POC] films coated with fibronectin, collagen or laminin at concentrations [ $\mu\text{g}/\text{cm}^2$ ] as indicated (n=3, mean + SD, \*\*\* indicates  $p < 0.001$ ).

myocytes and then diluted 1:10 and 1:100 as detailed in Section 2.3.2. After 18 hours of incubation on the surfaces, HL-1 cells were imaged.

Figure 4-3 shows images of area coverage per protein per concentration. These data were analysed and is summarised in Figure 4-4. The graph shows that cells seeded on POC films coated with fibronectin covered a larger area than those seeded on collagen and laminin coated films. This result is consistent with the high seeding efficiency reported by Boublik *et al* when fibronectin was used in their cardiac constructs [150]. Alternative coatings to the suggested by the supplier of HL-1 cells were considered as collagen is an important part of the cardiac ECM, representing more than 85% of the cardiac ECM. On the other hand, laminin is recommended as a coating for primary cardiac cells in most of the isolation and culture protocols available. Previous studies have also shown that ECM proteins influence cardiac cell morphology, motility, gene expression, survival of adherent cells and physiology. Lungdren *et al* found that after two weeks of culture, myocytes seeded on dishes coated with collagen and laminin formed a denser monolayer than those cultured on uncoated plastic dishes, and also exhibited spontaneous contraction [178].

Fibronectin used at a concentration of  $400 \mu\text{g}/\text{cm}^2$  showed a  $90\% \pm 5\%$  HL-1 cell area coverage in contrast to  $32\% \pm 4\%$  with the same protein coated at  $40 \mu\text{g}/\text{cm}^2$  and to  $11\% \pm 1\%$  when the concentration of the fibronectin was the lowest ( $4 \mu\text{g}/\text{cm}^2$ ). It can be alleged that initial concentrations are not the same for the three proteins in this study; however the concentrations used are the optimal values for each ECM protein according to the existing information.

Cell coverage on collagen and laminin coated films showed inferior area coverage when compared to fibronectin coated materials. The cell coverage for

laminin was only comparable to that of the PBS controls. In these studies, cell coverage also decreased as the protein concentration reduced, reaching the same levels of attachment as uncoated films with the lowest concentrations.

Results indicated that fibronectin was the best of these three ECM protein because not only enhanced myocyte adhesion to the POC film but most importantly maintained the cell morphology. This could possibly be related to the fact that a higher level of fibronectin expression is associated with cell proliferation and migration at the embryonic stage of heart development whilst during heart growth, fibronectin levels decrease and laminin and collagen levels increase. Also in contrast to smooth muscle cells, cardiomyocytes are not capable of fibronectin synthesis but only of type IV collagen and laminin synthesis [152]. An increased attachment ratio with fibronectin is also explained by fibronectin being recognised by ten different binding receptor integrins [179]. This supports the finding that a fibronectin coating was advantageous for obtaining high area coverage of cells and expressing the cardiac phenotype, and therefore this protein was used to coat the POC scaffolds for the remaining cellular studies.

#### **4.3.4 Analysis of the effect of different porosities on the proliferation of HL-1s**

Following surface modification studies, porosity of the POC scaffolds was examined as another factor for cell attachment and survival. HL-1 cells were seeded statically in these scaffolds to assess how the porosity affected cell survival. As previously discussed a minimal value of porosity is needed for

cells to proliferate and differentiate. Highly porous structures are thought to promote cell phenotype and physiology and to support migration, which is desired for tissue engineering ingrowth in the scaffold [180].

Cell number analysis as determined by alamar blue after 24 hours revealed no significant differences between cell proliferation for the three different porosities (Figure 4-5). Table 4-1 illustrates a minor trend of increasing cell concentration in more porous scaffolds; however considering the standard variation for these analyses, the differences are not significant with p values greater than 0.05 when comparing results of 60% and 80% porous and p greater than 0.19 in the other cases. Furthermore, Figure 4-6 presents fluorescent images of live cells where the same phenotype and adhesion levels were observed for the three different porosities. This study established little change in HL-1 survival on POC scaffolds whether the porosity varied between 60% and 80% and therefore this was not a factor to consider when deciding the best scaffold to culture HL-1 cells on. The changes in the mechanical properties dependant upon porosity were more relevant for this project. It was hence decided to use 70% porous as these POC scaffolds satisfied the requirements of a highly porous structure with mechanical integrity. The mechanical properties of 80% porous constructs were much more compromised than those 60% and 70% porous.

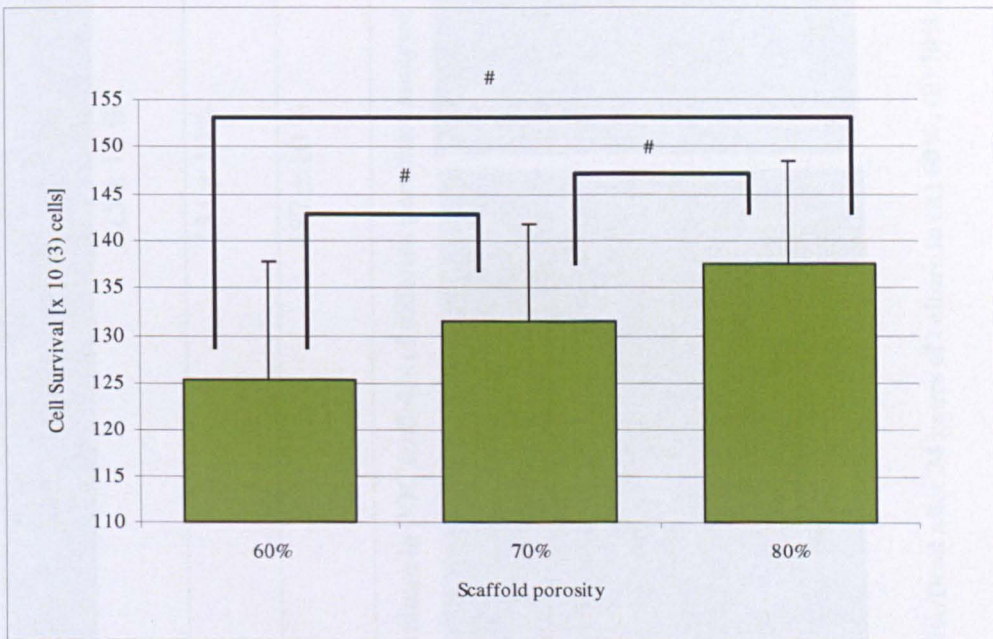
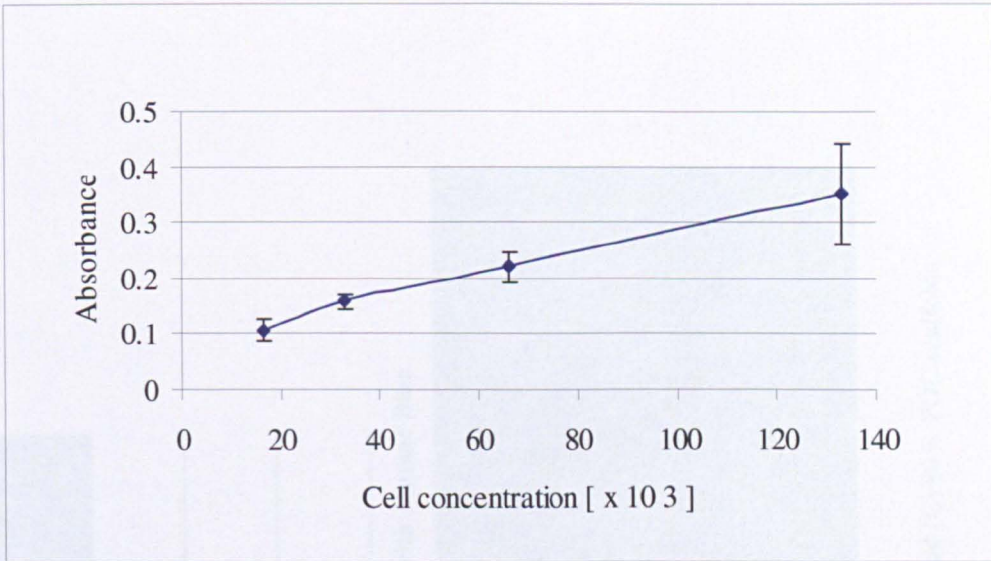


**Figure 4-5 (A) Standard curve for number cell and Alamar blue absorbance and (B) Survival of HL-1 cells after 24 hours when seeded on POC scaffolds with different porosities (mean  $\pm$  SD, n=9, # indicates  $p > 0.05$ ).**

POROSITY	RELATIVE SURVIVAL ( $\pm$ STD) [ $\times 10^3$ CELLS]
60 %	125 $\pm$ 12 %
70 %	131 $\pm$ 10%
80%	137 $\pm$ 10 %

**Table 4-2 Relative survival of HL-1 cells after 24 hours of culture in POC scaffolds of different porosities analysed with Alamar Blue**

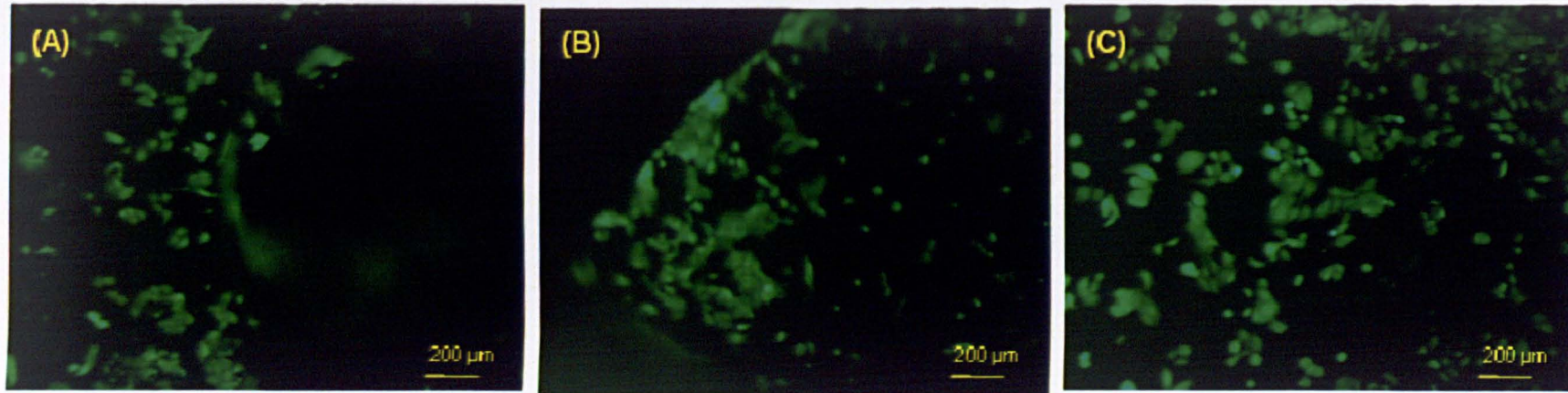


**Figure 4-6 Fluorescent images of HL-1 cells stained with Live/Dead after 24 hours of culture in (A) 60%, (B) 70% and (C) 80% POC scaffolds**

### **4.3.5 3D culture - Static vs. dynamic seeding**

After establishing the use of 70% porous scaffolds and fibronectin coating for further cellular studies, seeding conditions in 3D scaffolds were assessed to determine if seeding efficiency could be improved.

C2c12 myoblasts and HL-1 cardiomyocytes were seeded under static and dynamic techniques as described previously in Section 2.23. HL-1 cells were seeded on POC scaffolds by static, centrifugal and agitated seeding at 100, 200 and 300 rpm; whilst C2c12 cells were only assessed for static and dynamic seeding at 100 rpm due to a cell availability limitation. Cells were incubated using the experimental conditions for 24 hours before evaluating cell number and morphology of the cells on the scaffold.

SEM allowed visualisation of HL-1 and c2c12 cells after 24 hours of culture on POC scaffolds (Figures 4-7 and 4-8). Transversal imaging of the constructs was not possible because of the thinness of the scaffolds (2 mm); hence internal distribution could not be confirmed. Representative images of HL-1 cells seeded by centrifugation demonstrated low attachment and survival; however the few cells that adhered to POC, presented the typical phenotype. Normal cell morphology was thought to be as a result of the static incubation after the centrifugation seeding step. Although centrifugation concentrates the cells available in the cell suspension in a certain volume, seeding HL-1 cells by this method did not increase the number of cells within the scaffold. This was explained as a technical issue resulting from the morphology of the scaffold complicating the homogeneous deposition of cells throughout the whole structure. Godbey *et al* overcame this by designing a special rotor to centrifuge

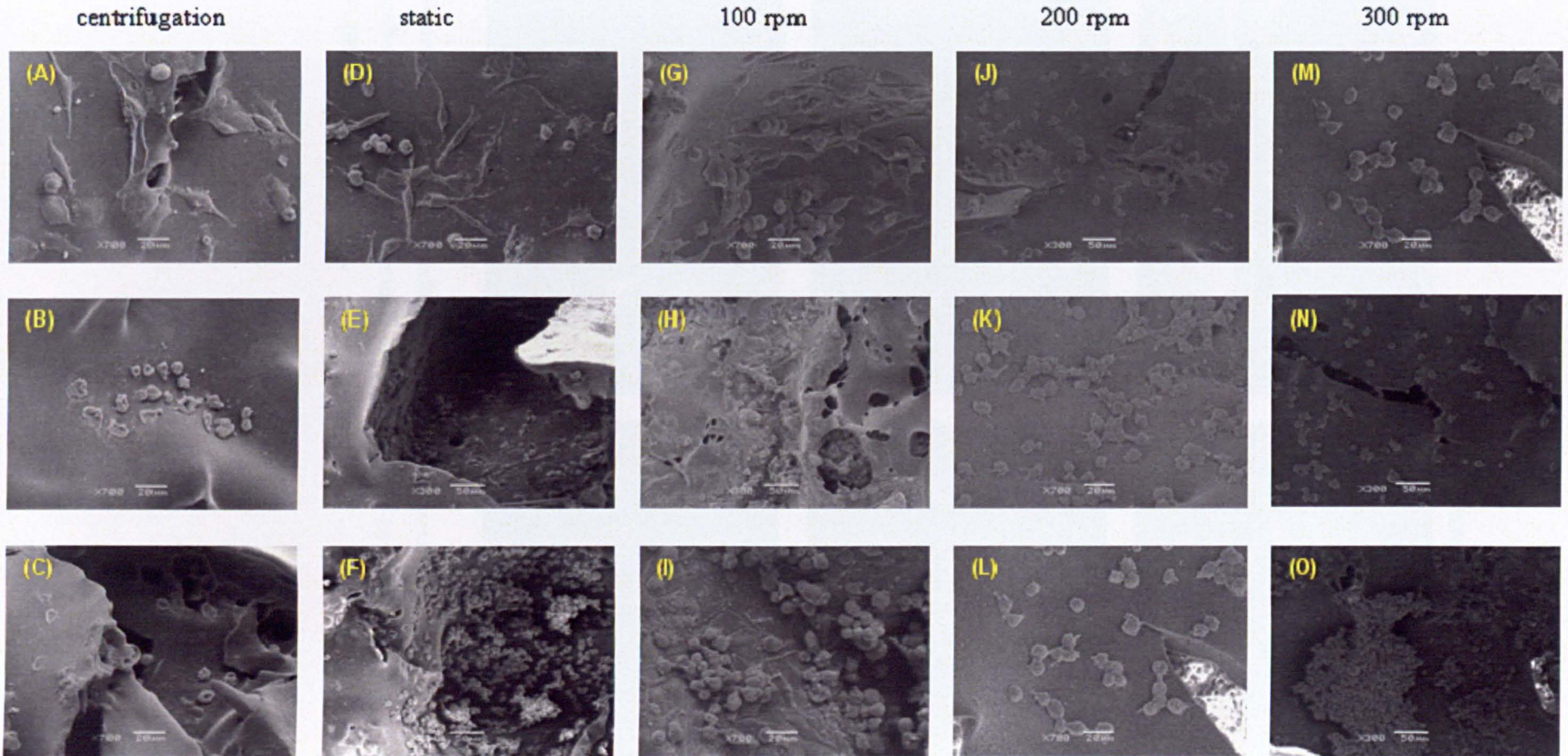


Figure 4-7 Images of HL-1 cells after 24 hours of culture in POC 70% scaffolds coated with fibronectin at  $400 \mu\text{g}/\text{cm}^2$  seeded by (A-C) centrifugation, (D-F) static, (G-I) 100 rpm, (J-L) 200 rpm and (M-O) 300 rpm

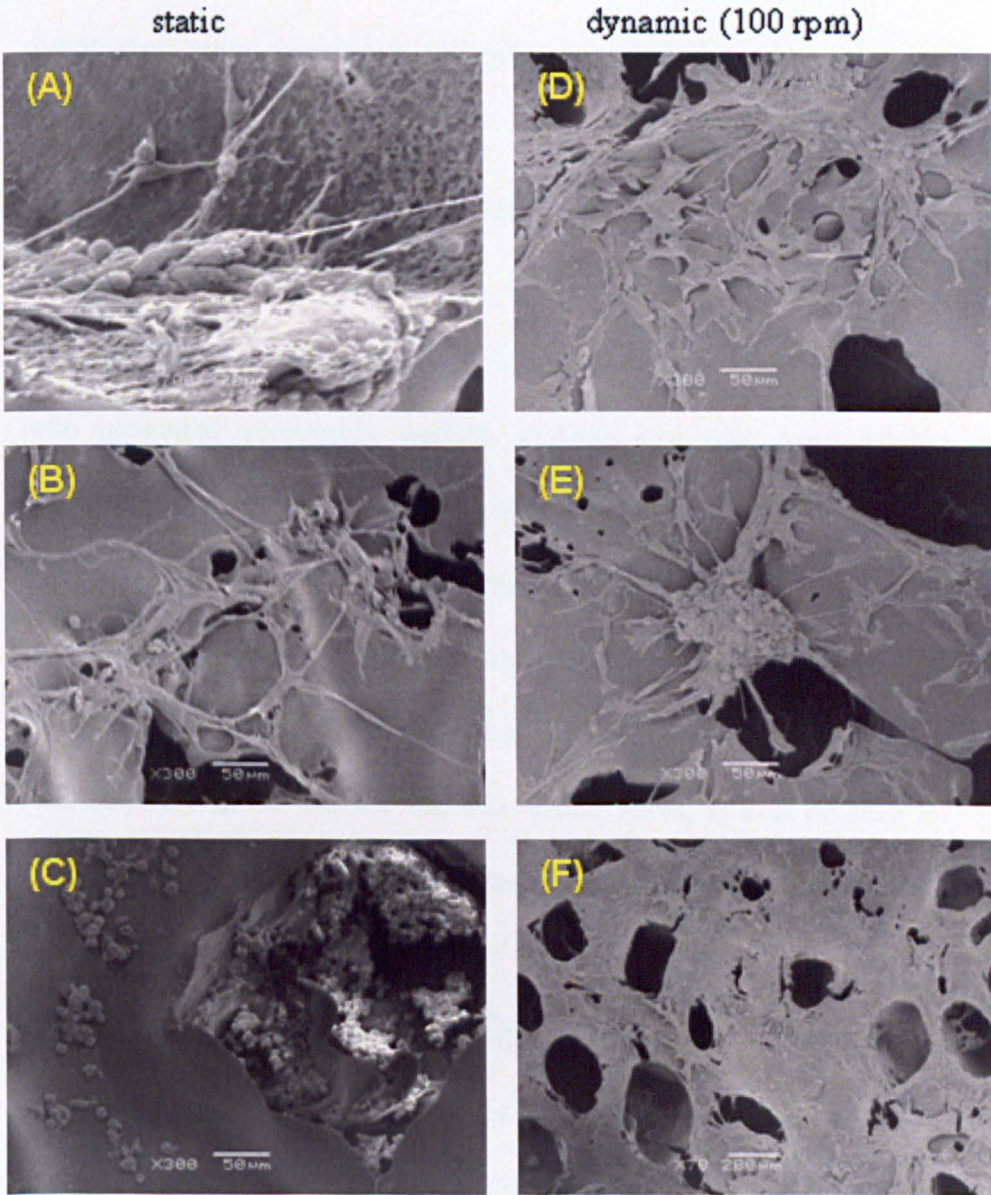


Figure 4-8 Images of c2c12 cells after 24 hours of culture when seeded on 70% POC film scaffolds coated with fibronectin at 400  $\mu\text{g}/\text{cm}^2$  seeded by (A-C) static method and by (D-F) 100 rpm dynamic seeding.

cylindrical constructs to ensure that the axis of rotation ran through the central lumen of the scaffolds. It was found that seeding efficiency, time and distribution were superior in centrifuged constructs compared to static and spinner flask [173].

Cells seeded statically showed not only a high ratio of attachment and normal phenotype but also greater viability, 162%, when compared to those seeded at 100 rpm after 24 hours (Figure 4.9). Dynamic seeding at this low agitation ratio presented acceptable viability (112%) but cells were smaller when compared to fully differentiated cardiomyocytes. When specimens were analysed by fluorescent stereo-microscopy, those seeded by centrifugation at 200 and 300 rpm showed no sign of the presence of live cells. In contrast, POC scaffolds seeded with HL-1 cells either statically or at 100 rpm, displayed live cells not only in the surface but also inside pores, as can be seen in Figure 4.10. It was impossible to image dead cells (stained red) due to partial auto-fluorescence of the POC.

Increasing the seeding speed to 200 and 300 rpm led to minimal cell attachment after 24 hours. The effect of agitation speed was negative in cell adhesion for speeds greater than 100 rpm as cells did not exhibit cardiac phenotype when seeded with these treatments. Differences in cell density, DNA content and metabolic activity between dynamic seeding techniques can also be caused by the vessel configuration. Carrier *et al* compared seeding neonatal rat cardiomyocytes in a rotating vessel and in mixed flasks. This group reported that cell damage in dynamic seeding was mainly due to turbulent flow in contrast to laminar flow which reduces cell damage [79]. Xiao *et al* reported that the combination of a dynamic technique for seeding

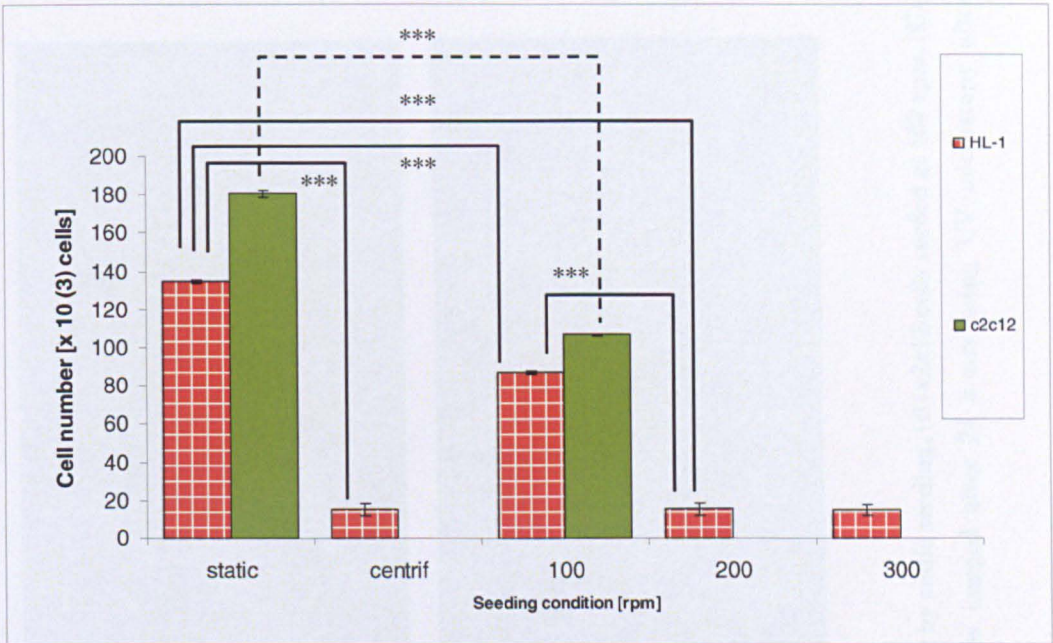
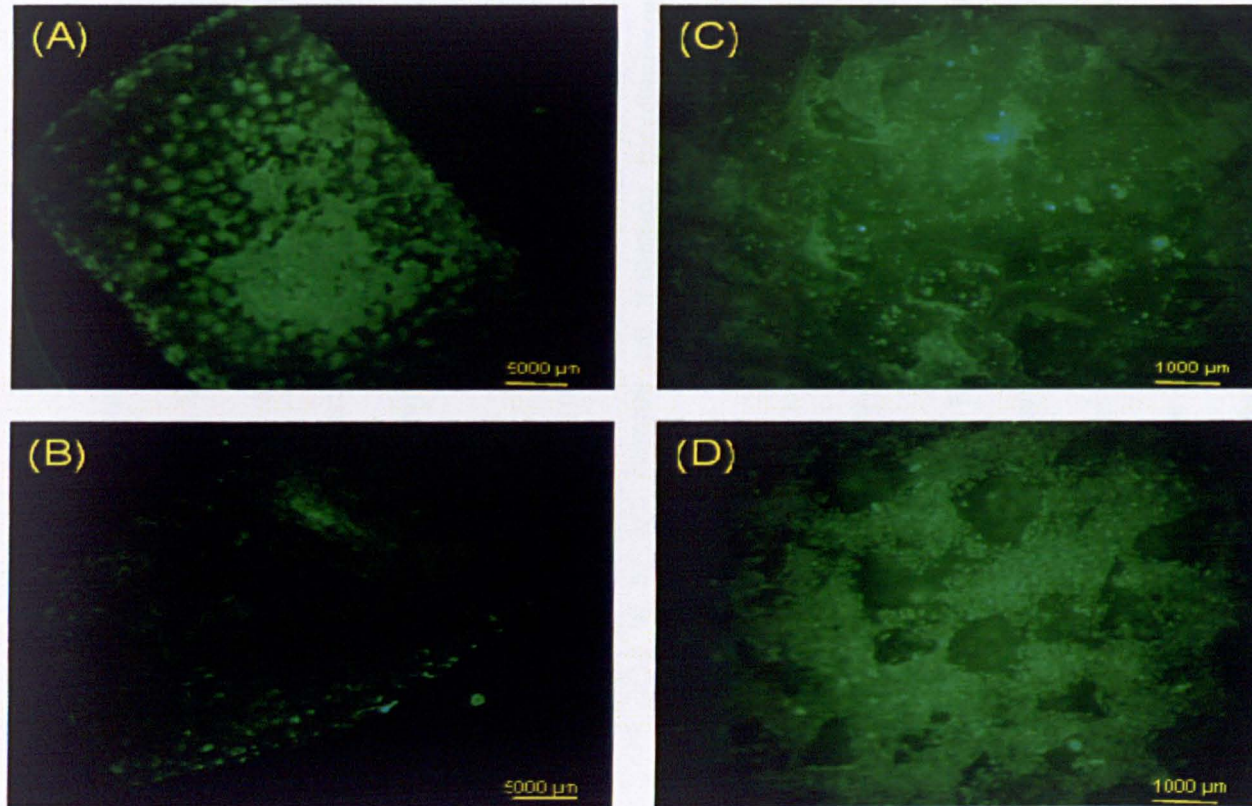


Figure 4-9 Graph of cell survival of HL-1 and c2c12 cells after 24 hours of being seeded statically, by centrifugation of at 100, 200 or 300 rpm (n=9, mean  $\pm$ SD, \*\*\* indicates  $p < 0.001$ ).



**Figure 4-10** Fluorescent images of 70% POC film scaffolds seeded with (A) c2c12 cells by static seeding, (B) c2c12 cells seeded at 100 rpm, (C) HL-1 cardiomyocytes statically and (D) HL-1 cardiomyocytes seeded dynamically at 100 rpm. Samples imaged after 24 hours using UV microscopy after Live/Dead staining.

following by static incubation of constructs was more beneficial for the cells than only dynamic or static methods [177]. Burg *et al* also experimented with different seeding/incubation methods and found that a dynamic seeding followed by bioreactor incubation for a week proved to increase metabolic activity and cellular infiltration. However, static methods were not the most inferior method [181]. In this study SEM demonstrated that the survival and differentiation of cardiomyocytes within these POC scaffolds were highly affected by agitation speed. Static seeding appeared to be the most favourable condition to seed HL-1s in 70% porous POC scaffolds.

C2c12 cells were imaged by SEM as shown in Figure 4-8. Constructs seeded either statically or at 100 rpm contained high number of cells, 225% vs. 137% survival respectively. Static seeding was also confirmed to be more advantageous condition for seeding c2c12s in POC scaffolds based on a superior viability. This was also confirmed by fluorescent live/dead staining as shown in Figure 4-10.

Radisic *et al* indicated that perfusion is the only seeding method that provides oxygen during the seeding, maintaining viability, high cell density and uniform distribution [182]. However the use of this seeding technique is restricted by the construct architecture and by the compatibility of the perfusion system with the bioreactor for long-term culture.

#### **4.4 Conclusions**

Scaffold surface and architecture as well as seeding strategy are fundamental factors when working with 3D models. Before introducing another variable, mechanical stimulation, it was crucial to establish the best possible seeding and culture conditions specific to the cell lines and the biomaterial.

The results presented in this chapter sought to compare several conditions to improve cell adhesion of myocytes in a novel flexible biomaterial. It was confirmed that myocytes require certain biochemical properties on the surface to adhere to POC. The surface modification study proved that fibronectin was a more advantageous coating compared to collagen and laminin. For each protein, a clear trend of decreased attachment was found when the protein concentration decreased on the surface.

Changes in the architecture of the scaffold showed little impact on cell survival at porosities between 60% and 80%, making the mechanical properties of the construct the fundamental factor to decide the most suitable porosity to be used in the following studies.

After testing static and dynamic seeding strategies, it was found that POC, being a highly hydrophilic material, enhances cell attachment and supports a better cell survival and differentiation when static conditions are applied. It was also concluded that the optimum seeding conditions did not vary between c2c12 and HL-1 cell types.

These optimisation studies led to the parameters established for the work in the mechanical bioreactor as presented in the next chapter.

## **5 Comparison of culture of cardiomyocyte constructs on a mechanical stimulated bioreactor and static culture**

*This chapter is mainly concerned with the effect of mechanical stimulation on cardiomyocytes. Cardiac constructs are cultured in Tencell, a dynamic bioreactor, and assessed for morphology, survival and gene expression.*

## 5.1 Introduction

### 5.1.1 Mechanical stimuli in cardiomyocytes

Mechanical forces play a significant role on muscle organogenesis and growth by modulating cellular proliferation, metabolic activity, ECM composition, gene regulation and protein expression and organisation. Cardiomyocytes are terminally differentiated cells that respond to excessive workload only by hypertrophy (an increase in cell size) and not by hyperplasia (increase in cell number) [183]. After increased cardiac load, cells adapt to the new conditions by modifying the gene program into hypertrophy and increasing contractile strength and peptide secretions [184-189]. Mechanical stimulation of *in vitro* myocytes has shown similar effects on cellular morphology and physiology when compared to *in vivo* cells subject to a mechanical force [179-183]. Vandeburgh *et al* reported that statically stretched skeletal myocytes showed increased levels of aminoacids, total proteins and particularly of myosin heavy chain (MHC) protein [190,193]. Reports of the effect of mechanical stimulation on cardiomyocytes are limited, mainly with information limited to cardiac loading also effect on myocyte by modifying fibre orientation and length leading to contraction rate/force changes [194]. Cardiomyocytes and cell types such as smooth muscle cells and endothelial cells, change their orientation in response to mechanical stimulation usually aligning on the direction of the stretching force [195-198]. Stretch regimes are also important for reaction and alignment in mammalian cells, Vandeburgh and Karlish also found that the cellular response of stretched cells in a slow uni-axial stretch affected fibre orientation and length in mammalian myocytes [199-200].

### 5.1.2 Cardiac gene markers

Molecular markers have been used to monitor changes in genetic expression levels and signalling pathways for transcriptional activation. One of the cellular responses after cardiac injury or overload is the reactivation of a program of immediate early gene expression; this up-regulates embryonic genes encoding for ANP, BNP,  $\beta$ -MHC and  $\alpha$ -skeletal actin [201-204]. The cardiac genes induced in response to cardiac load are classified by the response time. Immediate early genes which respond within one hour include BNP, c-fos, c-jun and c-myc. Intermediate response genes, responding after several hours, include ANP,  $\beta$ -MHC, skeletal  $\alpha$ -actin and Collagen III whereas late response genes, which show a response after days, are Collagen I and cardiac  $\alpha$ -actin [205-212].

#### ANF

Atrial natriuretic factor or peptide (ANF or ANP) is a hormone secreted by the heart and encoded by the gene *nppa*. This peptide is triggered by hemodynamic stress and regulates vasodilatation (blood pressure), diuresis and natriuresis [203, 213-215]. This hormone belongs to the family of natriuretic peptides and is present in important levels during embryogenesis and cardiac hypertrophy [216]. ANP importance has been highlighted by knockout models which showed that alterations in this gene cause hypertension [217-219]. It has also been reported that genetic variations are a factor in cardiac remodelling and hypertrophy; increased levels of ANP are considered a prognostic

indicator in cardiac failure [220-221]. King and Wilkins suggested that ANP also plays a role in the protection of the myocardium by inhibiting cardiac fibrosis and myocyte hypertrophy; as it was shown that ANP inhibits collagen production and induces apoptosis [222]. Ruskoaho *et al* demonstrated that after overload the level of ANP mRNA is increased and that myosin heavy chain and skeletal alpha actin are equally increased although cardiac alpha actin mRNA decreased [223].

### **Cardiac actin gene (*actc*)**

The actin isoforms  $\alpha$ -Skeletal and cardiac are two of the twenty actin genes present in the human genome.  $\alpha$ -Skeletal actin is expressed after myoblast differentiation and is prevalent in the embryonic heart but down-regulated after birth. The *actc* gene encodes for cardiac actin, the sarcomere thin filament protein that regulates muscle contraction. Mutations in this gene have been shown to cause cardiomyopathies [224]. Previously, Black and Packer reported the use of smooth muscle alpha actin, correlated with skeletal alpha actin, as a molecular marker of pressure-overload hypertrophy [225].

### **Myosin heavy chain genes (*myh*)**

Myosin is a cardiac protein present in the sarcomere thick filament. The first isoforms,  $\beta$ -MHC is characteristic of embryonic and adult heart and is expressed in newly formed cardiomyocytes. Mutations in this gene can lead to enlargement of the left ventricle [226].

### 5.1.3 Dynamic Bioreactors

Bioreactors provide a culture environment conducive to cell aggregation and supply an instrument for study of tissue formation and cell physiology under variable biological and biochemical conditions (Table 5-1). Mechanical stimulation has been studied in culture systems that control the mechanical load applied *in vitro*. The first bio-mechanically active bioreactors for cell culture were perfusion and membrane bioreactors that induced shear stress but neither tensile nor compressive load. The first approach for more complex mechanical bioreactors was to design laboratory-scale bioreactors. However in the last decades, mechanical stimulated bioreactors have been manufactured to meet the researchers' needs and its market has grown due to more research groups involved in regenerative medicine. Current commercial models are limited and expensive and therefore there is still a need for some groups to design their own.

Dynamic bioreactors can be classified mainly in those that apply compression, tension or fluid shear stress. Compressive systems are commonly used for bone, cartilage or endothelial applications as these cells stand this load *in vivo*.

Shear stress has been used to evaluate its influence on protein expression, ion channels and cytoskeletal remodelling [227]. Tensile systems have been developed to stretch lung, bone, ocular, muscular and vascular cells. This uniaxial load has been applied by diverse actuators such as solenoids, electromagnets, pneumatic pistons and even by manual screws [228]. The following bioreactors are available for mechanical stretching stimulation (Figures 5-1 and 5-2).

	<b>SHEER STRESS</b>	<b>MASS TRANSFER</b>	<b>DIMENSIONALITY</b>	<b>CO-LOCATION OF DISSIMILAR CELL TYPES</b>	<b>CELL DENSITY</b>
<b>Static Culture System (T-Flasks)</b>	None	Adequate 2D	3-4 layers 2D	Limited	0.3-1x10 <sup>6</sup> cells/ml
<b>Static Matrix Cultures</b>	None	Limited 3D	Limited 3D	Limited	Low
<b>Roller Bottles</b>	Medium	Good 2D	3-4 layers 2D	Very Limited	1-5x10 <sup>6</sup> cells/ml
<b>Stirred Suspension Culture</b>	Medium/High	Good	Very Limited 3D	Very Limited	10 <sup>6</sup> -10 <sup>7</sup> cells/ml
<b>Airlift Bioreactors</b>	Medium/Low	Good	Very Limited 3D	Very Limited	10 <sup>6</sup> -10 <sup>8</sup> cells/ml
<b>Hollow Fibre Perfused Systems</b>	None	Good	Limited 3D	Limited	10 <sup>7</sup> -10 <sup>8</sup> cells/ml
<b>ITEMS</b>	Medium	Excellent	Excellent 3D	Excellent	N/A
<b>Dynagen</b>	Medium	Excellent	Excellent 3D	Excellent	N/A
<b>Flexcell</b>	Medium	Limited 2D	Limited 2D	Good	N/A
<b>Tencell</b>	Low	Limited	3D	Good	N/A

**Table 5-1 Characteristics of different bioreactors for cell culture [243]**

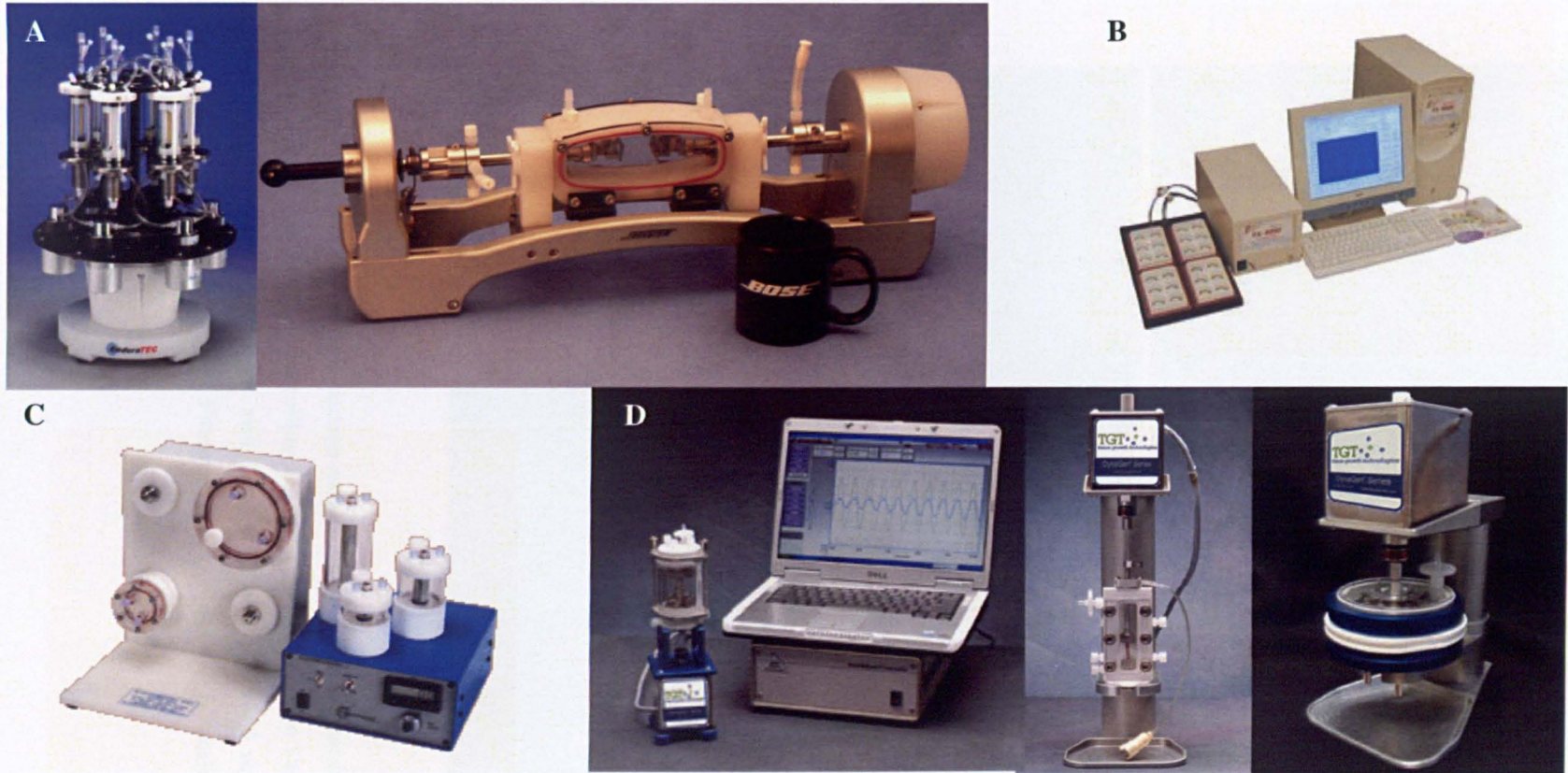
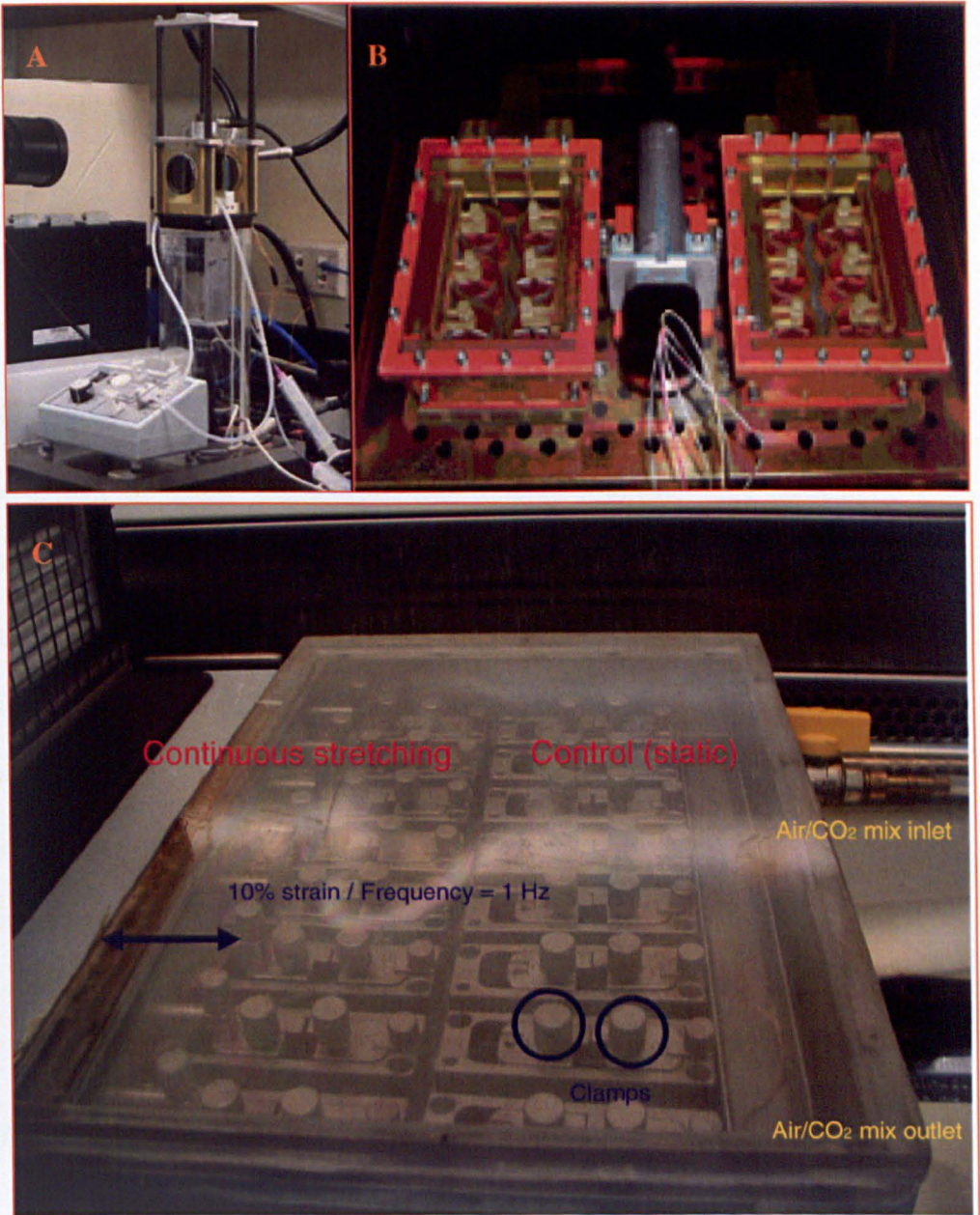


Figure 5-1 Commercial dynamic bioreactors (A) BioDynamics by Bose/Enduratec, (B) Flexcell, (C) RCCS, and (D) DynaGens by TGT [232-236]



**Figure 5-2** Digital images of custom-made multi-station dynamic bioreactors: (A) Miniature Load and Strain-Controlling Bioreactor (Northeastern University, USA), (B) Bioreactor for controlled stretch and flexure of soft biological materials under cell-culture conditions (University of Pittsburgh, USA) and (C) Tencell (Leeds University, UK) [92, 229, 230].

## **Custom-built Bioreactors**

Researchers require specific bioreactors that were not available up till now. This problem and the high cost of commercial systems made tissue engineers work together with engineers to design and build bioreactors that apply the forces researchers need.

A miniature load and strain controlling bioreactor was designed and built by researchers of Northeastern University in Boston, USA, to analyse the mechanics of tissue when a tensile load is applied. This bioreactor was developed to study the mechanical properties, deformation and growth of collagen in tissues [229]. Another research group from Pittsburgh University has designed several mechanical bioreactors, including a bioreactor for controlled stretch and flexure of soft biological materials under cell-culture conditions. This system was designed to study the effect of dynamic stimulation in tissue engineered heart valves. This bioreactor applies uni- and bi-directional cyclic flexure to specimens arranged in 6-wells plates contained in chambers. The frequency, amplitude, acceleration, and deceleration profiles are controlled by the software operating the bioreactor [230].

Tencell is a dynamic bioreactor that applies controlled cyclic tensile strain to constructs in a controlled setting. Leeds University researchers designed Tencell to culture cell-seeded collagen gels and tissue equivalents in order to study the biological response of biomaterials in a functional environment. This bioreactor contains 16 individual chambers in a sealed vessel, 8 of which are coupled to a uni-axial mechanical actuator that can be set up either to apply tension or compression loads. Tencell has previously been used to study orthopaedic implants, skin models and tissue engineered aortic heart valves

[92]. Zhonggang *et al* has also reported the design, fabrication and performance of an electro-tensile bioreactor. This system was developed to simulate the electrical and mechanical stimuli in cardiomyocyte-seeded collagen gels and other cardiovascular constructs [231].

### **Rotary Cell Culture System (RCCS) (Synthecon Incorporated)**

The Rotary Cell Culture System is a bioreactor developed by the National Aeronautics and Space Administration (NASA, USA) which enables the study of three-dimensional cultures under microgravity conditions. The system was initially designed to protect tissue samples during space flight but because of the unique microgravity environment it was exploited as a bioreactor. The RCCS integrates a culture system with high mass transfer of nutrients, metabolic products and gases in addition to providing a low shear environment. Inside the vessel, the particles are suspended by rotation as its centrifugal force equalises the gravity force preventing sedimentation. Cells can be cultured in suspension or in constructs up to several months. This bioreactor is commercialised by several companies and used for research such as tissue regeneration, cancer research, *in vitro* toxicology and production of monoclonal antibodies, proteins and pharmaceuticals [232-233].

### **Flexcell**

Flexcell is a “computer-regulated” pneumatic bioreactor which enables the creation of three-dimensional cultures under strain conditions. This system provides strain by applying vacuum pressure to the cells seeded on special 6-

well flexible plates. Static and cyclic strain or compression can be applied to monolayer cultures in different frequency and amplitude regimens. Flexcell supports the creation of three-dimensional cell-seeded gels [234].

### **Intelligent Tissue Engineering via Mechanical Stimulation (ITEMS) Bioreactor**

The ITEMS Bioreactor is an EnduraTEC / Electroforce (Bose) system that provides a biodynamic environment for three-dimensional constructs. This bioreactor is able to apply mechanical stresses and strains to constructs contained in the “closed-loop nutrient-flow subsystem”. The ITEMS is controlled by software that also allows the user to perform real time mechanical analysis. In addition to this, pressure and flow frequency and regimen can be varied. ITEMS can be arranged for one module or multi-station with 6 chambers, each of which can be loaded with axial and/or shear stress [235].

### **DynaGen ®**

The DynaGen bioreactor, by Tissue Growth Technologies, is the generic name for the series of bioreactors that are customised for diverse tissue engineering applications, including bone, cartilage, vascular and ligament. The DynaGen provides a mechanical stimulated 3D culture environment. These bioreactors apply tension and compression through mechanical pulsatile pressure combined with low and high flow rates. The system is fully integrated to a computer for the control of flow and load configurations [236].

#### **5.1.4 Aims**

The aim of this chapter was to assess the effect of culturing HL-1 cardiomyocyte on 70% porous POC scaffolds under dynamic conditions in the Tencell bioreactor. The first objective was to evaluate the seeding and culture conditions to then incubate the constructs for one week under continuous and discontinuous stretching regimes. The evaluation of this dynamic culture was to be done by comparing the relative expression of cardiac genes, survival, morphology and distribution of cardiomyocytes in the 70% porous POC scaffolds.

## **5.2 Materials and methods**

### **5.2.1 Preparation of Scaffolds**

Scaffolds were manufactured and prepared for cell-seeding as explained in Sections 2.1.2.b, 2.3.1 and 2.3.2. Scaffold surface modification was carried out using fibronectin according to the results of Section 4.3.3.

### **5.2.2 Cell culture**

HL-1s, obtained from Dr. Claycomb, were cultured as described in Section 2.2.1.

### **5.2.3 Culture of cell-seeded scaffolds**

For the initial seeding study, scaffolds were statically seeded with HL-1 cells as outlined in Section 2.3.4 at a density of  $0.55 \times 10^6$  and  $1.1 \times 10^6$  cells per

mL per scaffold and then transferred to the Tencell bioreactor for static incubation for 20 hours at 37°C and 5% CO<sub>2</sub>.

For the mechanical stimulated study, cells were seeded directly in the Tencell at  $0.55 \times 10^6$  cells per mL per scaffold and incubated for 60 hours before starting the stretching regimen according to Section 2.3.6. Constructs were either stimulated continuously or discontinuously 4 hours per day. All cultures were maintained for 1 week in the stretching regimen.

#### **5.2.4 Analysis of constructs**

Following one week of mechanical stimulated culture, constructs were removed from the bioreactor and washed in PBS. From the eight constructs in each condition, three were placed in RNAlater buffer for further qRT-PCR analysis. Alamar blue assay was performed in three other constructs and then washed in PBS to be prepared for SEM imaging. Live/Dead assay was carried out in the last two constructs, one of which was also immunostained for actin.

##### **Alamar blue**

Alamar blue assay was performed to assess the cell survival for each scaffold according to Section 2.4.1. The number of cells was calculated using the calibration curve for the HL-1s.

##### **Quantitative RT-PCR**

Samples were preserved in RNAlater at -20° before being analysed as described in Section 2.4.2.

### **Immunofluorescence staining of sarcomeric actin**

One sample was cut in two halves to be stained for Live/Dead and for sarcomeric actin. The immunofluorescence was carried out as previously described in Section 2.5.2 to confirm the presence of the protein

### **Live/Dead assay and Confocal microscopy**

Constructs were washed and incubated for Live/Dead Assay before being imaged in a Stereo and a confocal microscope as detailed in Section 2.5.3.

### **SEM**

Constructs were fixed in glutaraldehyde before SEM processing and imaging as described in Section 2.5.4.

### **Statistical analysis**

The statistical significance of these results was evaluated using Microsoft Excel 2002 (Microsoft Corporation 2002, USA). Results are expressed as mean  $\pm$  standard deviation (SD) when available. Data was analysed on triplicates unless otherwise stated in the analysis. T-tests of two samples assuming equal variances were performed as described in Section 2.6 to compare culturing conditions results.

## 5.3 Results and Discussion

### 5.3.1 Differences in seeding concentration and *in situ* incubation

The first approach for these studies was to seed HL-1 cells onto the scaffold and then transferring the seeded constructs into the Tencell bioreactor. It was hypothesised that seeding directly into the Tencell could have an effect in seeding efficiency. It was also speculated that the initial seeding concentration could affect cell survival. POC scaffolds were prepared for cell culture and then HL-1s were seeded in POC scaffolds at  $55 \times 10^3$  and  $110 \times 10^3$  cells per scaffold and incubated for 20 hours either in a TCP plate or seeded directly into the Tencell chambers. POC scaffolds were cut into the chamber dimensions and prepared for cell culture. Figure 5-3 shows the scaffold before the conditioning process and after the cells were seeded into the Tencell and cultured in it. Because of the geometry of the bioreactor, HL-1s concentrated in the central part of the scaffold between the clamps. Clamped areas were marked by a darker zone because of the reaction of the materials; this was attributed to a reaction of the metal to the elastomer. This has been observed with all other biomaterials used in the Tencell without affecting proliferation or survival [237].

Visually there was a difference between seeding in plates or in the Tencell (Figure 5-4 and 5-5). When seeding at low initial cell concentration, mean survival of cells in constructs incubated in plates for 20 hours was 123,000 cells compared to the 100,000 cells found on the construct of the Tencell; this difference was not statistically significant (Figure 5-6). Low survival can be

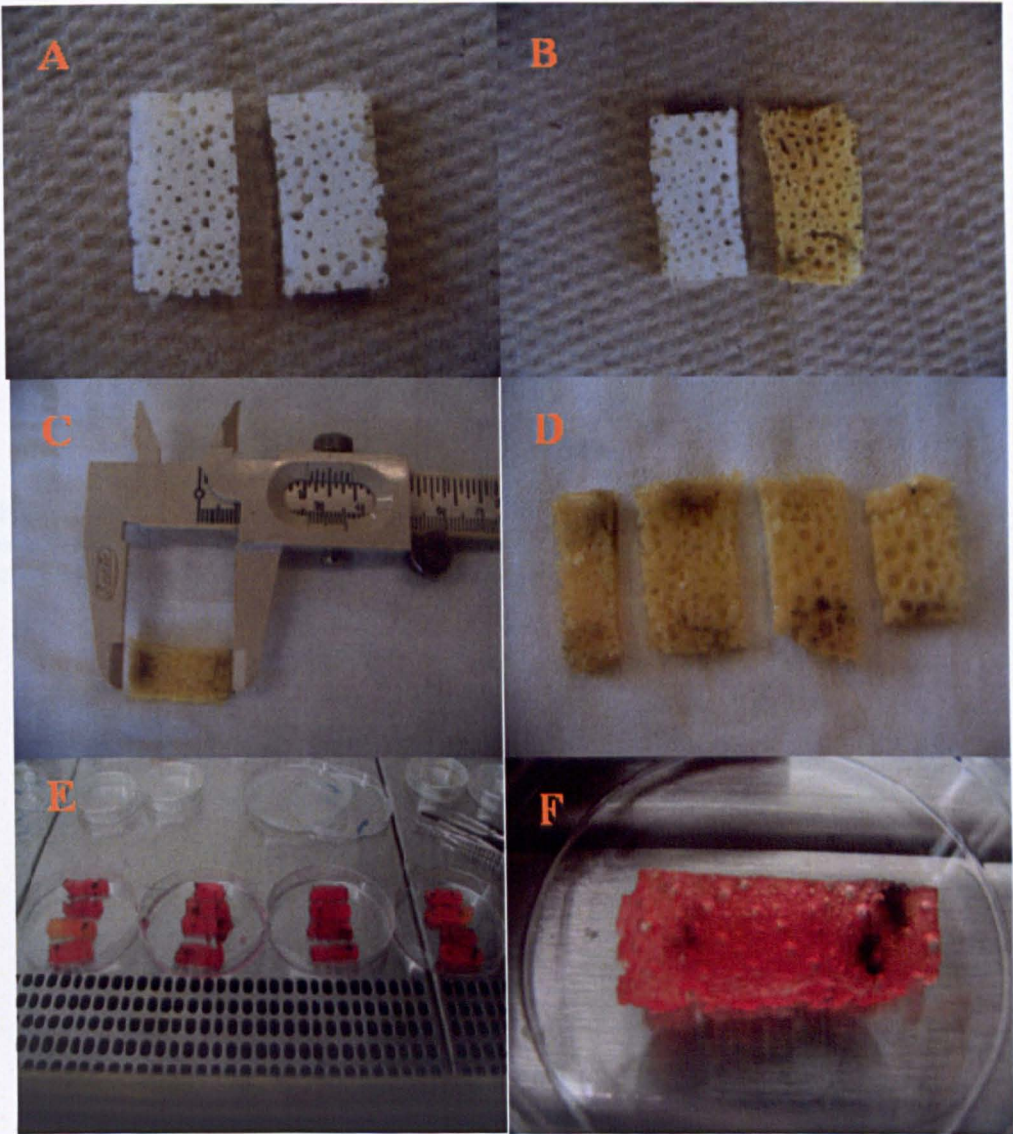


Figure 5-3 Digital images of 70% porous POC scaffolds (A) before cell culture preparation and (B) compared to a pH buffered scaffold characterised by the change of colour from white to pale yellow. POC scaffolds dimensions (C) and clamp marked areas (D) are shown. Resultant constructs after cell culture in the Tencell with change of colour caused by the culture medium (E) and clamp marks (F)

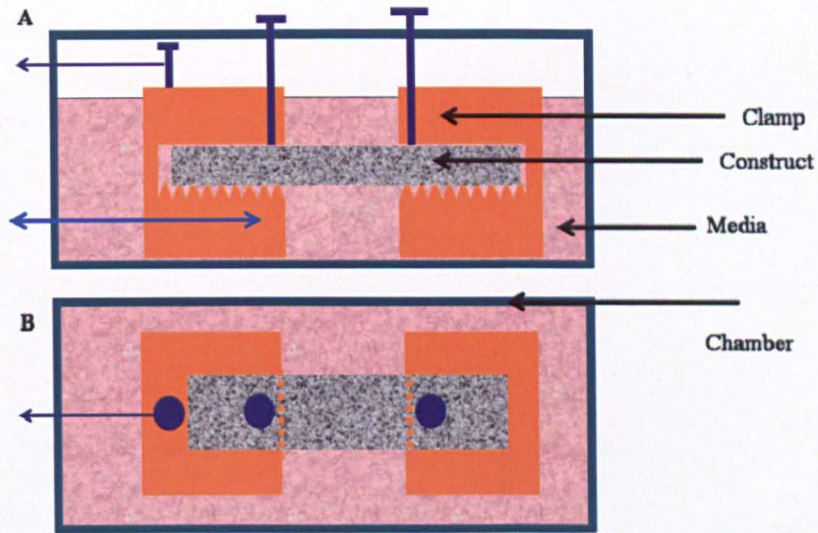


Figure 5-4 Diagram of a Tencell chamber showing (A) lateral view of a construct held by one static clamp and by one mechanically coupled clamp. (B) Superior view of the chamber containing the construct surrounded by media.

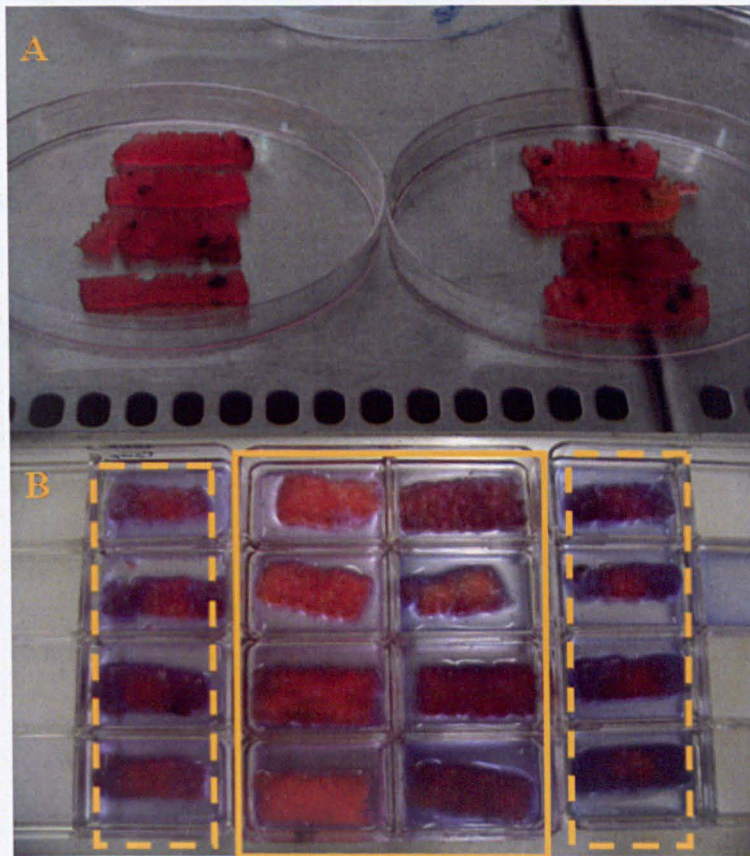
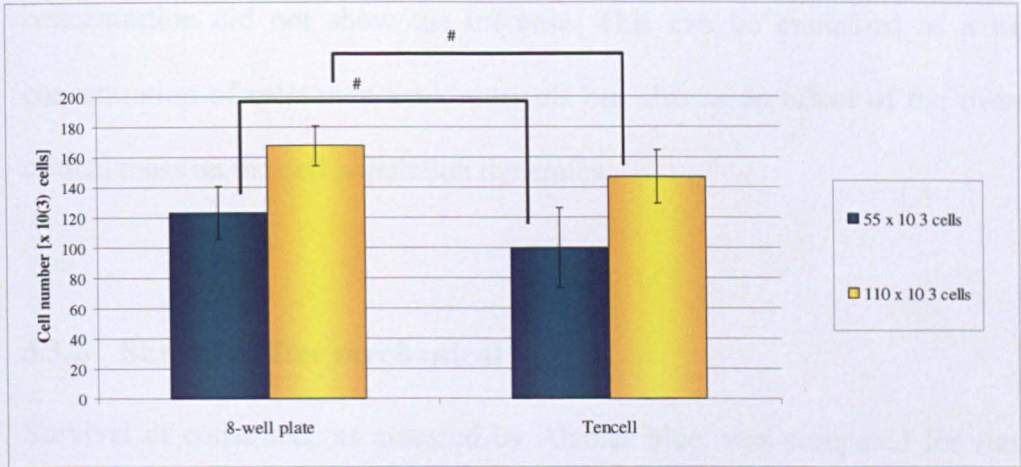


Figure 5-5 Digital image of HL-1/POC constructs (A) after 20 hours of static culture in the Tencell. (B) Constructs incubated in Alamar blue exhibit a change in colour from purple/blue to bright pink. Constructs in the central box were incubated in a plate whereas constructs in the discontinuous line box were in the Tencell. No metabolic activity can be seen where the clamps were whilst the central constructs show metabolic activity through all the structure.



**Figure 5-6 Survival of HL-1 cells after 20 hours of static culture. Cells were seeded at two different concentrations,  $55 \times 10^3$  cells and  $110 \times 10^3$  cells per scaffold; and in two conditions: incubated in 8-well non tissue cultured plates or directly into the Tencell chambers. There was no statistical significant difference in the survival of any of the groups (mean  $\pm$  SD, # indicates  $p > 0.05$ ,  $n=3$ ). However, when seeded at lower concentration, the overall survival was higher than seeded at higher concentration.**

explained because the Tencell clamps held the construct in the chambers and therefore the adhesion area was reduced.

Differences between initial seeding concentration were not significant, however when seeding at low concentration, survival was increased by 2 fold compared to the initial seeding concentration, whilst those seeded at higher concentration did not show the increase. This can be explained as a high concentration of cells may limit nutrients but also as an effect of the overall critical mass on the cell population dynamics.

### **5.3.2 Survival after mechanical load**

Survival of constructs, as assessed by Alamar blue, was compared for static, continuously and discontinuously stretching conditions. Figure 5-7 shows the survival after 1 week with no significant difference between static and continuously loaded at 10% of amplitude and 1 Hz. This can be explained by the fact that the cells had no time to proliferate and differentiate due to mechanical strain. A significant difference was seen with discontinuous regimen, explained by cells bearing an intermittent load. Cyclic stretching of constructs allows a better nutrient and waste exchange through the constructs stretching and compressing the pores and by agitating the media. It has been established that strain forces also induce an autocrine/paracrine reaction in cardiac myocytes as biochemical factors are released into the media as demonstrated by Sadoshima and Izumo. They stretched 20% a set of constructs and then switched non-stimulated cells to the stimulated media resulting in a mimicked effect of stretch in the non-stretched cells. Mechanical stimulation at

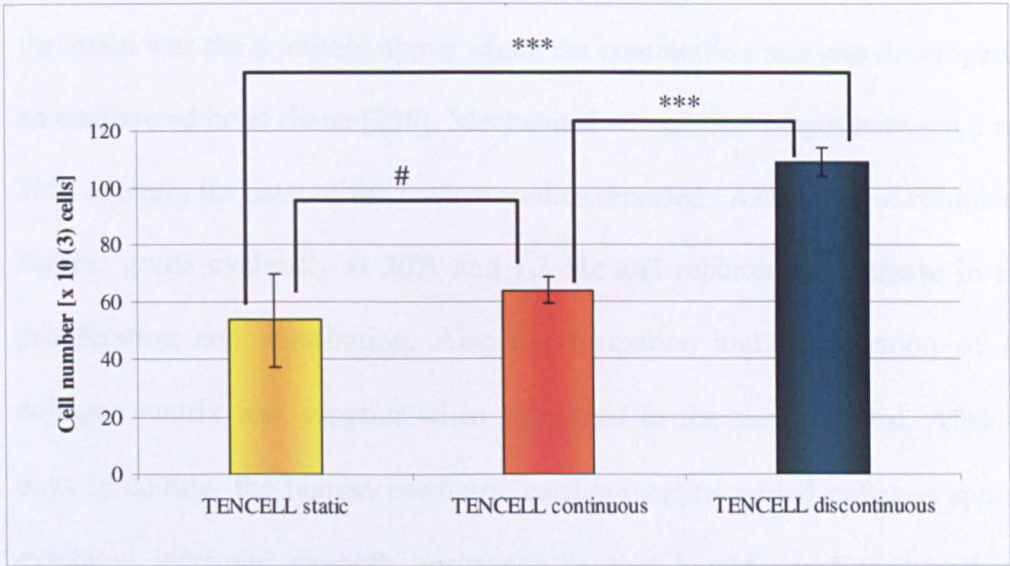


**Figure 5-7 Survival of HL-1 cells after 1 week of culture in the Tencell cultured at different stretching regimen. There is a significant difference between survival in the Tencell static culture and the stretching for four hours per day but not between static and continuous culture (mean  $\pm$  SD, \*\*\* indicates  $p < 0.001$ , # indicates  $p > 0.05$ ,  $n = 3$ )**

this scale caused no cell injury as proved by the lack of lactate dehydrogenase or creatine kinase in the media [186]. Fink *et al* found that 3% of amplitude in the strain was the threshold above which the contractile force was developed in an engineered heart tissue [238]. Mechanical stimulation ranges between 3 and 20% of strain for most of the *in vitro* studies reported. Akhyari *et al* stimulated cardiac grafts cyclically at 20% and 1.3 Hz and reported an increase in cell proliferation and distribution. Also the formation and organisation of the collagen matrix was superior when compared to the static control. After 14 days in culture, the human paediatric cardiomyocyte-seeded collagen sponge exhibited increased strength, resistance to stretch and an aligned collagen matrix. This study confirmed that mechanical stimulation positively affects cell morphology, proliferation and ECM formation. [239]. Zhao *et al* stretched cardiomyocyte constructs at 10% at 2 Hz and found orientated bundles, terminal differentiation and synchronous beating [240]. Yu and Russell stimulated neonatal rat cardiomyocytes by also stretching the constructs at 10% but at one, two, three and four hours. They found that there was a morphological change in the sarcomeres for all the conditions but the major difference was found after three hours of static strain [241]. Other groups have stretched at 20% of static strain finding induction of early genes causing hypertrophy in neonatal myocytes and hyperplasia in non-myocytes [188]. Tobita *et al* worked with embryonic cells in silicon constructs, and after 48 hours of cyclic stretch at 4% and 8%, they found hyperplasia instead of hypertrophy demonstrating that the lack of proliferation in cardiac constructs is caused by the differentiated cardiomyocyte and not by the mechanical stimuli [242]

It has also been demonstrated that cells are reversibly deformed by stretching the substrate and sustain no cell injury or slippage from the substrate [174]. Although mechanical stimulation is not indispensable to obtain functional grafts as demonstrated by Huang *et al* who obtained a contractile “bioengineered heart muscle” by static culture using fibrin, it is desirable to mimic the native conditions [243]. Alternatively perfusion has been used to induce stress to cardiac constructs. Yang *et al* used a pulsatile flow system to mimic biomechanical signals [244] Park also investigated the perfusion system but at lower rate and found that this improved the cell survival because perfusion enhances mass transport in the interior of the construct [245].

The next step in mimicking the cardiac environment is the mechano-electrical stimulation. Radisic *et al* have already explored electrical stimulation using collagen sponges and stimulated cyclically 2 milliseconds at 5 V/cm finding cell alignment and coupling synchronous contractions [246].

### **5.3.3 Gene expression**

Quantitative real-time Polymerase Reaction Chain (PCR) is an accurate method to determine levels of specific DNA or RNA sequences in cell or tissue samples. The method consists of the quantification of a fluorescent signal produced during the amplification of the sequence by PCR technology [93]. Three genes were evaluated with monolayer HL-1 cells on fibronectin-coated TCP: *myh6*, *actc1* and *nppa*. However when processing the cDNA of the Tencell samples with the primers for *myh6* (Myosin heavy chain) it appeared that the primers generated two products, probably because of splice

variants, and therefore the results were not reliable and hence not used (Figure 5-8). Initially *hprt1* and *rpl32* were used as housekeeping genes but after analysing the qRT-PCR results, it was seen that the values for the *hprt1* gene were too disperse. When analysed the relative expression of the target genes, *hprt1* expressions were unreliable. Willems *et al* consider *hprt1* an unsuitable reference gene because of its instability as previously reported by Murphy and Polak [247-248]. *Rpl32* was used as the only housekeeping gene to normalise *actc1* and *nppa* results as it was reported that the ribosomal protein family sequences are effective reference genes [249].

Although the graphics show a noteworthy up-regulation of *actc1* in both stretching regimes, and an intermediate up-regulation in the *nppa*, statistical analysis of the normalised results reported no statistically significant difference in the expression of *actc1* and *nppa* when the constructs were stretched either continuously or discontinuously (Figure 5-8). Nevertheless, continuous stretching presented a greater expression of both genes when compared to the discontinuous regime. Previously Auluck *et al* reported that ECM remodelling was up-regulated dependant upon strain type, amplitude and frequency. This group evaluated myogenic cells seeded in gelfoams stimulated at 7.5% and 15% amplitude. Constructs were evaluated under two stretching regimes: continuous for 6 hours or cyclic at 12 cycles/h for 6 hours. It was found that at greater amplitude and under continuous stretching, a greater response matrix-metalloprotease 2 was induced [240] The up-regulation found in the Tencell coincides with Sadoshima *et al* who reported that skeletal alpha actin gene was up-regulated when cardiomyocytes were stretched *in vitro*. However they also mentioned that actin may not be the best marker for hypertrophy because it can

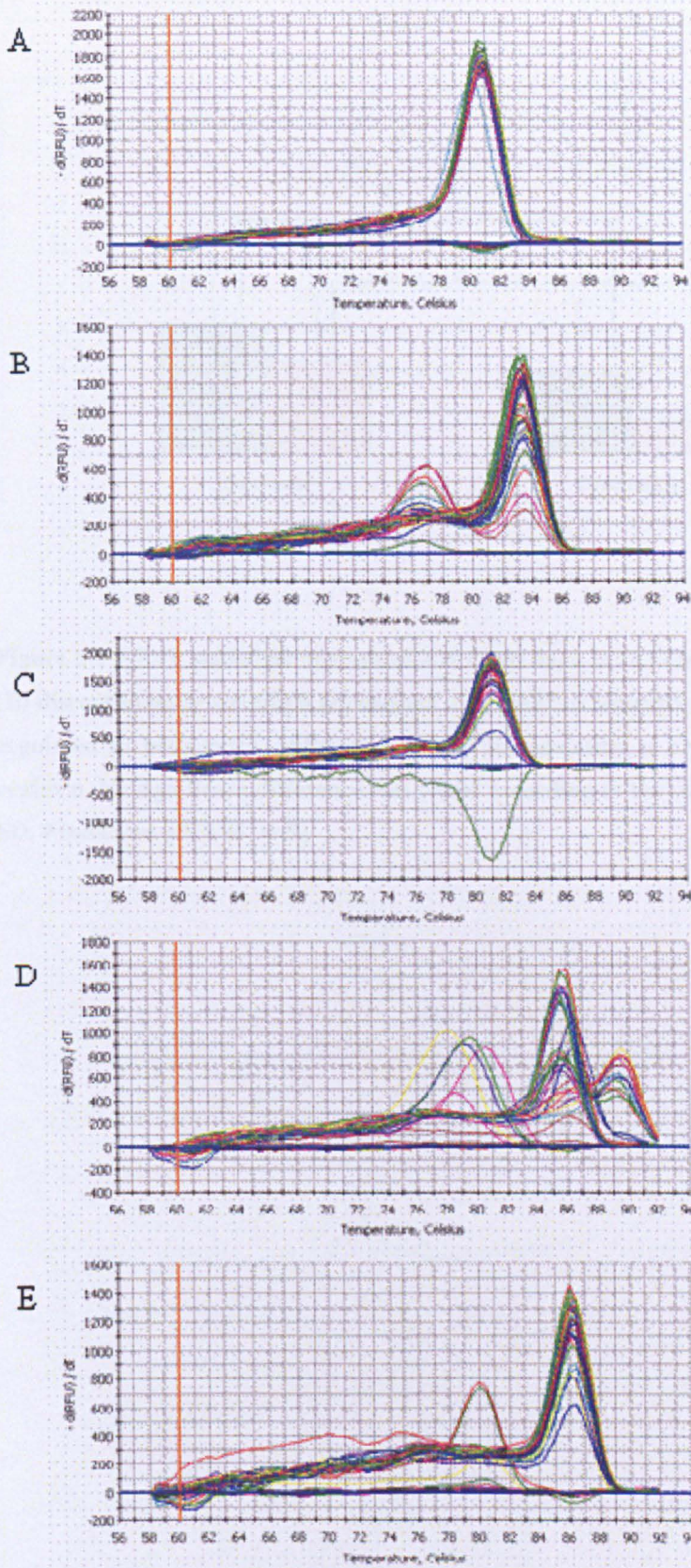
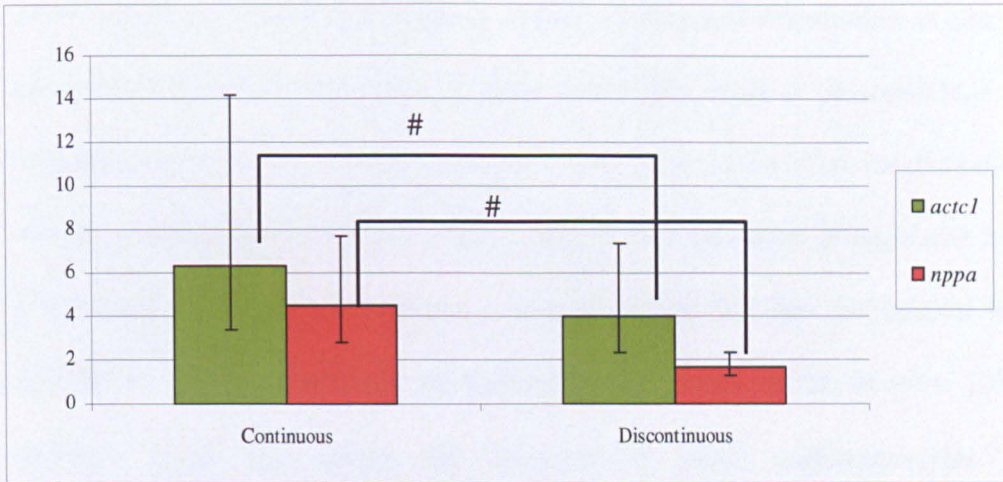


Figure 5-8 Melt curves of the primers for (A) *hprt1*, (B) *rpl32*, (C) *act1*, (D) *myh6* and (E) *nppa*. Several peaks are observed in the *myh6* melt curve indicating the amplification of additional sequences.



**Figure 5-9 REST statistical analysis of *actc1* and *nppa* in (A) continuously stretched and (B) discontinuously stretched normalised with *rpl32* as housekeeping gene. *Actc1* was up-regulated in both cases, although a 4-fold up-regulation is observed in discontinuous regimen. No significant difference was found according to the statistical method (mean  $\pm$  SD, # indicates  $p > 0.05$ ,  $n=9$ )**

be up-regulated even after the hyperplasia stadium in contrast to  $\beta$ -MHC and ANF which are stable late markers [184]. Mechanical stimulation is not the only cause of the up-regulation of these genes. Brown *et al* demonstrated up-regulation of ANF when cardiomyocytes were cultured on a fibronectin-coated silicon surface; their findings suggest that gene expression is regulated by a remodelled ECM [228]. Komuro *et al* also found that the mechanical load applied to silicon constructs up-regulated gene transcription *in vitro* [251]. Authors agree that genes are up-regulated when cardiomyocytes are mechanically stimulated; nevertheless a down-regulation of actin expression has also been reported when cardiomyocytes were cultured in a dynamic bioreactor using a collagen matrix [252].

### **5.3.4 Protein expression**

Alpha-cardiac actin was stained to confirm the presence of protein indicated by the gene expression. The limited number of constructs per experiment only allowed for one protein to be stained. Figure 5-9 illustrates the presence of actin filaments in HL-1 cells cultured in the Tencell bioreactor. No major differences were found between cells stretched discontinuously or continuously.

### **5.3.5 Imaging of constructs**

Cell proliferation and differentiation were evaluated by staining for live cells. Unfortunately POC is an auto-fluorescent material in the red channel and therefore it is only possible to visualise live cells. After incubating in the

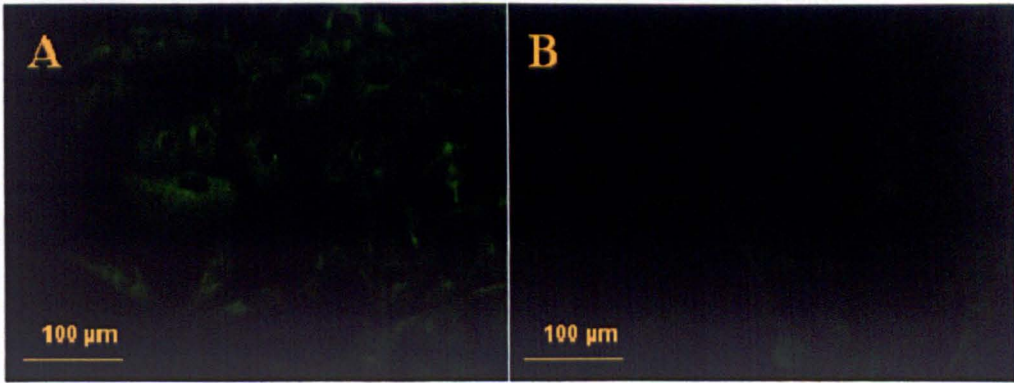


**Figure 5-10** Fluorescent micrographs of actin filaments in HL-1 cells stretched (A) discontinuously and (B) continuously loaded in the Tencell bioreactor.

Tencell the constructs, it was obvious that the clamped area did not support cell attachment or proliferation as can be seen in Figure 5-10. In the central areas of the construct, elongated cells were observed populating the POC scaffolds (Figure 5-11). No apparent difference was detected in cell distribution and morphology between continuous and discontinuously stretched samples when fluorescent images were analysed (Figure 5-12 and 5-13).

Figures 5-14 and 5-15 illustrate the cell distribution and differentiation of HL-1s in POC when visualised under the SEM. Cardiomyocytes statically cultured either on TCP or POC, presented clusters of dead cells but also areas of elongated cells organised into myofibres and aligned in the same direction. Constructs stretched continuously exhibited a larger area of dead cells whereas discontinuous stretched scaffolds shown fewer dead cells and an increased surface of organised elongated cells as can be seen in Figure 5-15. No major variation can be concluded from SEM images, although in this case SEM evaluated random areas and could not give a comprehensive analysis of the entire specimen due to the nature of the scaffold.

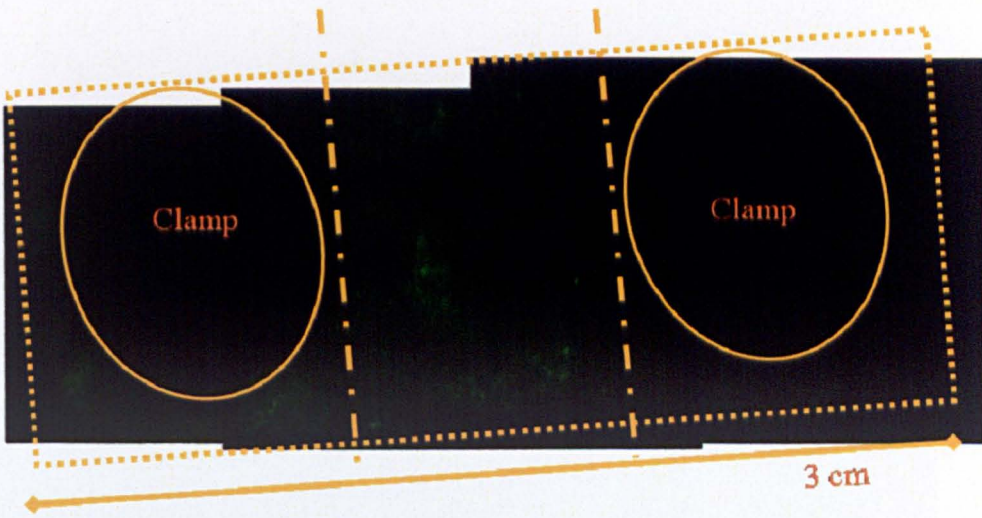


**Figure 5-11** Composed image of fluorescent stereo-micrographs of a HL-1/POC construct cultured in the Tencell stained for Live/Dead. Non-fluorescent lateral areas correspond to the clamps that hold the construct in position and therefore no cell attachment nor proliferation is visible.

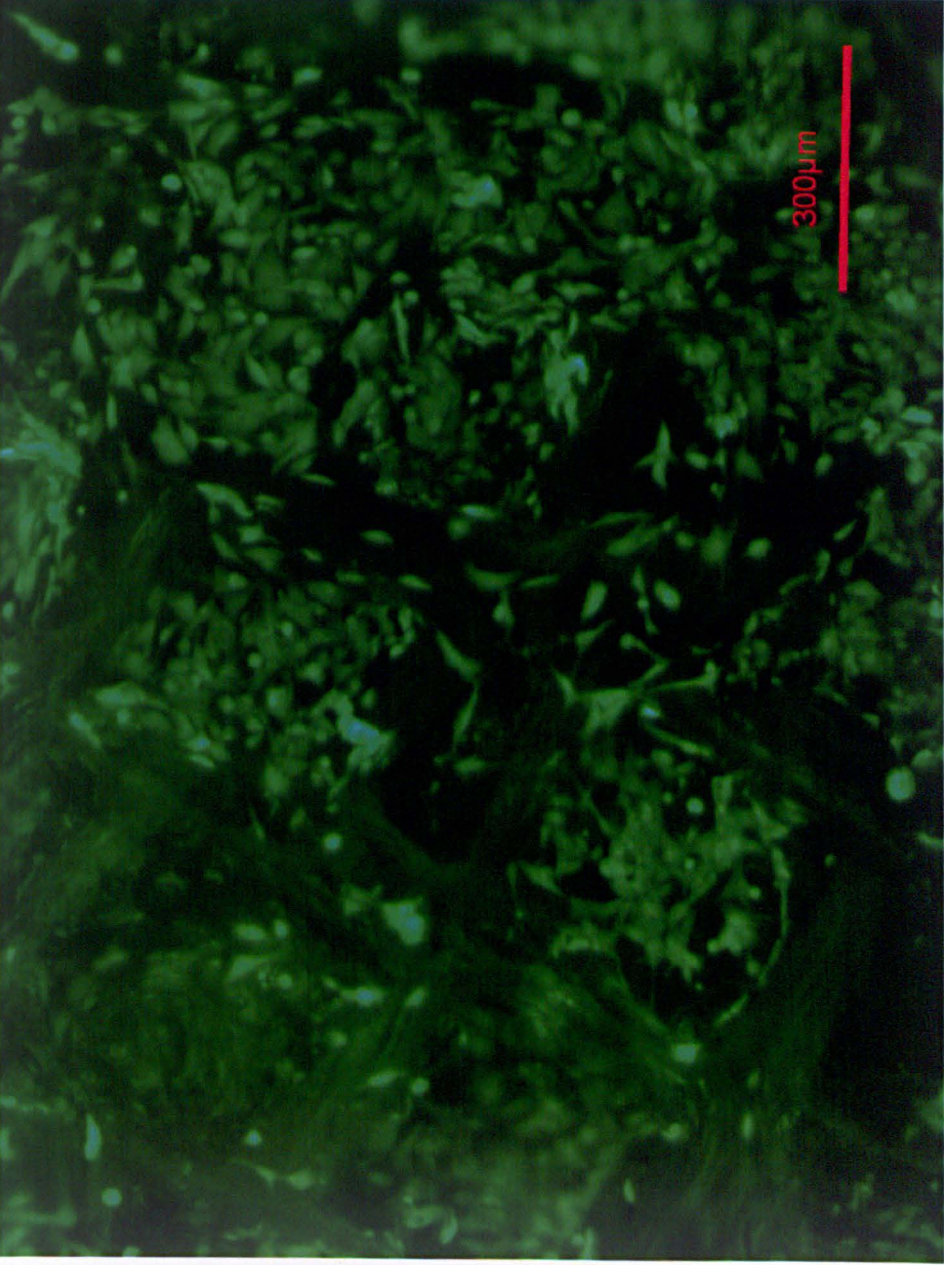
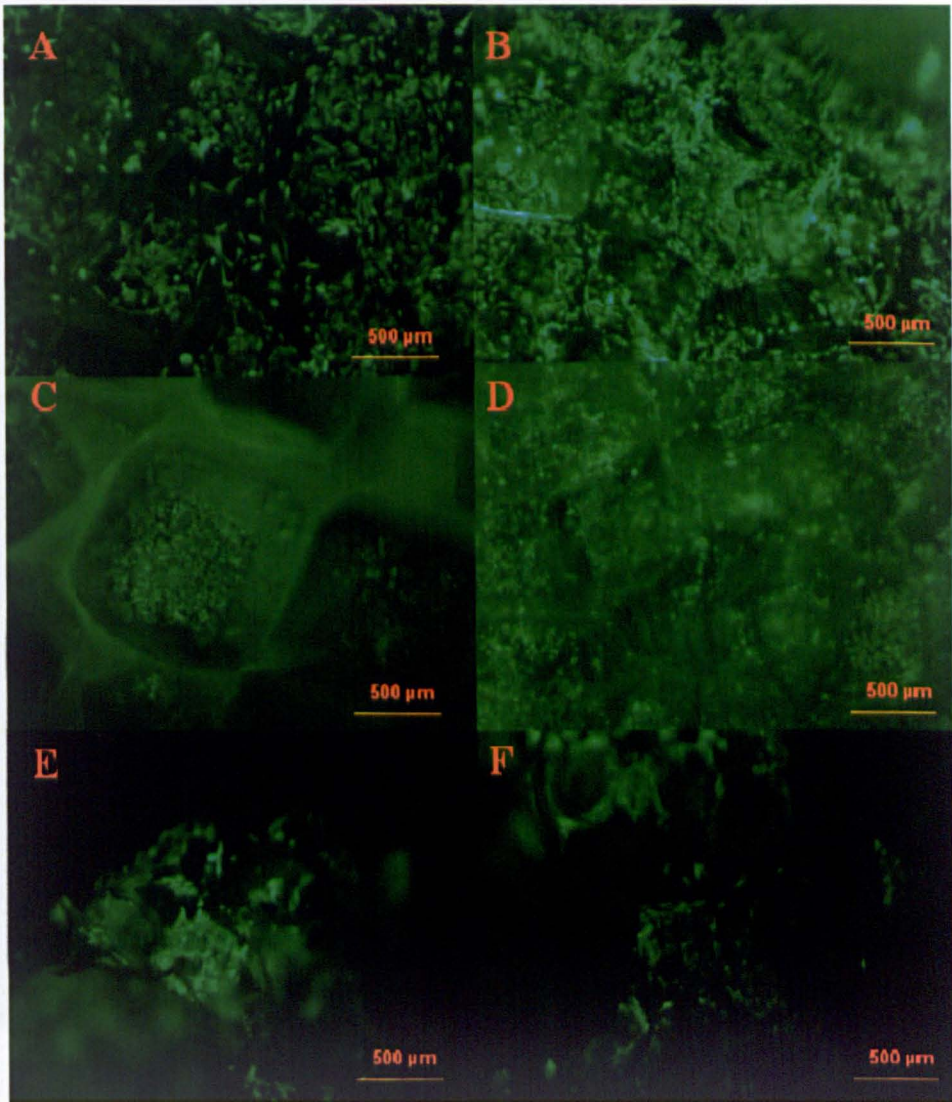


Figure 5-12 Fluorescent image of HL-1 cells in a POC scaffolds



**Figure 5-13** Fluorescent stereo-micrographs of HL-1 constructs cultured (A, B) statically, (C, D) under continuous mechanical load and (E,F) in a stretching regime of four hours per day

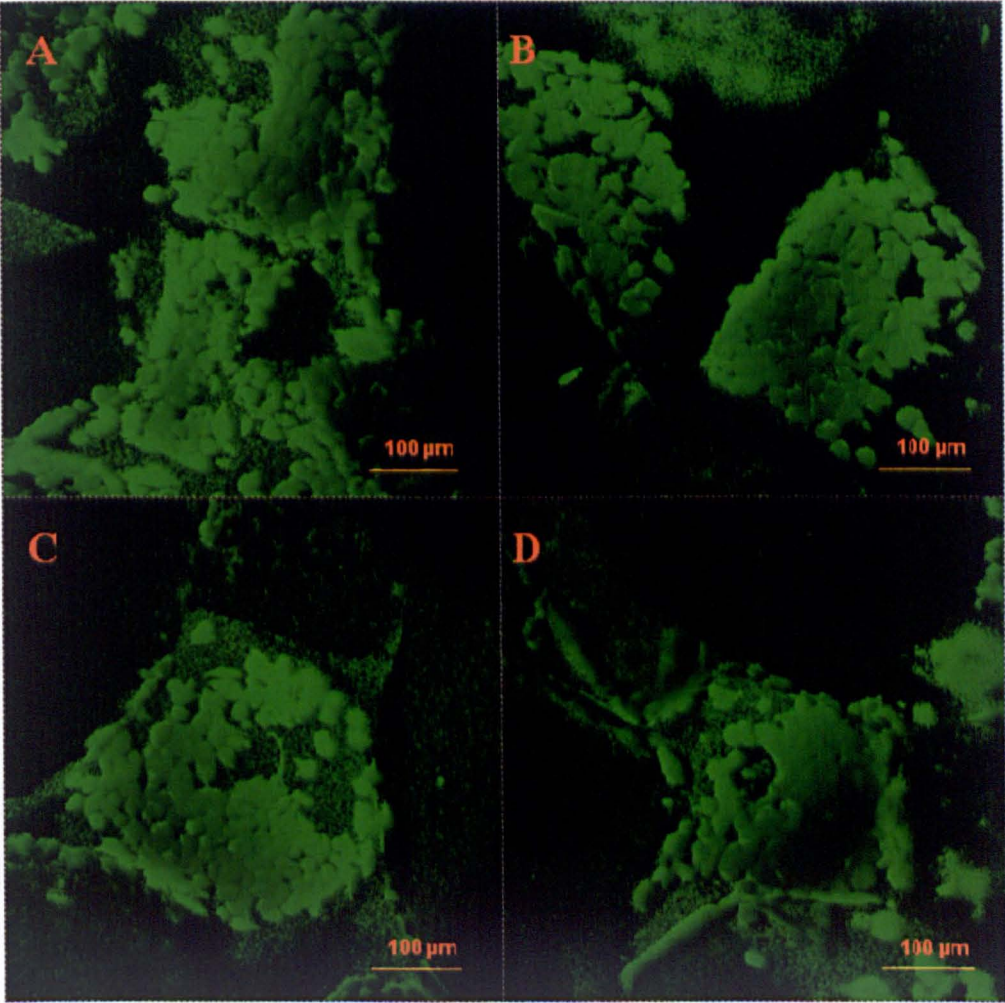
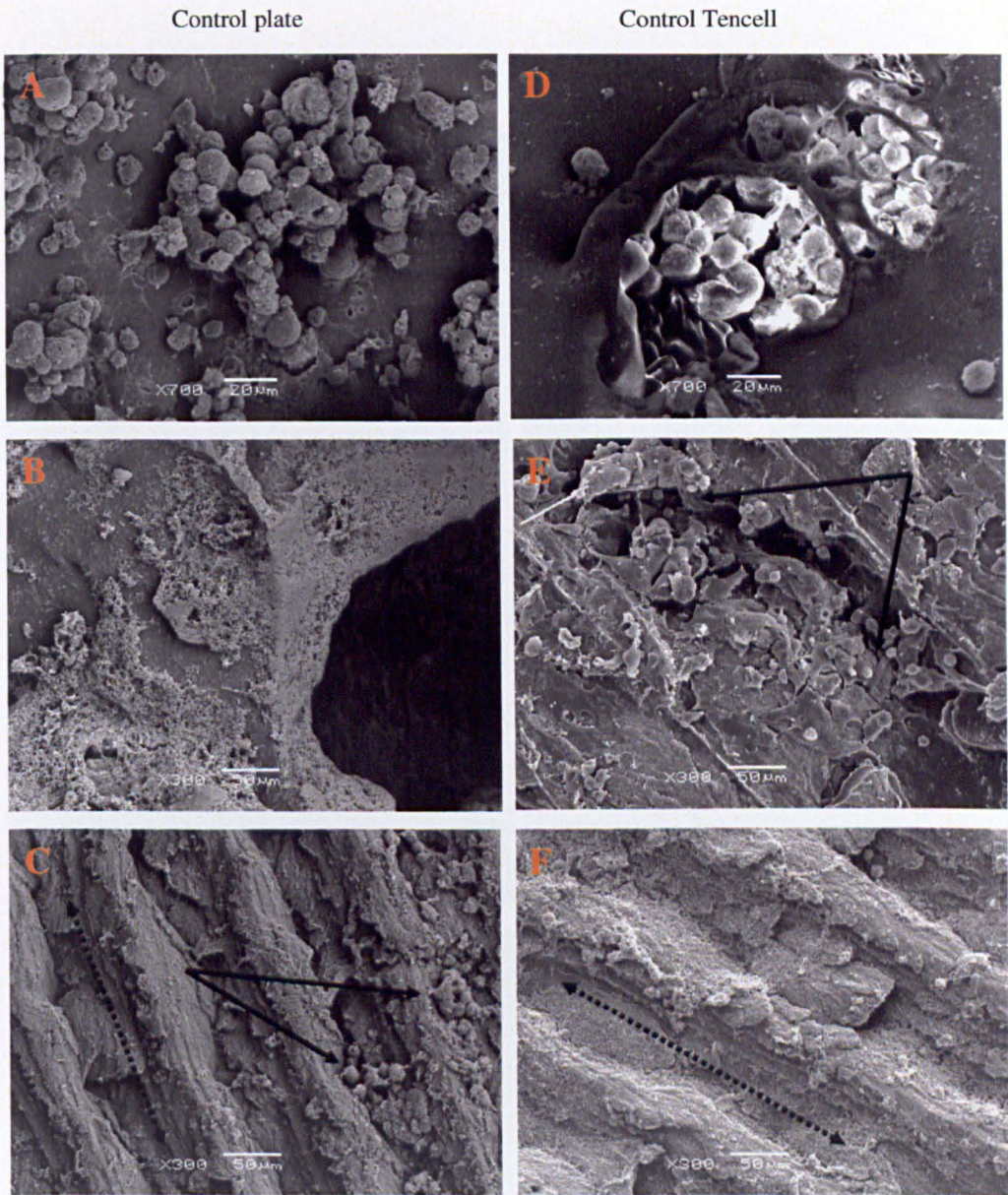
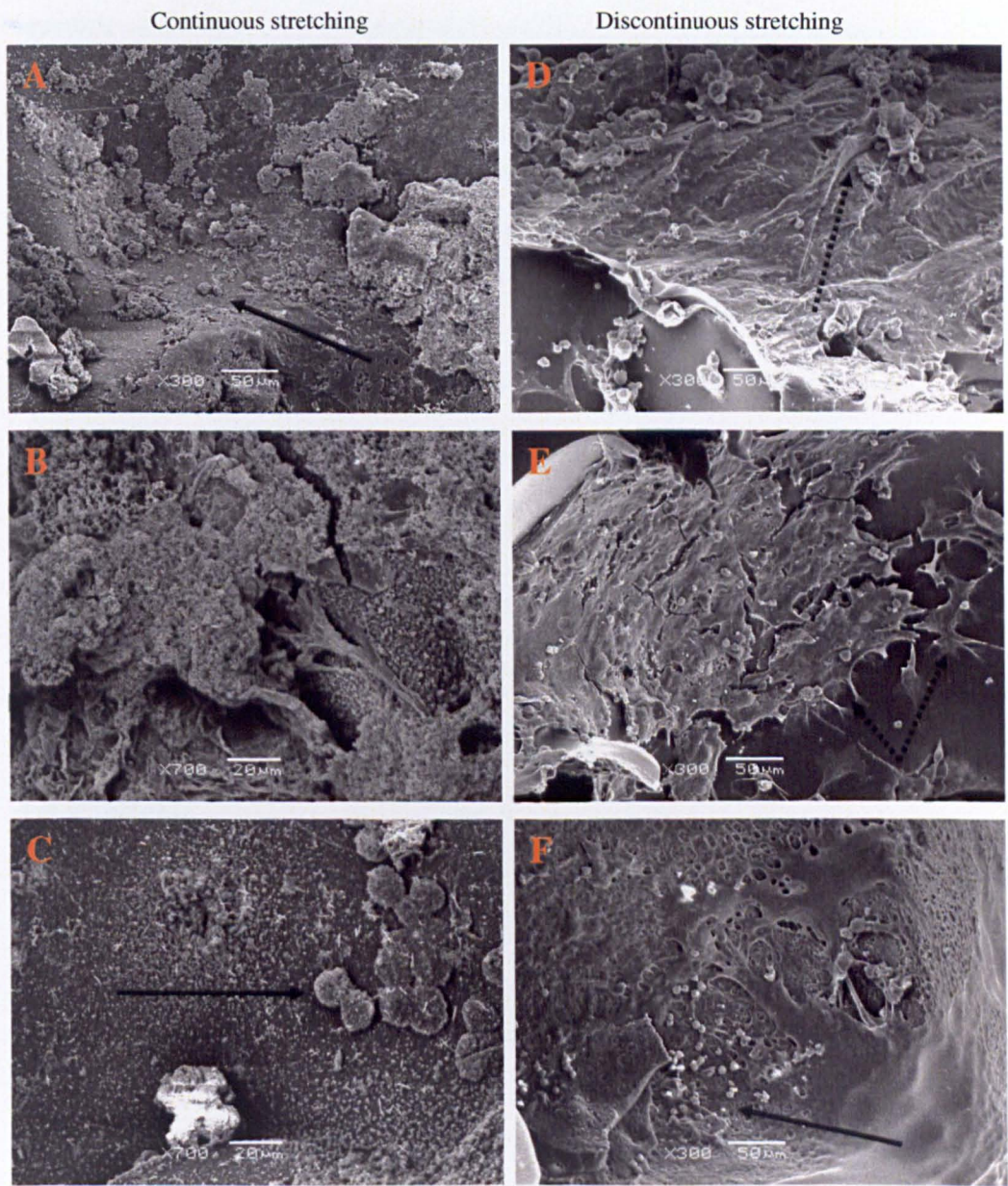


Figure 5-14 Confocal micrographs of HL-1s cultured (A,B) statically and (C,D) in the Tencell.



**Figure 5-15 SEM microphotographs of POC constructs seeded with HL-1 cells and statically cultured for a week in a 8-well plate and in the Tencell. Continuous arrows indicate dead cells and discontinuous arrows show structures that resemble aligned myofibres.**



**Figure 5-16 SEM microphotographs of POC constructs seeded with HL-1 cells and cultured for a week in the Tencell with continuous and discontinuous stretching regime. Continuous arrows indicate dead cells and discontinuous arrows show cardiomyocytes of typical phenotype.**

## 5.4 Conclusions

Barron *et al* reported that the use of bioreactors allowed the development of cardiac constructs by providing the conditions for a resultant graft with better morphological characteristics compared to static culture [243]. In this case this dynamic system did not produce a better construct overall. Mechanical stimulation did elicit an up-regulation of *actc1* and *nppa* genes, although these findings coincide to what has been previously described by other groups, the variation in the results was considerably high and therefore the difference between the stretching regimes was not significant. However, these stretching regimes proved to impact the construct with an increased survival of the cardiomyocytes in the discontinuous regime compared to the survival of non-stretched structures. It was also shown that cardiomyocytes attach, proliferate and exhibit their typical phenotype in POC scaffolds and survive in a dynamic environment.

## 6 General Discussion and Conclusions

Cardiac diseases have been treated with cellular cardiomyoplasty and drugs as an alternative to the shortage of transplant organs. Cardiac tissue engineering seeks to offer an additional advantage to cellular cardiomyoplasty: the immediate functionality and the possibility to use the engineered cardiac muscle also as a screening technique and as an alternative to animal models. Cardiac tissue engineering has exploited the use of dynamic bioreactors to mimic the electro-mechanical environment of the heart. Mechanical stimuli have been proved to be of major relevance for cellular alignment and biochemical signalling when primary cardiomyocytes have been cultured onto flexible materials under these dynamic conditions; however, no work has been done using the HL-1 cardiac cell line on the novel POC elastomer [183-186]. There is therefore the need to assess if the use of this polymer when culturing a cardiac cell line in a stretching regime could prove beneficial for cardiac tissue formation.

The aims of this work were to culture HL-1s/POC constructs in the dynamic bioreactor Tencell and to assess the effect of mechanical stimulation under optimised parameters. Prior to this, it was considered the need to process and characterise POC scaffolds before modifying them to enhance cell adhesion.

The first hypothesis was that POC could be processed into porous scaffolds suitable for cardiac tissue engineering. This work demonstrated that POC can be processed to create porous scaffolds using the salt leaching method but not by  $scCO_2$  processing as was thought. POC monomers resulted not solvent in  $CO_2$  and therefore the elastomer could not be foamed effectively. Porosity was

modified by altering the porogen concentration in the salt leaching method. The resulting scaffolds were characterised using SEM which allowed the qualitative analysis of the resulting scaffolds as well as the measurement of pore size. MicroCT provided pore size distribution and porosity as well as demonstrated pore connectivity and the effect of degradation overtime. Pore size correlated well between SEM and microCT measurements.

Porosity and storage method significantly affected the mechanical properties of the scaffold. Solid POC ultimate elongation was previously reported at 260% with a Young's modulus of 2.6 MPa [42]. In this study, POC porous structures only reached a Young's modulus of 3.3 kPa with 160% of ultimate elongation. Mechanical properties were proportionally weaker in scaffolds 70% and 80% porous when compared to those of 60% porous. It was also found that structures stored at low temperature exhibited a weaker Young's modulus than those stored at room temperature; however the ultimate elongation was higher as a result of a less stiff material. In addition to this, when the material was tested at high strain rates, the Young's modulus was higher than when the same material was evaluated at lower strain. This performance was explained as testing at low strain equals testing the material at low temperature, hence a stiffer behaviour.

Incorporating cellulose to the scaffold improved the mechanical strength of the scaffolds with a Young's modulus of 13 kPa but the limited ultimate elongation (only 70%) in addition to the degradation profile of cellulose in the human body limited their use. Degradation profiles of 60%, 70% and 80% POC scaffolds showed no significant difference between these. All the scaffolds had a rapid initial degradation to then slow than and degrade totally by the 27<sup>th</sup>

week regardless the porosity. POC degradation profile would allow enough time to populate and support cell infiltration and proliferation and to degrade over time allowing the remodelling of the tissue with the newly produced ECM.

Although POC is a hydrophilic polymer, it was expected to present poor cell adhesion because of its synthetic nature. Residual acidic monomers were also a concern due to its effect on pH. After assessing the mechanical properties, this material was evaluated for cell attachment and proliferation using the c2c12 and HL-1 cell lines. Because of the low pH of the scaffolds when in aqueous media, it was needed to wash all the acid residues.

The second hypothesis was that POC scaffolds could be modified to improve cell attachment. Results demonstrated that only when POC was modified with an ECM protein, cell adhesion was supported. Fibronectin, collagen and laminin were used to coat POC films at their optimal concentrations for myocytes and then evaluated for cell viability. In the results presented, fibronectin proved to be the most advantageous coating with nearly 90% of area coverage after 24 hours. Collagen and laminin did not provide the same biochemical cues and area coverage was minimal in surfaces coated with these compared to that of fibronectin. Because the use of proteins can present disadvantages on clinical applications, such as contamination, rejection and short-life, it may be considered to replace fibronectin with RGD before the construct goes into therapeutic stage [180]. ECM native proteins signal biological as well as mechanical stimuli. Ghosh *et al* demonstrated that cells on stiffer substrates exhibited higher elastic properties and cytoskeleton with more

stretched and organised actin filaments; cells on these also migrated and proliferated [254].

With respect to the effect of the porosity when seeding cardiomyocytes onto POC scaffolds, difference was not significant when cell survival was evaluated in 60%, 70% and 80% porous structures. Cells exhibited the same typical phenotype regardless the porosity used. The next step on biomaterial science is the design of “smart materials” which will respond to alterations in the local cellular environment such as temperature, acidity, enzymatic and biochemical signals. This response could vary from change in the biodegradation rate, release of active molecules or activation of specific factors [255].

The third hypothesis was that the seeding method would impact cell survival. Prior to dynamic culture in the stretching bioreactor, Tencell, seeding strategies were evaluated to determine the most suitable method for this system. Static, centrifugal and dynamical seeding was evaluated in c2c12 and HL-1 cells. Dynamic seeding has been used with more success with hydrophobic scaffolds to improve infiltration and contribute to a homogeneous seeding density; under these conditions, dynamic seeding usually increases viability and retention [174]. In the results presented, it was shown that static seeding proved to be the most beneficial seeding for these cells in 70% porous scaffolds, coated previously with fibronectin as determined in the previous studies. Centrifugal seeding, assessed in HL-1 cells, was limited by the scaffold morphology. Dynamic seeding, carried out by shaking at 100, 200 and 300 rpm the constructs, showed that at low speed, cell survival and morphology are not too different from the static seeding; however after 24 hours of agitation at 200 and 300 rpm, cells did not survive. Hence, it was concluded that no agitation or

minimal was required to ensure cell attachment and proliferation of myocytes in POC scaffolds.

The last hypothesis was that mechanical stimulation would promote cardiac tissue formation. The use of bioreactors in tissue engineering is mainly because of the need of improve mass transfer; however in this case the bioreactor also allowed for the constructs to be mechanically stimulated. In terms of culturing the HL-1s/POC constructs in the Tencell, it was first demonstrated that there was no significant difference when the constructs were seeded in 8-well plates and later transferred to the bioreactor or when seeded *in situ*. Dynamic culture was compared as a regime of continuous stretching of 10% of the construct against a discontinuous regime of 4 hours of mechanical stimulation at the same amplitude followed by 20 hours of static culture. After one week of dynamic culture, larger number of cells proliferated under discontinuous stretching compared to the other two conditions; cell viability was similar under static and continuous stretching. Constructs imaged by SEM, stereo and confocal microscopy revealed that HL-1s exhibited a typical phenotype when cultured statically and discontinuously but not so much when stretched continuously, where more dead cells were found. These results highlighted the importance of conditioning the cells without continuous stretching to allow the cells to attach and proliferate without mechanical strain. The effect of the mechanical stimuli in the constructs was also assessed at molecular level. Gene expression analysis of *actc1* and *nppa* revealed an up-regulation in both cases although no significant difference was obtained when comparing the continuous and the discontinuous regimes. It was thought that mechanical stimulation would provide an ideal environment for the

cardiomyocytes to form cardiac tissue; however results were not conclusive as not all the data was significantly better. Although cell survival was improved by discontinuous stretching, no myofibres formation was observed whilst up-regulation of gene expression reached acceptable levels.

In conclusion, POC scaffolds were characterised and modified for *in vitro* cardiac culture. In addition, cell imaging and biochemical assays have demonstrated that myocytes can attach, proliferate and exhibit their typical phenotype in POC scaffolds and survive in a dynamic environment.

## References

1. Komura I and Y Yazaki. Control of Cardiac Gene Expression by Mechanical Stress. *Annu Rev Physiol* 1993; 55:55-75
2. British Heart Foundation. 2004. [www.bhf.org.uk](http://www.bhf.org.uk)
3. Rayner M and S Petersen. European cardiovascular disease statistics 2000. 2000. [www.dphpc.ox.ac.uk/bhfhprg](http://www.dphpc.ox.ac.uk/bhfhprg): 80 p.
4. American Heart Association. 2004. [www.americanheart.org](http://www.americanheart.org).
5. Opie LH. The Heart: physiology, from cell to circulation. 1998: Lippincot-Raven. Philadelphia, USA
6. Narula J *et al.* (Ed). Heart failure:pathogenesis and treatment. Martin Dunitz Ltd. UK 2002
7. Essential Cardiology: Principles and Practice, ed. C. Rosendorff. 2001: Saunders. 895 p.
8. Lecture notes on Cardiology, ed. H.H. Gray. 2002: Blackwell Science. 274 p.
9. Anversa P, Leri A, Kajstura J and B Nadal-Ginard. Myocyte growth and cardiac repair. *J Mol Cell Card* 2002; 34(2): 91-105.
10. Engel FB, Hauck L, Cardoso MC, Leonhardt H, Dietz R and R von Harsdorf. A mammalian myocardial cell-free system to study cell cycle reentry in terminally differentiated cardiomyocytes. *Circ Res* 1999; 85(3): 294-301.

11. Shachar M and RJ Cohen. Cardiac Tissue Engineering, Ex-Vivo: Design Principles in Biomaterials and Bioreactors. *Heart Fail Rev* 2003; 8: 271-276.
12. Weber KT, Sun Y and LC Katwa. Myofibroblasts and local angiotensin II in rat cardiac tissue repair. *Int J Biochem Cell Biol* 1997; 29(1): 31-42.
13. Zandstra PW, Bauwens C, Yin T, Liu Q, Schiller H, Zweigerdt R, Pasumarthi KBS and LJ Field. Scalable production of embryonic stem cell-derived cardiomyocytes. *Tissue Eng* 2003; 9(4): 767-778.
14. Heart failure: Molecules, Mechanisms and therapeutic targets. John Wiley & Sons. UK 2006
15. Fukuda K. Progress in myocardial regeneration and cell transplantation. *Circ J* 2005; 69(12): 1431-1446
16. Cardiac cell and gene transfer: principles, protocols, and applications, ed. J.M. Metzger. 2003: Humana Press. 253 p.
17. Kehat I, Amit M, Gepstein A, Khimovich L, Feld Y, Itskovitz-Eldor J and L Gepstein. Functional integration of human embryonic stem cell derived cardiomyocytes with preexisting cardiac tissue: Implication for myocardial repair. *Circ* 2001; 104(17): 618.
18. Carraro U, Barbiero M, Docali G, Cotogni A, Rigatelli G, Casarotto D and C Muneretto. Demand dynamic cardiomyoplasty: Mechanograms prove incomplete transformation of the rested latissimus dorsi. *Ann Thorac Surg* 2000; 70(1): 67-73.

19. Mouquet F, Susen S, Van Bell E, Bauters C and B Jude. Cell therapy to treat heart failure. *Rev Med Int* 2003; 24(6): 401-404.
20. Siminiak T and M Kurpisz. Myocardial replacement therapy. *Circ* 2003; 108(10): 1167-1171.
21. [www.bioheartinc.com/about.php](http://www.bioheartinc.com/about.php) Biohert Inc. 2008
22. Leier, C V. Latissimus Dorsi Cardiomyoplasty. *ACC Current J Rev* 1998; 7(1):57-60
23. McDevitt TC, Woodhouse KA, Hauschka SD, Murry CE and PS Stayton. Spatially organized layers of cardiomyocytes on biodegradable polyurethane films for myocardial repair. *J Biomed Mat Res* 2003; 66A(3): 586-595.
24. Langer R and JP Vacanti. Tissue Engineering. *Science* 1993; 260: 920-926
25. National Science Foundation. 1988. [www.nsf.gov](http://www.nsf.gov)
26. Stocum DL. Regenerative Biology and Medicine. Academic Press-Elsevier. UK 2006
27. Rabkin E and FJ Schoen. Cardiovascular tissue engineering. *Cardiovasc Pathol* 2002; 11(6): 305-317.
28. Pearson RG, Bhandari R, Quirk RA and KM Shakesheff. Recent Advances in Tissue Engineering: An Invited Review. *J Long-Term Eff Med Implants* 2002; 12(1): 1-33.

29. Vunjak-Novakovic G and RI Freshney Ed. Culture of Cells for Tissue Engineering. Wiley USA 2006.
30. Claycomb WC, Lanson NA, Stallworth BS, Egeland DB, Delcaprio JB, Bahinski A and NJ Izzo. HL-1 cells: A cardiac muscle cell line that contracts and retains phenotypic characteristics of the adult cardiomyocyte. *Proc Nat Acad Sci USA* 1998; 95(6): 2979-2984.
31. Neilan, C. L., E. Kenyon, M.A. Kovach, K. Bowden, W.C. Claycomb, J.R. Traynor and S.F. Bolling. An immortalized myocyte cell line, HL-1, expresses a functional delta-opioid receptor. *J Mol Cell Cardiol* 2000; 2(12): 2187-2193.
32. Sartiani L, Bochet P, Cerbai E, Mugelli A and R Fischmeister. Functional expression of the hyperpolarization-activated, non-selective cation current I<sub>f</sub> in immortalized HL-1 cardiomyocytes. *J Physiol-London* 2002; 545(1): 81-92.
33. Ikada, Y. Tissue Engineering Fundamentals and applications. Elsevier UK 2006
34. Hench, LL and JR Jones Ed. Biomaterials, artificial organs and tissue engineering. Woodhead Publishing Limited. England 2005.
35. Callister WD. Materials Science and Engineering. an introduction, 6<sup>th</sup> edition. NY, Wiley, 2003
36. Ratner, BD *et al* Ed. Biomaterials Science: An introduction to Materials in Medicine. Elsevier UK 2004.

37. Rezwan K, Chen QZ, Blaker JJ and AR Boccaccini. Biodegradable and bioactive porous polymer/inorganic composite scaffolds for bone tissue engineering. *Biomater* 2006; 27(18):3413-3431
38. Thermoplastic elastomers (Department of polymer Science, University of Southern Mississippi). 2004. [www.psrc.usm.edu/macrog/tpe.htm](http://www.psrc.usm.edu/macrog/tpe.htm)
39. Saltzman, WM. Tissue Engineering: Engineering Principles for the Design of replacement organs and tissues. Oxford University Press. USA 2004
40. Ahn BD, Kim SH, Kim YH and JS Yang. Synthesis and characterization of the biodegradable copolymers from succinic acid and adipic acid with 1,4-butanediol *J Appl Pol Sci* 2001; 82:11, 2808-2826
41. Yang J, Webb AR and GA Ameer. Novel Citric acid-based Biodegradable Elastomers for Tissue Engineering” *Adv Mat* 2004; 16 (6): 511-516
42. Chemical Land 21. 2004. [www.chemicalland21.com](http://www.chemicalland21.com)
43. Bronzino, J (Ed). Tissue Engineering and Artificial organs. Taylor & Francis. USA 2006
44. Prendergast PJ and PE McHugh (Eds.) Topics in Bio-Mechanical engineering. 2004. Trinity centre for bioengineering and national centre for biomedical engineering science. Dublin, Ireland

45. Howard D, Buttery LD, Shakesheff KM and SJ Roberts. Review: Tissue engineering: strategies, stem cells and scaffolds. *J Anat* 2008. online early article doi:10.1111/j.1469-7580.2008.00878.x
46. Sung HJ, Carson M, Johnson C and ZS Galis. The effect of scaffold degradation rate on three-dimensional cell growth and angiogenesis. *Biomater* 2004; 25(26):5735-5742
47. Alsberg E, Kong HJ, Hirano Y, Smith MK, Albeiruti A and DJ Mooney. Regulating Bone Formation via Controlled Scaffold Degradation. *J Dent Res* 2003; 82(11): 903-908
48. Sales VL, Engelmayer GC, Johnson JA, Gao J, Wang Y, Sacks MS and JE Mayer. Protein Precoating of Elastomeric Tissue-Engineering Scaffolds Increased Cellularity, Enhanced Extracellular Matrix Protein Production, and Differentially Regulated the Phenotypes of Circulating Endothelial Progenitor Cells. *Circ.* 2007;116:I-55 – I-63.
49. Masood SH, Singh JP and Y Morsi. The design and manufacturing of porous scaffolds for tissue engineering using rapid prototyping. *Int J Adv Manuf Tech* 2005; 27(3-4):415-420.
50. Yang S, Leong KF, Du Z, Chua CK. The design of scaffolds for use intissue engineering. Part I. Traditional factors. *Tissue Eng* 2001; 7: 679-689
51. Leong KF, Cheah CM, Chua CK. Solid freeform fabrication of three-dimensional scaffolds for engineering replacement tissues and organs. *Biomaterials* 2003; 24(13):2363-78.

52. Antonios GM and JS Temenoff. Formation of highly porous biodegradable scaffolds for tissue engineering. *Electron. J. Biotechnol.* 2000; 3(2): 1-6
53. Reis RL and J San Roman (Eds). Biodegradable systems in tissue engineering and regenerative Medicine. CRC Press. USA 2005.
54. Howdle SM, Watson MS, Whitaker MJ, Popov VK, Davies MC, Mandel FS, Wang JD and KM Shakesheff. Supercritical fluid mixing: preparation of thermally sensitive polymer composites containing bioactive materials. *Chem Comm* 2001; 1:109-110
55. Elvassore N, Baggio M, Pallado P and A Bertucco. Production of different morphologies of biocompatible polymeric material by supercritical CO<sub>2</sub> antisolvent techniques. *Biotech Bioeng* 2001; 73: 449-457
56. Cooper AI. Recent developments in materials synthesis and processing using supercritical CO<sub>2</sub>. *Adv Mat* 2001; 13:1-4
57. Barry JJA, Guidda HS, Scotchford CA and SM Howdle. Porous methacrylate scaffolds: supercritical fluid fabrication and *in vitro* chondrocyte responses. *Biomaterials* 2004; 25: 3559-2568.
58. Bursac N, Papadaki M, Cohen RJ, Schoen FJ, Eisenberg SR, Carrier R, Vunjak-Novakovic G and LE Freed. Cardiac muscle tissue engineering: toward an *in vitro* model for electrophysiological studies. *Am J Physiol-Heart Circ Physiol* 1999; 277(2): H433-H444.

59. Shimizu T, Yamto M, Kikuchi A and T Okano. Two-Dimensional Manipulation of Cardiac Myocyte Sheets Utilizing Temperature-Responsive Culture Dishes Augments the Pulsatile Amplitude. *Tissue Eng* 2001; 7(2): 141-151.
60. Sodian R, Sperling JS, Martin DP, Egozy A, Stock U, Mayer JE and JP Vacanti. Fabrication of a trileaflet heart valve scaffold from a polyhydroxyalkanoate biopolyester for use in tissue engineering. *Tissue Eng* 2000; 6(2): 183-188.
61. Polonchuk L, Elbel J, Eckert L, Blum J, Wintermantel E and HM Eppenberger. Titanium dioxide ceramics control the differentiated phenotype of cardiac muscle cells in culture. *Biomaterials* 2000; 21(6): 539-550.
62. Shin M, Ishii O, Sueda T and JP Vacanti. Contractile cardiac grafts using a novel nonfibrous mesh. *Biomaterials* 2004; 25: 3717-3723.
63. Schmidt CE and JM Baier. Acellular vascular tissues: natural biomaterials for tissue repair and tissue engineering. *Biomaterials* 2000; 21(22): 2215-2231.
64. Ye Q, Zund G, Benedikt P, Jockenhoevel S, Hoerstrup SP, Sakyama S, Hubbell JA and M Turina. Fibrin gel as a three dimensional matrix in cardiovascular tissue engineering. *Eur J Cardio-Thorac Surg* 2000; 17(5): 587-591.

65. Kim BS and DJ Mooney. Scaffolds for engineering smooth muscle under cyclic mechanical strain conditions. *J Biomech Eng-Trans ASME* 2000; 122(3): 210-215.
66. Costa KD, Lee EJ and JW Holmes. Creating alignment and anisotropy in engineered heart tissue: Role of boundary conditions in a model three-dimensional culture system. *Tissue Eng* 2003; 9(4): 567-577.
67. Pego AP, Poot AA, Grijpma, DW, Feijen J. Biodegradable elastomeric scaffolds for soft tissue engineering. *J Cont Release* 2003;87:69-79
68. Radisic M, Vunjak-Novakovic G. Cardiac tissue engineering. *J Serb Chem Soc* 2005;70(3);541-556
69. Evans HJ, Sweet JK, Price RL, Yost M and RL Goodwin. Novel 3D culture system for study of cardiac myocyte development. *Am J Physiol-Heart Circ Physiol* 2003; 285(2): H570-H578.
70. Radisic M, Euloth M, Yang LM, Langer R, Freed LE and G Vunjak-Novakovic. High-density seeding of myocyte cells for cardiac tissue engineering. *Biotech Bioeng* 2003; 82(4): 403-414.
71. Kofidis T, Lenz A, Boublik J, Akhyari P, Wachsmann B, Stahl KM, Haverich A and RG Leyh. Bioartificial grafts for transmural myocardial restoration: a new cardiovascular tissue culture concept. *Eur J Cardio-Thorac Surg* 2003; 24(6): 906-911.

72. Dar A, Shachar M, Leor J and S Cohen. Cardiac tissue engineering - Optimization of cardiac cell seeding and distribution in 3D porous alginate scaffolds. *Biotech Bioeng* 2002; 80(3): 305-312.
73. Hubbell, JA. Bioactive Materials. *Curr Op Biotech* 1999; 10: 123-129.
74. Zisch AH, Schenk U, Schenses JC, Sakiyama-Elbert SE and JA Hubbell. Covalently conjugated VEGF-fibrin matrices for endothelialization. *J Control Release* 2001; 72(1-3): 101-113.
75. Papadaki M, Bursac N, Langer R, Merok J, Vunjak-Novakovic G and LE Freed. Tissue engineering of functional cardiac muscle: molecular, structural, and electrophysiological studies. *Am J Physiol-Heart Circ Physiol* 2001; 280(1): H168-H178.
76. Akhyari P *et al.* Mechanical stretch regimen enhances the formation of bioengineered autologous cardiac muscle grafts. *Circ* 2002;106(suppl I):I137-I142
77. Carrier RL, Rupnick M, Langer R, Schoen FJ, Freed LE and G Vunjak-Novakovic. Effects of oxygen on engineered cardiac muscle. *Biotech Bioeng* 2002; 78(6): 617-625.
78. Sodian R, Lemke T, Fritsche C, Hoerstrup SP, Fu P, Potapov EV, Hausmann H and R Hetzer. Tissue-engineering bioreactors: A new combined cell-seeding and perfusion system for vascular tissue engineering. *Tissue Eng* 2002; 8(5): 863-870.

79. Carrier RL, Rupnick M, Langer R, Schoen FJ, Freed LE and G Vunjak-Novakovic. Perfusion improves tissue architecture of engineered cardiac muscle. *Tissue Eng* 2002; 8(2): 175-188.
80. Carrier RL, Papadaki M, Rupnick M, Schoen FJ, Bursac N, Langer R, Freed LE and G Vunjak-Novakovic. Cardiac tissue engineering: Cell seeding, cultivation parameters, and tissue construct characterization. *Biotech Bioeng* 1999; 64(5): 580-589.
81. Solan A, Mitchell S, Moses M and L Niklason. Effect of pulse rate on collagen deposition in the tissue- engineered blood vessel. *Tissue Eng* 2003; 9(4): 579-586.
82. Sugden PH. Mechanotransduction in cardiomyocyte hypertrophy. *Circ* 2001; 103(10): 1375-1377.
83. Ruwhof C, van Wamel AET, Egas JM and A van der Laarse. Cyclic stretch induces the release of growth promoting factors from cultured neonatal cardiomyocytes and cardiac fibroblasts. *Mol Cell Biochem* 2000; 208(1-2): 89-98.
84. Kada K, Yasui K, Naruse K, Kamiya K, Kodama I and J Toyama. Orientation change of cardiocytes induced by cyclic stretch stimulation: Time dependency and involvement of protein kinases. *J Mol Cell Card* 1999; 31(1): 247-259.
85. Reffelmann T and RA Kloner. Cellular cardiomyoplasty - cardiomyocytes, skeletal myoblasts, or stem cells for regenerating

myocardium and treatment of heart failure?. *Cardiovasc Res* 2003; 58(2): 358-368.

86. Digisens 2007 [www.digitalscanservice.com/tomography.php](http://www.digitalscanservice.com/tomography.php)

87. Chu, CC. The in-vitro degradation of poly(glycolic acid) suture-effect of pH. *J. Biomed Mater Res* 1981; 15: 795

88. Chu, CC. An in-vitro degradation study of the effect of buffer on the degradation of poly(glycolic acid) sutures. *J Biomed Mater Res* 1981;15:19

89. Itano N, Okamoto S, Zhang D, Lipton SA and E Ruoslahti. Cell spreading controls endoplasmic and nuclear calcium: a physical gene regulation pathway from the cell surface to the nucleus. *PNAS* 2003; 100(9):5181-6.

90. Lien YC, Lin SM, Nithipongvanitch R, Oberley TD, Noel T, Zhao Q, Daosukho C, and DK St Clair. Tumor necrosis factor receptor deficiency exacerbated Adriamycin-induced cardiomyocytes apoptosis: an insight into the Fas connection. *Mol Cancer Ther.* 2006 Feb; 5(2):261-9.

91. Imanaka-Yoshida K, Hiroe M, Nishikawa T, Ishiyama S, Shimojo T, Ohta Y, Sakakura T and T Yoshida. Tenascin-C modulates adhesion of cardiomyocytes to extracellular matrix during tissue remodelling after myocardial infarction. *Lab Inves.* 2001 Jul;81(7):1015-24

92. Ingham E and J Fisher. Development of Physically interactive bioreactors for study of cell and tissue responses to biomechanical stimulation in vitro. *Eur Cell Mat* 2003 6(2):5
93. Ahmed SA, Gogal RM Jr and JE Walsh. A new rapid and simple non-radioactive assay to monitor and determine the proliferation of lymphocytes: an alternative to [<sup>3</sup>H]thymidine incorporation assay. *J. Immunol. Methods* 1994; 170:211-224.
94. Rozen S and H Skaletsky. "Primer3 on the WWW for general users and for biologist programmers". In: Krawetz S, Misener S (eds) *Bioinformatics Methods and Protocols: Methods in Molecular Biology*. Humana Press, 2000. Totowa, NJ, pp 365-386
95. Koressaar T and M Remm. Enhancements and modifications of primer design program Primer3. *Bioinform* 2007; 23(10):1289-1291
96. Grove DS. Quantitative real-time polymerase chain reaction for the core facility using TaqMan and the Perkin-Elmer/Applied Biosystems Division 7700 Sequence Detector. *J Biomol Tech* 1999; 10: 11-16
97. Pfaffl MW, Horgan GW and L Dempfle. Relative expression software tool (REST ©) for group-wise comparison and statistical analysis of relative expression results in real-time PCR. *Nucleic Acids Res* 2002; 30(9):e36
98. Lemanski L and Z Tu. Immunofluorescent studies for myosin, actin, tropomyosin and  $\alpha$ -actinin in cultured cardiomyopathic hamster heart cells. *Develop Biol* 1983;97(2):338-348

99. Fluorescent staining of living cells. Johnson I. *Microscopy and histology for molecular biologists: A user's guide*, Eds. Kiernan JA, Mason I, 2002. pp. 92-101
100. Bancroft, J.D., Stevens. A. eds. *Theory and practice of histological techniques*. 4th Ed. London: Churchill Livingstone, 1996.
101. Jancar J, Slovikova A, Amler E, Krupa P, Kecova H, Planka L, Gal P and A Necas. Mechanical response of porous scaffolds for cartilage engineering. *Physiol Res* 2007; May 31
102. Gorna K and S Gogolewski. Biodegradable porous polyurethane scaffolds for tissue repair and regeneration. *J Biomed Mater Res A*. 2006;79(1):128-38
103. Bhat S. *Biomaterials*, 2nd Ed. Alpha Science International LTD, UK. 2005
104. "Plasticizers", Ullmann's Encyclopaedia of Industrial Chemistry, Volume A 20, 1992; 439-458
105. Tai H, Popov VK, Shakesheff KM and SM Howdle. Putting the fizz into chemistry: applications of supercritical carbon dioxide in tissue engineering, drug delivery and synthesis of novel block copolymers. *Biochem Soc Trans*. 2007; 35(3):516-21
106. Arora KA, Lesser AJ and TJ McCarthy. Preparation and characterization of microcellular polystyrene foams processed in supercritical carbon dioxide. *Macromolecules* 1998;31:4614-4620

107. Shieh Y-T, Su J-H, Manivannan G, Lee PHC, Sawan SP and WD Spall. Interaction of supercritical carbon dioxide with polymers. I. Crystalline polymers. *J Appl Polymer Sc.*1996;59(4); 695-705
108. Goel SK and EJ Beckman. Generation of microcellular polymeric foams using supercritical carbon dioxide. I: Effect of pressure and temperature on nucleation. *Polymer Eng Sc* 1994; 34(3): 1137-1147
109. Cooper AI. Polymer synthesis and processing using supercritical carbon dioxide. *J Mat Chem* 2000; 10(2):207-234
110. Cooper AI. Porous materials and supercritical fluids. *Adv Mat* 2003; 15:1049-1059
111. Alavi SH, Gogoi BK, Khan M, Bowman BJ and SSH Rizvi. Structural properties of protein-stabilized starch-based supercritical fluid extrudates. *Food Res International* 1999; 32(2): 107-118
112. Mooney DJ, Baldwin DF, Suh NP, Vacanti JP and R Langer. Novel approach to fabricate porous sponges of poly(D,L-lactic-co-glycolic acid) without the use of organic solvents. *Biomaterials* 1996;17(14):1417-22
113. Harris L, Kim BS and D J Mooney. Open pore biodegradable matrices formed with gas foaming. *Biomed Mater Res* 1998; 42, 396-402
114. Richardson TP, Peters MC, Ennett AB and DJ Mooney. Polymeric system for dual growth factor delivery. *Nat Biotechnol* 2001;19(11):1029-34

115. Kanczler J, Barry J, Ginty P, Howdle SM, Shakesheff KM and ROC Oreffo. Supercritical carbon dioxide generated vascular endothelial growth factor encapsulated poly(dl-lactic acid) scaffolds induce angiogenesis in vitro. *Biochem Biophys Res Commun.* 2007; 352(1):135-141
116. Hile DD, Amirpour ML, Akgerman A and MV Pishko. Active growth factor delivery from poly(d,l-lactide-co-glycolide) foams prepared in supercritical CO<sub>2</sub>. *J Contr Rel* 2000; 66(2): 177-185
117. Howdle SM, Watson MS, Whitaker MJ, Popov VK, Davies MC, Mandel FS, Wang JD, and KM Shakesheff. Supercritical fluid mixing: preparation of thermally sensitive polymer composites containing bioactive materials. *Chem Commun.* 2001: 109-110
118. Ginty PJ, Howard D, Rose FR, Whitaker MJ, Barry JJ, Tighe P, Mutch SR, Serhatkulu G, Oreffo RO, Howdle SM and KM Shakesheff. Mammalian cell survival and processing in supercritical CO<sub>2</sub>. *Proc Natl Acad Sci* 2006;103(19):7426-31
119. Heyde M, Partridge KA, Howdle SM, Oreffo ROC, Garnett MC and KM Shakesheff. Development of a Slow Non-Viral DNA Release System From PDLLA Scaffolds Fabricated Using a Supercritical CO<sub>2</sub> Technique. *Biotechnol Bioeng* 2007; 98 679-693
120. Sachlos E and JT Czernuszka. Making tissue engineering scaffolds work. Review: the application of solid freeform fabrication technology to

the production of tissue engineering scaffolds. *Eur Cell Mater* 2003;5:29-39

121. Liao C-J, Chen C-F, Chen J-H, Chiang S-F, Lin Y-J and K-Y Chang. Fabrication of porous biodegradable polymer scaffolds using a solvent merging/particulate leaching method. *J Biomed Mat ReS* 2002; 59(4): 676-681
122. Murphy WL, Dennis RG, Kileny JL and DJ Mooney. Salt fusion: an approach to improve pore interconnectivity within tissue engineering scaffolds. *Tissue Eng.* 2002 ;8(1):43-52
123. Scanco Medical 2007 [www.scanco.ch](http://www.scanco.ch)
124. Charles-Harris M, del Valle S, Hentges E, Bleuët P, Lacroix D and JA Planell. Mechanical and structural characterisation of completely degradable polylactic acid/calcium phosphate glass scaffolds. *Biomaterials* 2007; 28(30): 4429-38.
125. Cartmell S, Huynh K, Lin A, Nagaraja S and R Guldberg. Quantitative microcomputed tomography analysis of mineralization within three-dimensional scaffolds in vitro. *J Biomed Mater Res A.* 2004;69(1):97-104
126. Van Vlierberghe S, Cnudde V, Dubruel P, Masschaele B, Cosijns A, De Paepe I, Jacobs, Van Hoorebeke L, Remon JP and E Schacht. Porous Gelatin Hydrogels: 1. Cryogenic Formation and Structure Analysis *Biomacromol*; 2007; 8(2):331-337

127. Merret K *et al.* "Surface analysis methods for characterizing polymeric biomaterials" in *Cells, Proteins and Materials: Festschrift in Honor of the 65th Birthday of Dr. John L. Brash*. Sheardown H (Ed). VSP, The Netherlands 2003
128. Silva MMCG. Porous polymeric scaffolds for tissue engineering: a supercritical fluid approach. 2005. Thesis (PhD) - University of Nottingham, UK
129. Askady A and A Astahov. Polymers with elasticity Gradients. *Mat World*, 1997 (5):10 p 587
130. Ishizaki K, Shridar K and M Nanko. *Porous Materials: Process Technology and Applications*. Kluwer Academic Publishers 1998
131. Kovacik J. Correlation between Young's modulus and porosity in porous materials. *J Mat Sci Letters* 1999; 18: 1007-1010
132. Reed-Hill RE and R Abbaschian. *Physical Metallurgy Principles*. 3rd ed. Boston: PWS Publishing Company, 1994,
133. Callister WD Jr. *Materials Science and Engineering, an Introduction*. 3rd ed. New York: John Wiley & Sons, Inc., 1994,
134. Svensson A, Nicklasson E, Harrah T, Panilaitis B, Kaplan DL and M Brittberg. Bacterial cellulose as a potential scaffold for tissue engineering of cartilage. *Biomaterials* 2005;26:419-431

135. Müller FA, Müller L, Hofmann I, Greil P, Wenzel MM and R Staudenmaier. Cellulose-based scaffold materials for cartilage tissue engineering. *Biomater.* 2006; 27(21):3955-63.
136. Entcheva E, Bien H, Yin L, Dhung CY, Farell M and Y Kostov, Functional cardiac cell constructs on cellulose-based scaffolding. *Biomaterials* 2004; 25: 5753-5762
137. Katz S. Degradation of Polymers. *Mat World* 1995:377-78
138. Black J. Biological performance of materials: Fundamentals of Biocompatibility. 4th Ed. Taylor and Francis. USA 2006
139. Yamaguchi M. Rheological properties of linear and crosslinked polymer blends: relation between crosslink density and enhancement of elongational viscosity. *J Polymer Sc Part B: Polymer Phys.* 2000; 39(2): 228-235
140. Sheridan MH, Shea LD, Peters MC and DJ Mooney. Bioabsorbable polymer scaffolds for tissue engineering capable of sustained growth factor delivery. *J Contr Rel* 2000; 64(1): 91-102
141. Yang J, Motlagh D, Webb AR and GA Ameer. Novel biphasic elastomeric scaffold for small-diameter blood vessel tissue engineering. *Tissue Eng* 2005; 11(11/12): 1876-1886
142. Mirsky I, Ghista DN and H Sandler. "Cardiac mechanics: physiological, clinical and mathematical considerations". USA, Wiley, 1974

143. Wang Y, Ameer GA, Sheppard BJ and R Langer. A tough biodegradable elastomer. *Nat Biotechnol* 2002; 20(6): 602-606
144. Stankus JJ, Guan J and WR Wagner. Fabrication of biodegradable elastomeric scaffolds with sub-micron morphologies. *J Biomed Mater Res A* 2004; 70(4): 603-14
145. Poirier Y, Nawrath C, and C Somerville. Production of polyhydroxyalkanoates, a family of biodegradable plastics and elastomers, in bacteria and plants. *Biotechnol (NY)* 1995; 13(2): 142-150
146. Guan J, Fujimoto KL, Sacks MS and WR Wagner. Preparation and characterization of highly porous, biodegradable polyurethane scaffolds for soft tissue applications. *Biomaterials* 2005; 26: 3961-3971
147. Eastwood M *et al.* Effect of precise mechanical loading on fibroblast populated collagen lattices: morphological changes. *Cell Motil Cytoskeleton* 1998; 40: 13-21
148. Aygden MM and E Braunwald. Studies on Starling's law of the heart: mechanical properties of human myocardium studied in vivo. *Circ* 1962; XXVI: 516-524
149. Hiroshi Y. "Strength of biological materials", USA, Williams & Wilkins, 1970
150. Boublik J *et al.* Mechanical Properties and remodelling of hybrid cardiac constructs made from heart cells, fibrin, and biodegradable, elastomeric knitted fabric. *Tissue Eng* 2005; 11(7/8): 1122-1132

151. Davis JM (Ed). Basic Cell Culture. Oxford University Press, 2<sup>nd</sup> Ed. USA 2002
152. Corda S, Samuel JL and L Rappaport. Extracellular matrix and growth factors during heart growth. *Heart Fail Rev* 2000; 5: 119-130.
153. Agnetti G *et al.* Activation of glucose transport during simulated ischemia in H9c2 cardiac myoblasts is mediated by protein kinase C isoforms. *Life Sc* 2005; 78(3): 264-270
154. White SM, Constantin PE and WC Claycomb. Cardiac physiology at the cellular level: use of cultured HL-1 cardiomyocytes for studies of cardiac muscle cell structure and function *Am J Physiol Heart Circ Physiol.* 2004; 286(3): H823-9
155. Alfarano C, Sartiani L, Nediani C, Mannucci E, Mugelli A, Cerbai E and L Raimondi. Functional coupling of angiotensin II type 1 receptor with insulin resistance of energy substrate uptakes in immortalized cardiomyocytes (HL-1 cells). *Br J Pharmacol.* 2008; 153(5): 907-14.
156. Nguyen *et al*, Hypoxia regulates the expression of the adrenomedullin and HIF-1 genes in cultured HL-1 cardiomyocytes. *Biochem Biophys Res Commun* 1999; 265(2): 382-6
157. Filipeanu CM, Zhou F, Lam ML, Kerut KE, Claycomb WC and G Wu. Enhancement of the recycling and activation of beta-adrenergic receptor by Rab4 GTPase in cardiac myocytes. *J Biol Chem* 2006; 281(16): 11097-103

158. Filipeanu CM, Zhou F, Claycomb WC and G Wu. Regulation of the cell-surface expression and function of angiotensin II type 1 receptor by Rab1-mediated ER-to-Golgi transport in cardiac myocytes. *J Biol Chem.* 2004; 279(39): 41077-84
159. Ikeda K, Tojo K, Otsubo C, Udagawa T, Kumazawa K, Ishikawa M, Tokudome G, Hosoya T, Tajima N, Claycomb WC, Nakao K and M Kawamura. 5-hydroxytryptamine synthesis in HL-1 cells and neonatal rat cardiocytes. *Biochem Biophys Res Commun.* 2005; 328(2): 522-5
160. Vunjak-Novakovic G and RI Freshney Ed. Culture of Cells for Tissue Engineering. Wiley 2006
161. Boateng SY, Lateef SS, Mosley W, Hartman TJ, Hanley L and B Russell. RGD and YIGSR synthetic peptides facilitate cellular adhesion identical to that of laminin and fibronectin but alter the physiology of neonatal cardiac myocytes. *Am J Physiol Cell Physiol* 2005; 288: C30-C38
162. Gstraunthaler G. Alternatives to the use of fetal bovine serum: serum-free cell culture. *ALTEX* 2003; 20(4): 275-81
163. Weber KT, Sun Y, Tyagi SC and Cleutjens JP. Collagen network of the myocardium: Function, structural remodeling and regulatory mechanisms. *J Mol Cell Cardiol* 1994; 26: 279-292.
164. Cleutjens JPM and EEJM Creemers. Integration of concepts: cardiac extracellular matrix remodelling after myocardial infarction. *J Cardiac Fail* 2002; 8(6); S344-S348

165. Boluyt MO and OHL Bing. Matrix gene expression and decompensated heart failure: The age SHR model. *Cardiovasc Res* 2000; 46: 239-249
166. Tamura N *et al.* Cardiac fibrosis in mice lacking brain natriuretic peptide. *PNAS* 2000; 97(8): 4239-4244.
167. Van Tienen TG, Heijkants RGJC, Buma P, de Groot JH, Pennings AJ and RPH Veth. Tissue ingrowth and degradation of two biodegradable porous polymers with different porosities and pore sizes. *Biomaterials* 2002; 23(8): 1731-1738.
168. Zeltinger J, Sherwood JK, Graham DA, Müller R and LG Griffith. Effect of Pore Size and Void Fraction on Cellular Adhesion, Proliferation, and Matrix Deposition. *Tissue Eng* 2001; 7(5): 557-572
169. O'Brien FJ, Harley BA, Yannas IV and LJ Gibson. The effect of pore size on cell adhesion in collagen-GAG scaffolds. *Biomaterials* 2005; 26(4): 433-41
170. Narayan D, Venkatraman SS. Effect of pore size and interpore distance on endothelial cell growth on polymers. *J Biomed Mater Res A*. 2008; Feb 15 [Epub ahead of print]
171. Li Y, Ma T, Kniss DA, Lasky LC and ST Yang. Effects of filtration seeding on cell density, spatial distribution and proliferation in nonwoven fibrous matrices. *Biotechnol Prog* 2001; 17: 935-944
172. Godbey WT, Hindy BSS, Sherman ME and A Atala. A novel use of centrifugal force for cell seeding into porous scaffolds. *Biomaterials* 2004;25(14):2799-2805167

173. Yang TH, Miyoshi H and N Ohshima. Novel cell immobilization method utilizing centrifugal force to achieve high-density hepatocyte culture in porous scaffold. *J Biomed Materials Res* 2001; 55(3): 379 – 386
174. Solchaga L, Tognana E, Penick K, Baskaran H, Goldberg VM, Caplan AI and JF Welter. A rapid seeding technique for the assembly of large cell/scaffold composite constructs. *Tissue Eng* 2006;12(7):1851-1863
175. Radisic M, Yang L, Boublik J, Cohen RJ, Laner R, Freed LE and G Vunjak-Novakovic. Medium perfusion enables engineering of compact and contractile cardiac tissue. *Am J Physiol Heart Circ Physiol* 2004;286:H507-516
176. Shimizu K, Ito A, Arinobe M, Murase Y, Iwata Y, Narita Y, Kagami H, Ueda M and H Honda. Effective cell-seeding technique using magnetite nanoparticles and magnetic force onto decellularized blood vessels for vascular tissue engineering. *J Biosci Bioeng.* 2007; 103(5): 472-8
177. Xiao YL, Riesle J and CA. Van Blitterswijk. Static and dynamic fibroblast seeding and cultivation in porous PEO/PBT scaffolds. *J Mat Science: Mat Med* 1999;10(12) : 773-777
178. Lundgren E, Terracio L, Mardh S and TK Borg. Extracellular matrix components influence the survival of adult cardiac myocytes *in vitro*. *Exp Cell Res* 1985;58(2):371-381
179. S, Svineng G, Wennerberg K, Armulik A and L Lohikangas. Fibronectin-integrin interactions. *Front Biosc* 1997; 2 :d126-146.

180. Hersel U, Dahmen C and H Kessler. RGD modified polymers: biomaterials for stimulated cell adhesion and beyond. *Biomaterials* 2003; 24: 4385-4415.
181. Burg KJL *et al.* Comparative study of seeding methods for three-dimensional polymeric scaffolds. *J Biomed Mater Res* 2000; 51: 642-649
182. Radisic M, Park H, Geretch S, Cannizzaro C, Langer R and G Vunjak-Novakovic. Biomimetic approach to cardiac tissue engineering. *Phil Trans Soc B* 2007; 362: 1357-1368
183. Komuro I and Y Yazaki. Control of cardiac gene expression by mechanical stress. *Annu Rev Physiol* 1993; 55: 55-75
184. Sadoshima J and S Izumo. Mechanical stretch rapidly activates multiple signal transduction pathways in cardiac myocytes: potential involvement of an autocrine/paracrine mechanism. *EMBO J.* 1993; 12: 1681-1692
185. Yamazaki T, Komuro I, Kudoh S, Zou Y, Shiojima I, Hiroi Y, Mizuno T, Maemura K, Kurihara H, Aikawa R, Takano H & Y Yazaki. Endothelin-1 is involved in mechanical stress-induced cardiomyocyte hypertrophy. *J Biol Chem* 1996; 271: 3221-3228
186. Sadoshima J and S Izumo. The cellular and molecular response of cardiac myocytes to mechanical stress. *Annu. Rev. Physiol.* 1997; 59: 551-571
187. Lorell BH & BA Carabello. Left ventricular hypertrophy: Pathogenesis, detection, and prognosis. *Circ* 2000; 102: 470-479

188. Sadoshima J, Jahn L, Takahashi T, Kulik TJ, and S Izumo. Molecular characterization of the stretch-induced adaptation of cultured cardiac cells. *J. Biol. Chem.* 1992; 267: 10551-10560
189. Carson JA and FW Booth. Effect of serum and mechanical stretch on skeletal  $\alpha$ -actin gene regulation in cultured primary muscle cells. *Am J Physiol Cell Physiol* 1998; 275: C1438-C1448
190. Vandeburgh HH and S Kaufman. An in vitro model for stretch-induced hypertrophy of skeletal muscle. *Science* 1979; 203: 265-268
191. Stewart, DM. The role of tension in muscle growth. In: Regulation of Organ and Tissue Growth. New York: Associated Press, 1972, p. 77-100
192. Goldspink DF, Cox VM, Smith SK, Eaves LA, Osbaldeston NJ, Lee DM, and D Mantle. Muscle growth in response to mechanical stimuli. *Am J Physiol Endocrinol Metab* 1995; 268: E288-E297
193. Powell CA, Smiley BL, Mills J, and HH Vandeburgh. Mechanical stimulation improves tissue-engineered human skeletal muscle. *Am J Physiol Cell Physiol* 2002; 283(5): C1557-C1565, 2002
194. Gans C and AS Gaunt. Muscle architecture in relation to function. *J Biomech* 1991; 24(Suppl 1): 53-65
195. Shirinsky VP, Antonov AS, Birukov KG, Sobolevsky AV, Romanov YA, Kabaeva NV, Antonova GN and VN Smirnov VN. Mechanochemical control of human endothelium orientation and size. *J Cell Biol* 1989; 109: 331-339

196. Terracio L, Miller B and TK Borg. Effects of cyclic mechanical stimulation of the cellular components of the heart: in vitro. *In Vitro Cell Dev Biol* 1988; 24: 53-58
197. Mills I, Cohen CR, Kamal K, Li G, Shin T, Du W and BE Sumpio. Strain activation of bovine aortic smooth muscle: study of strain dependency and the role of protein kinase A and C signalling pathways. *J Cell Physiol* 1997; 170: 228-234
198. Collinsworth AM, Torgan CE, Nagda SN, Rajalingam RJ, Kraus WE and GA Truskey. Orientation and length of mammalian skeletal myocytes in response to a unidirectional stretch. *Cell Tissue Res* 2000; 302: 243-251
199. Samuel JL and HH Vandeburgh. Mechanically induced orientation of adult rat cardiac myocytes in vitro. *In Vitro Cell Dev Biol* 1990; 26: 905-914
200. Vandeburgh HH and P Karlisch. Longitudinal growth of skeletal myotubes in vitro in a new horizontal mechanical cell stimulator. *In Vitro Cell Dev Biol* 1989; 25: 607-616
201. Chien KR, Knowlton KU, Zhu H and S Chien. Regulation of cardiac gene expression during myocardial growth and hypertrophy: molecular studies of an adaptive physiologic response. *FASEB J* 1991;5:3037-3046
202. Izumo S, Nadal-Ginard B and V Mahdavi. Protooncogene induction and reprogramming of cardiac gene expression produced by pressure overload. *PNAS* 1988; 85: 339-343

203. Ruskoaho H, Kinnunen P, Taskinen T, Vuolteenaho O, Leppäluoto J and TE Takala. Regulation of ventricular atrial natriuretic peptide release in hypertrophied rat myocardium. Effects of exercise. *Circ* 1989; 80: 390-400
204. Marttila M, Vuolteenaho O, Ganten D, Nakao K and H Ruskoaho. Synthesis and secretion of natriuretic peptides in the hypertensive TGR(mREN-2)27 transgenic rat. *Hypertension* 1996; 28: 995-1004
205. Lee HR, Henderson SA, Reynolds R, Dunnmon P, Yuan D and KR Chien. Alpha 1-adrenergic stimulation of cardiac gene transcription in neonatal rat myocardial cells. effects on myosin light chain-2 gene expression. *J Biol Chem* 1988; 263: 7352-7358
206. Lindpaintner K, Jin MW, Niedermaier N, Wilhelm MJ and D Ganten. Cardiac angiotensinogen and its local activation in the isolated perfused beating heart. *Circ Res* 1990; 67: 564-573
207. Takewaki S, Kuro-o M, Hiroi Y, Yamazaki T, Noguchi T, Miyagishi A, Nakahara K, Aikawa M, Manabe I and Y Yazaki. Activation of Na<sup>+</sup>-H<sup>+</sup> antiporter (NHE-1) gene expression during growth, hypertrophy and proliferation of the rabbit cardiovascular system. *J Mol Cell Cardiol* 1995; 27: 729-742.
208. Flesch M, Schwinger RH, Schiffer F, Frank K, Sudkamp M, Kuhn-Regnier F, Arnold G and M Bohm. Evidence for functional relevance of an enhanced expression of the Na<sup>+</sup>-Ca<sup>2+</sup> exchanger in failing human myocardium. *Circ* 1996 94: 992-1002

209. Crozatier B. Stretch-induced modifications of myocardial performance: From ventricular function to cellular and molecular mechanisms. *Cardiovasc Res* 1996; 32: 25-37
210. Schunkert H, Orzechowski HD, Bocker W, Meier R, Riegger GA and M Paul. The cardiac endothelin system in established pressure overload left ventricular hypertrophy. *J Mol Med* 1999; 77: 623-630.
211. Swynghedauw B. Molecular mechanisms of myocardial remodeling. *Physiol Rev* 1999; 79: 215-262
212. Dostal DE and KM Baker. The cardiac renin-angiotensin system: Conceptual, or a regulator of cardiac function? *Circ Res* 1999; 85: 643-650
213. de Bold AJ. Atrial natriuretic factor: a hormone produced by the heart. *Science* 1985; 230(4727): 767-770
214. Flynn TG, de Bold ML and AJ de Bold. The amino acid sequence of an atrial peptide with potent diuretic and natriuretic properties. *Biochem Biophys Res Commun* 1983; 117: 859-865
215. Atlas SA, Kleinert HD, Camargo MJ, Januszewicz A, Sealey JE, Laragh JH, Schilling JW, Lewicki JA, Johnson LK and T Maack. Purification, sequencing and synthesis of natriuretic and vasoactive rat atrial peptide. *Nature* 1984; 717-719
216. Saito Y, Nakao K, Arai H, Nishimura K, Okumura K, Obata K, Takemura G, Fujiwara H, Sugawara A and T Yamada. Augmented expression of atrial natriuretic polypeptide gene in ventricle of human failing heart. *J Clin Invest* 1989; 83: 298-305

217. Lopez MJ, Wong SK, Kishimoto I, Dubois S, Mach V, Friesen J, Garbers DL and A Beuve. Salt-resistant hypertension in mice lacking the guanylyl cyclase-A receptor for atrial natriuretic peptide. *Nature* 1995; 378: 65-68
218. Oliver PM, Fox JE, Kim R, Rockman HA, Kim HS, Reddick RL, Pandey KN, Milgram SL, Smithies O and N Maeda N. Hypertension, cardiac hypertrophy, and sudden death in mice lacking natriuretic peptide receptor A. *PNAS* 1997; 94: 14730-14735
219. Knowles JW, Esposito G, Mao L, Hagaman JR, Fox JE, Smithies O, Rockman HA and N Maeda. Pressure-independent enhancement of cardiac hypertrophy in natriuretic peptide receptor a-deficient mice. *J Clin Invest* 2001; 107: 975-984
220. Franco V, Chen Y-F, Oparil S, Feng JA, Wang D, Hage F and G Perry. Atrial Natriuretic Peptide Dose-Dependently Inhibits Pressure Overload-Induced Cardiac Remodeling. *Hypertension* 2004; 44: 746-750
221. Kuwahara *et al.* NRSF regulates the fetal cardiac gene program and maintains normal cardiac structure and function. *EMBO J.* 2003 Dec 1;22(23):6310-21
222. L King and MR Wilkins. Natriuretic peptide receptors and the heart. *Heart* 2002; 87: 314-315
223. Schwartz K, de la Bastie D, Bouveret P, Oliviero P, Alonso S and M Buckingham. Alpha-skeletal muscle actin mRNA's accumulate in hypertrophied adult rat hearts. *Circ Res* 1986; 59: 551-555

224. Olson TM, Doan TP, Kishimoto NY, Whitby FG, Ackerman MJ, and L Fananapazir. Inherited and de novo mutations in the cardiac actin gene cause hypertrophic cardiomyopathy. *J Mol Cell Cardiol* 2000; 32: 1687-1694
225. Black FM, Packer SE, Parker TG, Michael LH, Roberts R, Schwartz RJ and MD Schneider. The vascular smooth muscle alpha-actin gene is reactivated during cardiac hypertrophy provoked by load. *J Clin Invest* 1991; 88(5): 1581–1588
226. Vikstrom KL, and Leinwand LA. Contractile protein mutations and heart disease. *Curr Opin Cell Biol* 8: 97-105, 1996
227. Davies, P.F., Mundel, T. and Barbee, K.A. A mechanism for heterogeneous endothelial responses to flow in vivo and in vitro. *Journal of Biomechanics* 1995; 28: 1553–1560.
228. Brown TD. Techniques for mechanical stimulation of cells in vitro: a review. *J Biomechanics* 2000; 33(1): 3-14
229. Extracellular Matrix Engineering Research Laboratory (EMERL) Northeastern University, USA. 2007. [www1.coe.neu.edu/~jeffr/kelli.htm](http://www1.coe.neu.edu/~jeffr/kelli.htm)
230. Engineered Tissue Mechanics and Mechanobiology Laboratory (ETM<sup>2</sup>L) University of Pittsburgh, USA. 2007. [www.pitt.edu/~msacks/Laboratories.htm](http://www.pitt.edu/~msacks/Laboratories.htm)
231. Zhonggang F, Matsumoto T, Nomura Y and T Nakamura. An electro-tensile bioreactor for 3-D culturing of cardiomyocytes. *Eng Med Biol Magazine IEEE* 2005; 24 (4): 73 – 79
232. Synthecon Inc 2007 <http://smaplaboratory.uah.edu/~cmds/team/synth.html>

233. BioTeamPSC LLC 2007. [http://bioteampsc.com/\\_wsn/page3.html](http://bioteampsc.com/_wsn/page3.html)
234. Flexcell Int Corp 2008. <http://www.flexcellint.com/gallery.htm>
235. ElectroForce <http://www.bose-electroforce.com/product.cfm?pid=45>
236. Tissue Growth Technologies 2008. <http://www.tissuegrowth.com/>
237. Personal communication with Dr. J Ingram, Leeds University, May 2006.
238. Fink C, Ergun S, Kralisch D, Remmers U, Weil J and T Eschenhagen. Chronic stretch of engineered heart tissue induces hypertrophy and functional improvement. *FASEB J* 2000;14:669-679
239. Akyhyari P, Fedak PWM, Deisel RD, Lee TYJ, Verma S, Mickle DAG and RK Li. Mechanical stretch regimen enhances the formation of bioengineered autologous cardiac muscle graft. *Circ* 2002; 106(Supp I): 137-142
240. Zhao YS *et al.* Construction of a unidirectionally beating 3-dimensional cardiac muscle construct. *J Heart Lung Transplant* 2005; 24: 1091-1097
241. Yu JG and B Russell. Cardiomyocyte remodelling and sarcomere addition after uniaxial static strain in vitro. *J Histochem Cytochem* 2005; 53(7): 839-844
242. Tobita K *et al.* Engineered early embryonic cardiac tissue retains proliferative and contractile properties of developing embryonic myocardium. *Am J Physiol Heart Circ Physiol* 2006; 291: H1829-1837
243. Huang YC, Khait L and RK Birla. Contractile three-dimensional bioengineered heart muscle for myocardial regeneration. *J Biomed Mat Res* 2007; 80A: 719-731

244. Yang C, Sodian R, Luders C, Lemke T, Du J, Hubler M, Wenger Y, Meyer R and R Hetzer. In vitro fabrication of a tissue engineered human cardiovascular patch for future use in cardiovascular surgery. *Ann Thorac Surg.* 2006 ; 81(1): 57-63.
245. Park H, Radisic M, Lim JO, Chang BH and G Vunjak-Novakovic. A novel composite scaffold for cardiac tissue engineering. *In Vitro Cell Dev Biol-Animal* 2005; 41: 188-196
246. Radisic M, Park H, Shing H, Consi T, Schoen FJ, Langer R, Freed LE and G Vunjak-Novakovic. Functional assembly of engineered myocardium by electrical stimulation of cardiac myocytes cultured on scaffolds. *PNAS* 2004; 101(52): 18129-18134
247. Willems E, Mateizel I, Kemp C, Cauffman G, Sermon K and L Leyns. Selection of reference genes in mouse embryos and in differentiating human and mouse ES cells. *Int J Dev Biol* 2006 (50): 627-635.
248. Murphy CL and JM Polak. Differentiating embryonic stem cells: Gapdh, but neither hpert nor beta-tubulin is suitable as an internal standard for measuring ma levels. *Tissue Eng* 2002 (8): 551-559.
249. De Jonge HJM, Fehrmann RSN, de Bont ESJM, Hofstra RMW, Gerbens F, Kamps WA, de Vries EGE, van der Zee AGJ, te Meerman GJ and A ter Elst. Evidence Based Selection of Housekeeping Genes. *Plos One* 2007 (9):e898
250. Auluck A, Mudera V, Hunt NP and MP Lewis. A three-dimensional in vitro model system to study the adaptation of craniofacial skeletal muscle following mechanostimulation. *Eur J Oral Sci* 2005; 113: 218-224

251. Komuro I, Kaida T, Shibasaki Y, Kurabayashi M, Katoh Y, Hoh E, Takaku F and Y Yazaki. Stretching cardiac myocytes stimulates protooncogene expression. *J Biol Chem* 1990; 265(7): 3595-3598.
252. Stegemann JP and RM Nerem. Phenotype modulation in vascular tissue engineering using biochemical and mechanical stimulation. *Ann Biomed Eng.* 2003; 31(4): 391-402
253. Barron V, Lyons E, Stenson-Cox C, McHugh PE and A Pandit. Bioreactors for Cardiovascular Cell and Tissue Growth: A Review. *Ann Biomed Eng* 2003; 31(9): 1017-1030
254. Ghosh K *et al.* Cell adaptation to a physiologically relevant ECM mimic with different viscoelastic properties. *Biomaterials* 2007;28:671-679
255. Davis ME, Hsieh PCH, Grodzinsky AJ and RT Lee. Custom design of the cardiac microenvironment with biomaterials. *Circ Res* 2005;97:8-15

**Appendix 1 – Video of HL-1 cardiomyocytes, cultured  
in TCP, contracting at confluence**

## **Appendix 2 – Publications and Presentations**

Hidalgo-Bastida LA *et al.* Designing Flexible Degradable Scaffolds for Cardiac Tissue Engineering. *Eur Cell Mat* 2005; (10)2: 49.

Hidalgo-Bastida LA *et al.* “Mechanical Properties of a Flexible Scaffold for Cardiac Tissue Engineering” “First International Conference on Mechanics of Biomaterials and Tissues” Hawaii, USA 2005.

Hidalgo-Bastida LA *et al.* Cell Adhesion and Mechanical Properties of a Flexible Scaffold for Cardiac Tissue Engineering. *Acta Biomat* 2007; 3:457-462.

## Designing Flexible Biodegradable Scaffolds for Cardiac Tissue Engineering

LA Hidalgo-Bastida, JJA Barry, FRAJ Rose, LD Buttery, I Hall & KM Shakesheff,

*Tissue Engineering Group, School of Pharmacy, University of Nottingham, England, GB*

**INTRODUCTION:** Recently cardiovascular diseases have become the main cause of death not only in the western countries but also in many developing countries [1]. Current research has concentrated on new alternatives such as cellular therapy. The lack of physical support containing growth factors to induce specific differentiation in the cellular therapy suggest that a cardiac construct could provide more clinical benefits if is able to supply such support. Cardiac muscle engineering is focused on obtaining cardiomyocyte constructs by seeding cardiac cells on suitable scaffolds. According to some works additional mechanical stimuli on cell culture systems have been shown to improve protein expression and differentiation in mammalian cells [2]. Our aim is to produce a flexible scaffold able to support mechanical load during tissue regeneration and evaluate the effects on the resulting 3D cardiomyocyte construct.

**METHODS:** The elastomer Poly-(1,8-octanediol-co-citric acid) [POC] was processed to obtain a porous structure using the salt leaching method before it was completely crosslinked, porosity was increased by modifying the salt concentration [3]. Porosity was evaluated with micro-tomography ( $\mu$ CT) and scanning electron microscopy (SEM). POC films were precoated with Collagen type I, Fibronectin and Laminin at different concentrations to assess the effect on cell attachment and proliferation. The films were stored at room temperature in PBS and then seeded with a cardiac cell line, HL-1 [4]. The monolayer cultures were evaluated for morphology, proliferation and survival. Also, 3D porous scaffolds were seeded with HL-1 and the constructs evaluated for morphology, proliferation and survival.

**RESULTS:** The scaffolds obtained from the POC polymer resulted flexible interconnected porous structures with a mean pore size of  $350 \mu\text{m}$ , suitable for cardiac tissue engineering (Figure 1). Data showed that unreacted monomers should be washed after the scaffold is processed to avoid a drop in the pH. Two-dimensional culture of HL-1 cells on POC films showed an acceptable attachment to the surface, and this was improved in all the precoated films (Figure 2).

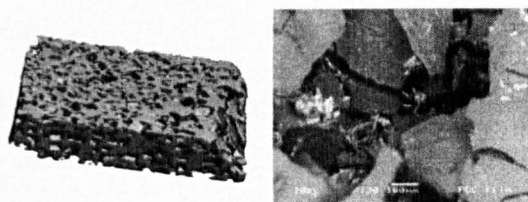


Fig 1: micro-tomography image (left) and SEM image (right) of a Poly-(1,8-octanediol-co-citric acid) [POC] scaffold

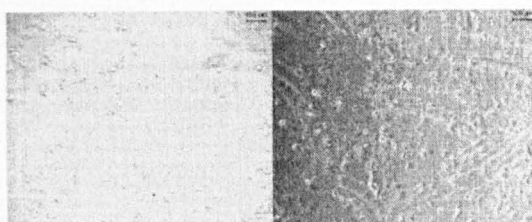


Fig 2: HL-1 cells after 24 hours of culture on POC film (left) and on POC film precoated with Fibronectin (right)

**DISCUSSION & CONCLUSIONS:** POC is a biodegradable and flexible material that can be processed to obtain elastic porous scaffolds suitable for cardiac engineering applications. Cell culture on POC showed cell attachment but the modification of the surface by the protein coating improved cell adhesion, making it a suitable material for cardiac tissue engineering. The composition of the POC scaffold is being optimized to meet the mechanical and biological parameters needed for this purpose. Further research on the constructs cultured on other systems will be carried out to assess the impact of different culture conditions in this material.

### REFERENCES:

- <sup>1</sup> World Health Organisation. (2005). [www.who.int](http://www.who.int)
- <sup>2</sup> W.H. Zimmermann et al. (2002) *Circ Res* **90**(2): 223-30.
- <sup>3</sup> J. Yang, A.R. Webb and G.A. Ameer. (2004) *Adv Mat* **16**( 6): 511-516
- <sup>4</sup> W. Claycomb et al. (1998) *PNAS* **95**(6): 2979-84

**ACKNOWLEDGEMENTS:** This project is funded by the Mexican Science & Technology Council and by the British Council.